STATUS OF THESIS

Title of thesis	**Studies on the oxidation of monoethanolamine using UV and H₂O₂ with post-biological treatment**

I, <u>**IDZHAM FAUZI B MOHD ARIFF**</u>

(CAPITAL LETTERS)

hereby allow my thesis to be placed at the Information Resource Centre (IRC) of Universiti Teknologi PETRONAS (UTP) with the following conditions:

1. The thesis becomes the property of UTP,

2. The IRC of UTP may make copies of the thesis for academic purposes only,

3. The thesis is classified as

    ☐ Confidential

    ☑ Non-confidential

If the thesis is confidential, please state the reason:

_____

_____

_____

The contents of the thesis will remain confidential for _____ years.

Remarks on disclosure:

_____

_____

Signature of Author

Permanent address:_____
S6, JLN TASIK PRIMA 3/1
TAMAN TASIK PRIMA
47150 PUCHONG, SELANGOR,
MALAYSIA

Date:____17/9/2010_____

Endorsed by

Signature of Supervisor

Name PROF DR VS MURUGESAN
Chemical Engineering Department
Universiti Teknologi PETRONAS

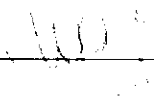Date:_____

UNIVERSITI TEKNOLOGI PETRONAS

STUDIES ON THE OXIDATION OF MONOETHANOLAMINE USING UV AND

H_2O_2 WITH POST-BIOLOGICAL TREATMENT

by

IDZHAM FAUZI BIN MOHD ARIFF

The undersigned certify that they have read, and recommend to the Postgraduate Studies Programme for acceptance this thesis for the fulfilment of the requirements for the degree stated.

Signature:

Main Supervisor:

PROF. DR. T. MURUGESAN
Chemical Engineering Department
Universiti Teknologi PETRONAS

Signature:

Co-Supervisor:

Signature:

Head of Department:

Date: 17/9/10

STUDIES ON THE OXIDATION OF MONOETHANOLAMINE USING UV AND

H_2O_2 WITH POST-BIOLOGICAL TREATMENT

by

IDZHAM FAUZI BIN MOHD ARIFF

A Thesis

Submitted to the Postgraduate Studies Programme

as a Requirement for the Degree of

MASTER OF SCIENCE

CHEMICAL ENGINEERING

UNIVERSITI TEKNOLOGI PETRONAS

BANDAR SERI ISKANDAR,

PERAK

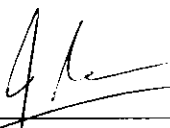SEPTEMBER 2010

DECLARATION OF THESIS

Title of thesis	**Studies on the oxidation of monoethanolamine using UV and H₂O₂ with post-biological treatment**

I, **IDZHAM FAUZI B MOHD ARIFF**

<div align="center">(CAPITAL LETTERS)</div>

hereby declare that the thesis is based on my original work except for quotations and citations which have been duly acknowledged. I also declare that it has not been previously or concurrently submitted for any other degree at Universiti Teknologi PETRONAS or other institutions.
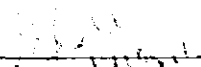
Witnessed by

_____
Signature of Author

_____
Signature of Supervisor

Permanent address: _Sb, JLN TASIK_
PRIMA 3/1, TAMAN TASIK
PRIMA, A'JISU Puchong
S'GOR, MALAYSIA

Name of Supervisor
PROF. DR. T. MURUGESAN
Chemical Engineering Department
Universiti Teknologi PETRONAS

Date: _17/9/2010_

Date:_____

iv

ACKNOWLEDGEMENT

In the name of God, The Most Gracious, The Most Merciful. Praise be to God, Lord of the worlds. May His Blessings be on the Prophet Muhammad, on his family and his companions.

I would like to express my heartfelt gratitude to all the individuals who have made this thesis possible. Firstly I wish to thank PETRONAS Research Sdn Bhd for allowing and supporting me to conduct this research project. This work would not be possible without the full support of Dr Shahidah M Shariff, General Manager of Novel Process and Advanced Engineering, who first persuaded me to register and then continued to be supportive and understanding of any difficulties that I faced. I would like to thank Pn Mahani Bt M Zain, Program Head for Bioremediation, who was tireless in ensuring the smooth administration of the scope of collaboration and agreement between PRSB and UTP.

I owe my deepest gratitude to Prof. Binay K. Dutta, who acted as my supervisor for the most part of the research work. His knowledge and guidance has made what seemed impossible at first to become challenges that were easily surmountable. His patience in responding to my many questions and the insights which he always provided were valuable and much appreciated.

My deepest thanks also to Prof. T. Murugesan who was willing to take me under his supervision despite his schedule and managed to guide me to the final stages of the thesis submission. His contribution in reviewing the written material is greatly acknowledged.

A special thanks to my family, Zakhinah, Haziq and Hana for their love and support and for enduring the extended period of me being a weekend husband/father.

ABSTRACT

In natural gas processing, alkanolamine solvents such as monoethanolamine (MEA) are widely used for removal of sour gases from natural gas. In natural gas processing plants, large volumes of alkanolamine solutions are routinely generated during periodic maintenance, cleaning and vessel safety inspections. Due to intermittent generation, high organic content and biological recalcitrance, these chemicals are generally not treatable in the conventional wastewater treatment systems available in these facilities and high costs can be incurred to segregate and dispose alkanolamine-contaminated wastewater. Advanced oxidation processes (AOPs) have been studied extensively as a promising pollution abatement strategy to rapidly oxidize many organic pollutants. The combination of UV radiation and hydrogen peroxide, called the UV/H_2O_2 process, is a widely studied AOP, and the degradation of synthetically-prepared MEA solution using the UV/H_2O_2 process is investigated in this work.

The effects of various parameters on the organics degradation of MEA under UV/H_2O_2 treatment was studied using the Taguchi approach to design of experiments based on the L-16 (4^5) modified orthogonal array. Experiments were conducted in a jacketed glass reactor using low-pressure UV lamps. Chemical oxygen demand (COD) was used as a measure of the degree of degradation of organics in the MEA solution. The parameters studied were UV dose, temperature, initial pH and initial H_2O_2 dose. The optimum conditions, predicted response (COD removal) and confidence interval were determined and a confirmation experiment was conducted. The results indicate that the main and controlling factor for the removal of COD in the experimental conditions used in this study is the UV dose. Other parameters did not have any statistically significant effect on the COD removal at the ranges used in this study. The response at optimum conditions was verified by confirmation experiment.

A more detailed study of UV/H$_2$O$_2$ degradation on MEA was conducted to determine the effects of various parameters, i.e. initial pH, temperature, UV dose (photon flux), and initial H$_2$O$_2$ dose at a broader range than the Taguchi study. In addition, the solution pH, H$_2$O$_2$ concentration, MEA concentration and some breakdown products were also investigated. The UV incident photon flux (i.e. UV dose) was quantified using hydrogen peroxide actinometry. It was found that COD removal and H$_2$O$_2$ decay are increased by raising the initial pH of the solution and more than 90% COD removal is achievable at high initial pH (8-9) after 60 minutes. Variation of solution temperature in the range studied did not have any appreciable effect on COD removal nor H$_2$O$_2$ decay. The COD removal and H$_2$O$_2$ decay increased with higher UV photon flux. Although the Taguchi study found no effect of initial H$_2$O$_2$ dose on COD removal at low H$_2$O$_2$ dosage, it was found that increase of initial H$_2$O$_2$ dose above 0.16 M concentration retarded the COD removal rate due to the scavenging of hydroxyl radicals by excess H$_2$O$_2$. The pseudo first-order kinetic constants for MEA degradation were estimated and ranged between 0.0090 to 0.0922 min^{-1} depending on the reaction conditions. The effects of the parameters on the kinetic constants were also evaluated. Several intermediate breakdown products were identified, including formate and nitrate. The formation of these acidic species resulted in the pH depression that was observed during the course of reaction. Significant concentration of ammonia was also formed during the course of the reaction.

A quasi-mechanistic kinetic rate model for the reduction of gross organic content (based on COD) during MEA oxidation using UV/H$_2$O$_2$ process was also developed. The kinetic model incorporates a set of literature rate constant values for the principal reactions involved in the photolysis of hydrogen peroxide by UV radiation to which is added the n-th order reaction of the substrate (COD) with ·OH radical. The kinetic model was validated using experimental COD and H$_2$O$_2$ degradation data and exhibited good agreement with measured values. The model results confirm that the increased COD removal at higher pH was a result of the formation of pH-dependent species and not due to the effect of H$_2$O$_2$ dissociation into hydroperoxide ion at high pH.

The biodegradability of MEA solution (in terms of COD) that has been partially degraded via UV/H$_2$O$_2$ was studied using batch growth reactor operated under aerobic conditions. The kinetic rate constants based on the Monod model formed the basis of comparison and were calculated by fitting the growth and utilisation data to a sigmoid equation. The acclimatization times were also studied. The results indicated that, for MEA solution which was partially treated with UV/H$_2$O$_2$ at 30% COD removal, the biomass growth rate, substrate utilisation rate and biomass yield was reduced compared to untreated MEA. The acclimatization time for aerobic biodegradation was unaffected. The only parameter that showed improvement was the half-saturation coefficient. This effect may be attributed to formation of some unidentified inhibitory compound at the level of pretreatment that was applied. Biodegradation of both MEA and partially treated MEA was found to generate high levels of ammonia as by-product.

ABSTRAK

Pelarut alkanolamina, contohnya monoetanolamina (MEA) digunakan secara meluas dalam penyingkiran gas-gas masam (*sour gases*) daripada gas asli. Dalam loji pemprosesan gas asli, larutan alkanolamina dalam isipadu yang besar seringkali dihasilkan akibat kerja-kerja penyelenggaraan berkala, pembersihan dan pemeriksaan keselamatan yang perlu dilakukan pada tangki-tangki pemprosesan. Pada umumnya, larutan kimia ini tidak dapat dirawat dengan berkesan menggunakan sistem rawatan air sisa konvensional yang biasanya terdapat di loji-loji tersebut. Ini disebabkan oleh beberapa faktor seperti kadar penghasilan larutan sisa yang tidak tetap, kandungan bahan organik yang tinggi serta keterbiodegradan yang rendah. Natijahnya, kos yang tinggi diperlukan untuk mengasingkan dan melupuskan air sisa yang dicemari dengan alkanolamina. Proses pengoksidaan lanjutan (AOP) yang berpotensi untuk mengoksidakan kebanyakan bahan cemar organik telah dikaji dengan meluas sebagai satu strategi penghapusan bahan cemar. Kombinasi sinar ultra ungu (UV) dan hidrogen peroksida yang juga dikenali sebagai proses UV/H_2O_2 adalah sejenis AOP yang sering mendapat perhatian di dalam kajian-kajian saintifik. Penggunaan proses UV/H_2O_2 dalam penguraian larutan MEA yang disediakan secara sintetik telah dikaji dan hasilnya dibentangkan di dalam kertas kerja ini.

Kesan-kesan beberapa faktor-faktor tertentu dalam menguraikan kandungan organik di dalam rawatan larutan MEA dengan proses UV/H_2O_2 telah dikaji menggunakan kaedah rekaan eksperimen Taguchi menggunakan aturan ortogonal (*orthogonal array*) L-16 (4^5). Reaktor kaca berjaket yang dilengkapi dengan lampu UV bertekanan rendah digunakan untuk tujuan eksperimen. Darjah penyingkiran bahan organik dalam larutan MEA telah diukur berdasarkan kandungan *chemical oxygen demand* (COD). Faktor-faktor yang dikaji adalah dos UV, suhu, pH permulaan, dan dos H_2O_2 permulaan. Tahap optimum bagi setiap faktor, hasil (tahap

penyingkiran COD) optimum dan selang keyakinan (*confidence interval*) bagi hasil optimum telah ditentukan. Hasil kajian menunjukkan bahawa faktor yang paling penting dalam proses penyingkiran COD di dalam keadaan-keadaan eksperimen yang dinyatakan adalah dos UV. Semua faktor-faktor lain tidak menampakkan kepentingan statistik dalam penyingkiran COD pada julat-julat yang digunakan dalam kajian ini. Hasil optimum telah disahkan dengan menjalankan eksperimen pengesahan.

Satu kajian yang lebih terperinci ke atas rawatan MEA menggunakan UV/H_2O_2 telah dijalankan bagi menentukan kesan-kesan daripada faktor-faktor tersebut pada julat-julat yang lebih besar daripada kajian sebelumnya. Selain daripada itu, pH larutan, kepekatan H_2O_2, kepekatan MEA dan hasil-hasil sampingan tindakbalas juga dikaji. Kaedah aktinometri hidrogen peroksida digunakan untuk mengukur tahap fluks foton UV dalam eksperimen. Penyingkiran COD dan kadar penyusutan H_2O_2 didapati meningkat dengan kenaikan pH larutan. Penyingkiran COD melebihi 90% selepas 60 minit boleh dicapai pada pH permulaan yang tinggi (8-9). Variasi pada suhu larutan tidak menunjukkan kesan yang ketara pada penyingkiran COD ataupun penyusutan H_2O_2. Penyingkiran COD dan penyusutan H_2O_2 juga meningkat dengan peningkatan fluks foton UV. Walaupun kajian sebelum ini mendapati bahawa dos H_2O_2 tidak memberi kesan kepada kadar penyingkiran COD pada dos H_2O_2 rendah, kajian terperinci menunjukkan bahawa kenaikan dos H_2O_2 permulaan melebihi 0.16 M mengakibatkan kadar penyingkiran COD menurun disebabkan oleh tindakbalas antara radikal hidroksil dan H_2O_2 berlebihan. Pemalar-pemalar kinetik palsu peringkat pertama (*pseudo first-order kinetic constants*) untuk degradasi MEA telah dianggarkan dan nilainya adalah di antara 0.0090 ke 0.0922 min^{-1} bergantung kepada keadaan-keadaan tindakbalas. Kesan daripada perubahan nilai-nilai faktor kepada pemalar-pemalar kinetik juga dikaji. Beberapa hasil-hasil sampingan tindakbalas berjaya dikenalpasti, termasuk ion-ion format dan nitrat. Penghasilan ion-ion berasid ini menjelaskan penurunan ketara pada nilai pH yang telah direkodkan dalam eksperimen. Ammonia juga telah dihasilkan pada kepekatan yang tinggi akibat tindakbalas yang berlaku.

Sebuah model kadar kinetik separa mekanistik telah dihasilkan untuk menghuraikan penyusutan kandungan organik (berdasarkan COD) semasa pengoksidaan MEA menggunakan proses UV/H_2O_2. Model kinetik tersebut menggunapakai nilai-nilai pemalar kadar daripada literatur bagi tindakbalas-tindakbalas utama yang terlibat di dalam proses fotolisis hidrogen peroksida dengan sinar UV, yang mana ditambah pula dengan tindakbalas peringkat n (n-th order) di antara substrat (COD) dan radikal $\cdot OH$. Model kinetik tersebut telah disahkan menggunakan data yang diperoleh semasa eksperimen dan persamaan yang baik diperolehi di antara anggaran model dengan nilai-nilai sebenar yang diukur semasa eksperimen. Hasil anggaran model tersebut juga mengesahkan bahawa peningkatan kadar penyingkiran COD pada pH tinggi adalah disebabkan penghasilan produk-produk sampingan tindakbalas yang sifatnya bergantung kepada nilai pH dan bukannya akibat daripada penceraian H_2O_2 kepada ion hidroperoksida pada pH tinggi.

Keterbiodegradan larutan MEA (berdasarkan ukuran COD) yang telah dirawat secara separa menggunakan proses UV/H_2O_2 telah dikaji menggunakan bioreaktor kelompok yang dioperasikan dalam keadaan aerobik. Pemalar-pemalar kadar kinetik berdasarkan model Monod membentuk asas bagi melakukan perbandingan dan ianya ditentukan dengan menyesuaikan data pertumbuhan biojisim dan penggunaan substrat kepada sebuah persamaan sigmoid. Jangka masa untuk penyesuaian (*acclimatization*) biojisim juga ditentukan. Hasil kajian mendapati, bagi larutan MEA yang telah dirawat melalui proses UV/H_2O_2 pada tahap penyingkiran COD sebanyak 30%, kadar pertumbuhan biojisim, kadar penggunaan substrat dan penghasilan biojisim didapati telah berkurang berbanding larutan MEA yang tidak dirawat, manakala masa penyesuaian untuk biodegradasi aerobik tidak terjejas. Satu-satunya parameter yang menunjukkan peningkatan adalah pekali separuh-penepuan. Kesan-kesan ini boleh dianggap berpunca daripada penghasilan sebatian perencat biologikal yang tidak dapat dikenalpasti.. Biodegradasi kedua-dua larutan MEA dan larutan MEA terawat didapati menghasilkan tahap kandungan ammonia yang tinggi sebagai hasil sampingan tindakbalas.

TABLE OF CONTENTS

LIST OF TABLES

LIST OF FIGURES AND ILLUSTRATIONS

LIST OF SYMBOLS

Symbol	Description	Units
E_0	Oxidation potential	V
TLV	Threshold limit value	ppmv
μ	Specific biomass growth rate	h^{-1}
k	Specific substrate utilisation rate, or	h^{-1}
	rate constant, or	depends on reaction order
	slope of sigmoid	$mg\ L^{-1}\ s^{-1}$
X	Biomass concentration	mg/L
S	Substrate concentration	mg/L
K_S	Half-saturation coefficient	mg/L
LP	Low-pressure (UV lamp)	
$Y_{X/S}$	Biomass yield	
MP	High-pressure (UV lamp)	
λ	Wavelength	nm
ε	Molar absorption coefficient	$L\ mol^{-1}\ cm^{-1}$
COD	Chemical oxygen demand	mg/L
TOC	Total organic carbon	mg/L
DOE	Design of experiments	
MLSS	Mixed liquor suspended solids	mg/L
MLVSS	Mixed liquor volatile suspended solids	mg/L
Φ	Quantum yield of photolysis	$mol\ Einstein^{-1}$
I_0	Volumetric UV photonic flux	$Einsteins \cdot L^{-1} \cdot s^{-1}$
D	Optical density of solution	
ANOVA	Analysis of variance	
C.I.	Confidence interval	
k_0	Pseudo first-order rate constant	min^{-1}

Symbol	Description	Units
t_R	Chromatogram peak residence time	min
$f_{H_2O_2}$	fraction of UV irradiation absorbed by hydrogen peroxide	
A	Solution absorbance = $2.303D$	
b	Path length	cm
K_a	Acid dissociation constant	
r	Reaction rate	mol L^{-1} s^{-1}
n	Reaction order	
a, b & c	Coefficients for sigmoid equation	

CHAPTER 1

INTRODUCTION

1.1. Background of Research

Monoethanolamine (MEA) is an alkanolamine that is widely used as an absorbent for the removal of acid gases (H_2S and CO_2) from natural gas (The Dow Chemical Company 2007). Although the MEA solution is continuously regenerated during desorption in a regenerator stripping tower, large volumes of MEA solutions are potentially generated as waste especially during periodic maintenance, cleaning and vessel safety inspections (Yassir 2006). In addition, accumulation of contaminants in the alkanolamine solution often lead to operational problems that may require either partial solution purging or complete inventory replacement, leading to the production of large volumes of contaminated, high-strength alkanolamine waste solutions (Abdi 2001). Although MEA itself is considered to be readily biodegradable, the release of MEA to the environment, especially to the surface water environment is a cause for concern (Robins, Houston and Sevigny 2002). On the other hand, off-site disposal of MEA waste solutions, typically by incineration, can be very expensive depending on local environmental waste regulations, especially if large volumes are generated. For example, in Malaysia, the applicable scheduled waste disposal rate for chemical organic waste can be between 570 to 951 USD per tonne of pumpable liquid depending on the composition (Malaysian Industrial Development Authority (MIDA) 2008).

In this regard, advanced oxidation processes (AOPs) have been studied extensively as a promising pollution abatement strategy to treat many persistent or recalcitrant organic pollutants. AOP is defined as an oxidation process in which the

1

dominant oxidative species is the hydroxyl radical (•OH) and are usually operated at or near ambient pressure and temperature (Glaze, Kang and Chapin 1987). There are different types of AOPs based on the method in which the oxidative species is generated. Some examples include UV/H_2O_2, O_3-based processes, Fenton's oxidation, electrochemical-based processes, and others. In this thesis, the degradation of MEA using the UV/H_2O_2 advanced oxidation process is reported. The effects of various operational factors were investigated and a kinetic model was developed to describe the process. Biological oxidation of UV/H_2O_2-treated MEA was studied to investigate the effect of AOP treatment on MEA biodegradability

1.2. Properties and Applications of MEA

MEA, (C_2H_7NO) is a clear, colorless, viscous liquid at ambient conditions with a mild, ammonia-like odor. It is an ethanolamine and has the properties of both amines and alcohols. MEA is completely miscible in water and is hygroscopic. MEA is also a primary amine and has a chemical structure as shown in Figure 1-1 below:

$$H{-}\overset{\displaystyle H}{\underset{\displaystyle H}{N}}{-}(CH_2)_2{-}OH$$
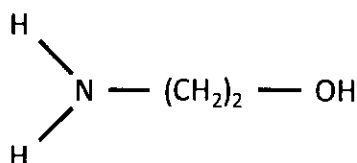
Figure 1-1: Chemical structure of MEA

MEA is used in a variety of applications such as cement manufacturing, gas treating, metalworking fluids, personal care products, pharmaceuticals, printing inks, textiles and wood-treating (The Dow Chemical Company 2007).

Although many alkanolamines are not readily biodegradable, MEA is considered to be readily biodegradable and does not bioaccumulate (The Dow Chemical Company 2007). Nonetheless, the release of MEA to the environment is a cause for concern, and it has been found that the MEA biodegradation in soil is

inhibited at high concentrations exceeding 1500 mg/kg (Mrklas, et al. 2004). The unintentional release of MEA in the surface water environment is potentially damaging to aquatic life, especially to aquatic plants and algae which are the most sensitive organisms to alkanolamine contamination. For these organisms, chronic effects are observed for MEA exposure between 1 – 80 mg/L (Robins, Houston and Sevigny 2002).

1.3. Gas Purification using MEA

Natural gas is a naturally-occurring mixture of light hydrocarbon (primarily methane) and non-hydrocarbon gases, and can be found either in non-associated dry gas wells (i.e. without crude oil) or in association with crude oils, either in contact with and/or dissolved in crude oil and is co-produced with it. Higher molecular weight paraffinic hydrocarbons (C_2-C_7) are usually present in smaller amounts with the natural gas mixture, and their ratios vary considerably from one gas field to another. Raw natural gases contain carbon dioxide, hydrogen sulfide, and water vapor in various amounts. Hydrogen sulfide must be removed from natural gas for domestic application because of its toxicity and its highly corrosive nature, especially to metallic equipment. Carbon dioxide is also undesirable, because it lowers the heating value of the gas and can solidify under high pressure and low temperatures conditions during natural gas transport (Kidnay and Parrish 2006).

Alkanolamines are often used in gas processing to remove these undesirable acid gases due to their ability to form salts with the weak acids formed by H_2S and CO_2 in aqueous solution. In the gas processing plant, alkanolamine solvents are used to remove these compounds by stripping them from the natural gas feed in a gas contactor. The solvent is then regenerated and recycled to generate a closed-loop process. Among the various alkanolamines, MEA is preferred for maximum removal of relatively low concentrations of acid gases, especially at lower operating pressures and is one of the most commonly used solvents for acid gas removal (Kohl and Nielsen 1997).

3

1.4. Advanced Oxidation Process

As previously noted, AOPs involve the generation of highly reactive radical intermediates at ambient conditions, especially hydroxyl radicals ($\cdot$OH). The importance of the $\cdot$OH radical in AOPs is due to the high reactivity of the radical and its high oxidizing power ($E_0 = 2.8$ V), which is second only to fluorine (Adams and Kuzhikannil 2000). Additionally, $\cdot$OH radicals react rapidly and non-selectively with most organic pollutants with second-order rate constants in the order of $10^8 - 10^9$ L/mole$\cdot$s, 3 – 4 orders of magnitude greater than other oxidants (Crittenden, Trussell, et al. 2005). AOPs can often lead to total mineralization of organics, given sufficient reagents and time. The combination of low selectivity, rapid reaction kinetics and capacity for total mineralization give AOPs a clear advantage compared to conventional chemical oxidation and other phase separation processes such as stripping, carbon adsorption and membrane separation.

1.5. AOP as a pretreatment to biological oxidation

Degradation of most soluble organic compounds can often be achieved economically using biological treatment processes. Biological or biochemical processes can be defined as processes that use living microorganisms to destroy or transform pollutants. They include aerobic processes such as the aerated lagoon, activated sludge system and the sequencing batch reactor and also anaerobic processes. However, it is widely known that biological processes are more effective than physical or chemical processes when pollutant concentrations are low. In particular, aerobic biodegradation systems such as the conventional activated sludge plants are only suitable for the removal of between 50 – 4,000 mg/L of COD and anaerobic systems are not effective above 50,000 mg/L COD (Leslie Grady Jr, Daigger and Lim 1999). In addition, biological treatment is often inhibited by presence of toxic or biorecalcitrant compounds. With respect to this, a number of researchers have indicated that pretreatment of certain polluted waters using AOP before biological treatment (i.e. coupling of AOP and biological oxidation) can improve the rate of organic degradation (Arslan-Alaton, Cokgor and Koban 2007) (Sarria, et al. 2002).

4

However, this result will be highly dependent on the nature of the pollutant; for example, Adams and Kuzhikannil (2000) found that AOP pretreatment was ineffective at improving biodegradability of certain amine surfactants. This means that laboratory or pilot scale testing of integrated AOP-biological oxidation systems need to be conducted before applying the process to degrade a particular organic compound.

1.6. Problem Statement

In the above context, this work has been conducted to investigate experimentally the degradation of MEA solution using UV/H_2O_2 process to investigate the potential of the process to solve the issue of treatment of MEA waste from gas processing plants. In addition, the suitability of the use of UV/H_2O_2 as a pretreatment for aerobic biological oxidation process will also be studied.

1.7. Objectives

The following are the specific objectives to address the above-stated hypothesis:

1. An overall view of the effects of various parameters on the degradation of organics in MEA solution under UV/H_2O_2 treatment will be studied using the Taguchi approach to design of experiments.

2. The effects of identified parameters on organic destruction, MEA degradation and residual H_2O_2 decay will be studied in detail and the formation of some degradation products will be identified. The effect of the identified parameters will be correlated to the pseudo first-order kinetic rate constants for MEA degradation.

3. A quasi-mechanistic rate model will be developed to adequately describe the kinetics of COD degradation and H_2O_2 consumption. The

model will then be generalized and validated using present experimental results.

4. Partially UV/H$_2$O$_2$-treated MEA will be tested for biodegradability using batch growth reactor operated under aerobic conditions. The effect to MEA biodegradability will be analysed based on the calculation of the Monod kinetic rate constants.

1.8. Scope of Work

The scope of this study covers the experimental investigation of the degradation of MEA solution using UV/H$_2$O$_2$ process to determine the effects of various reaction parameters on the efficiency of both organic destruction and MEA degradation rate. The experiments were carried out using synthetically-prepared MEA solutions at approximately 1 g/L concentration, to ensure reasonable COD reduction during the course of the reaction (1 hour). Parameters such as pH, hydrogen peroxide concentration, temperature and UV dose will be studied preliminarily using statistical design of experiment method followed by more detailed experimentation. Low-pressure Hg arc UV lamps will be used in the study, and variation of UV dose is constrained by the available lamp size and reactor configuration. The pH will be varied to maximum pH of approximately 10 for unbuffered samples, to prevent the spontaneous decomposition of H$_2$O$_2$ at higher pH range. The lower limit of pH was set at 2, since the amount of acid required to further reduce the pH is excessively large and unrealistic in large-scale practice, especially due to the alkalinity of the amine compound. The temperature range will be studied in the range of 20 to 45 °C in consideration of the practicality and cost-effectiveness of actual heating and cooling required in a full-scale system. A suitable kinetic rate model will be developed to model the degradation of organics and oxidant consumption in the process. This kinetic rate model is based on COD, not substrate (MEA) to investigate the overall organics behavior under oxidation and also to simplify the mathematical analysis. In addition, the effects of UV/H$_2$O$_2$ pretreatment on subsequent aerobic biological

6

oxidation will also be studied in batch mode using suitable kinetic models of biomass growth and substrate utilization.

CHAPTER 2

LITERATURE REVIEW

2.1. Natural Gas Treatment

Natural gas is primarily used for fuel and petrochemical feedstock. Of the various primary sources of fuel, natural gas provides close to 1-quarter of the global energy needs. Its popularity as an energy source is expected to grow significantly in the future, primarily due to the various environmental advantages compared to other sources such as crude oil and coal. In particular, natural gas is cleaner in terms of greenhouse gas emissions, since it is estimated that crude oil and coal produces 1.4 to 1.75 times more carbon dioxide emissions compared to the natural gas (Kidnay and Parrish 2006).

The size of the global total proven natural gas reserves is estimated at about 6040 trillion cubic feet (Tcf). Of this, Malaysia holds 83 Tcf of proven reserves as of January 2009. The production of natural gas in Malaysia has been steadily rising, reaching 2.3 Tcf during 2007. Malaysia is the second largest net exporter of natural gas, primarily in the form of liquefied natural gas (LNG) and in 2007, exported over 1 Tcf of LNG, equivalent to 13 % of total world LNG exports, mostly to Japan, South Korea, and Taiwan (United States Department of Energy 2009).

There are 3 primary objectives in the processing of natural gas for its usage as fuel and petrochemical feedstock as indicated below:

1. Purification

2. Separation

8

3. Liquefaction

In the purification process, undesirable materials in the gas that may inhibit its use as a fuel is removed. In separation, components in the gas that have greater value as industrial gas, petrochemical feedstocks or stand-alone fuel are separated and in liquefaction, the energy density of the natural gas is increased to facilitate storage and transportation. These processes are normally achieved in a gas processing plant, which will have some combination of the following unit processes or process sections, depending on the desired end product of the plant (Kidnay and Parrish 2006):

1. Inlet receiving

2. Inlet compression

3. Gas treating

4. Dehydration

5. Hydrocarbon recovery

6. Nitrogen rejection

7. Helium recovery

8. Outlet compression

9. Liquids processing

10. Sulfur recovery

11. Storage and transportation

12. Liquefaction

2.1.1. Gas treating

In the gas treating process, the primary aim is the reduction of contaminants to acceptable levels as defined according to requirements of safety, corrosion control, gas and/or liquid product specifications, freeze-out prevention at low temperatures, compression costs, prevention of catalyst poisoning in downstream facilities and environmental impact. The main contaminants of concern are the "acid gases" i.e. H_2S and CO_2, which can cause many problems in the gas stream. Both acid gases form weak acids in the presence of moisture leading to corrosion. H_2S in particular is highly toxic and has a threshold limit value (TLV) for prolonged exposure of 10 ppmv. At 1000 ppmv and greater, death occurs in minutes. If the gas is being fed to an LNG liquefaction facility, then the maximum CO_2 level is about 50 ppmv to prevent solids formation (Gas Processors Suppliers Association 2004).

The levels of acid gases that are present in the raw gas vary widely; as a consequence many processes are in use to remove acid gases from a natural gas stream, since no single process is superior to achieve all the treatment levels in every situation. These processes include solvent absorption, solids absorption, membranes, direct conversion and cryogenic fractionation. The selection of the most suitable gas treating process is subject to a number of considerations as outlined in Gas Processors Suppliers Association Engineering Data Book (2004).

2.1.1.1.   Chemical solvent absorption

Chemical solvent absorption processes are one of the most widely used processes in the industry. In chemical solvent absorption, H_2S and CO_2 are removed from the gas stream by a chemical reaction with the solvent, either reversibly or irreversibly. In a reversible process, the acid gases are removed in a contactor at high partial pressure and/or low temperature and the process is reversed in the stripper under conditions of low partial pressure and/or high temperature. The most widely used chemical solvents for removal of acid gases from natural gas are alkanolamines. Alkanolamines contain both amine and alcohol functional groups, the former being the reactive component and the latter functions to reduce the overall compound

10

volatility. Amines are basic, and react exothermically with weak acids formed when H_2S and CO_2 are dissolved in water forming a salt in the solution. Amine reactivity is dependent on the structure of the compound, whether it is a primary, secondary or tertiary amine. Sterically-hindered amines are amines where the functional amine group is shielded by neighbouring groups such that larger molecules have less access to the reactive center. Table 2-1 shows some commonly used amines and their chemical structures.

Table 2-1: Chemical structures of some common amines used in gas treating

Amine Type	Examples	
Primary amine	Monoethanolamine (MEA)	Diglycolamine (DGA)
Secondary amine	Diethanolamine (DEA)	Diisopropanolamine (DIPA)
Tertiary amine	Triethanolamine (TEA)	Methyldiethanolamine (MDEA)

A generic process flow of chemical solvent absorption process commonly used in gas treating is shown in Figure 2-1. In the contactor, the sour gas feed enters the bottom section at approximately 70 bar and 32 °C and flows upward, counter-current to the lean amine solution which flows downward. The contactor utilizes

11

trays or packing to increase contact between the lean amine solution and the sour gas feed and operates at higher-than-ambient temperatures with the maximum occurring near the bottom of the contactor tower. The rich amine leaves the bottom of the unit and enters a flash tank, where its pressure is reduced to 5 to 7 barg to flash off any dissolved hydrocarbons. The rich amine is then heated in a heat exchanger and enters the solvent regenerator (stripper) at temperatures in the range of 80 to 105°C. Vapor generated at the bottom flows upward, where it contacts the rich amine and strips the acid gases from the liquid that flows down. A stream of lean amine is removed from the stripper, cooled to about 45°C, and sent back to the contactor at the top to cool and condense the upward-flowing vapor stream. The vapor, which consists mostly of acid gases and water vapor, exits the top of the stripper and is generally processed for sulfur recovery. The lean amine exits the bottom of the stripper at about 130°C and exchanges heat with the rich amine stream before it enters the top of the contactor (Kidnay and Parrish 2006).
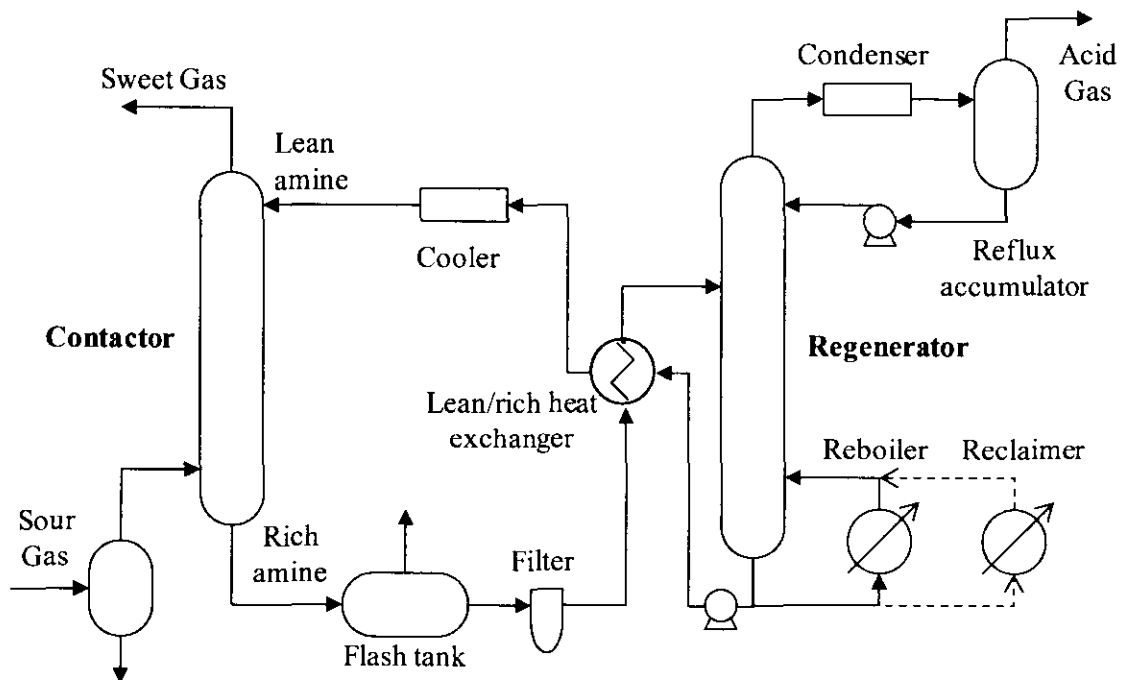
Figure 2-1: Simplified flow diagram for a typical acid gas removal unit.

2.1.1.2.   *Waste generation from solvent absorption process*

Since the solvent absorption process is a closed-loop system, buildup of non-regenerable contaminants often occurs, leading to operational difficulties such as foaming, corrosion, solids deposition, loss of amine strength and environmental issues.   Depending on the chemical structure of the amine and the operating conditions, the amine solvents can be irreversibly decomposed by chemical reaction with inorganic carbon and sulfur compounds such as CO_2, COS and CS_2, thermal degradation and oxidative degradation.   Nonvolatile contaminants and suspended solids from the gas feed can also accumulate in the solution and cause problems. Finally, heavier hydrocarbons that are not removed in the stripping tower may dissolve in the solution in the high temperatures and low pressure conditions in the absorption towers (Abdi 2001).   These contaminants need to be removed to prevent operational problems and loss of acid gas removal efficiency.   Although the most desirable remediation of these contaminant is by solvent reclamation either by absorption, ion exchange, catalytic reversal or distillation, at times certain operational and design limitation prevent these options from being implemented.   Instead, solution purging and replacement may need to be conducted as a short term solution. This will lead to the formation of large volumes of highly concentrated solvent waste, which could not be removed in conventional wastewater treatment processes available for the facility.

In addition, internal vessel inspections of the absorption and regeneration towers and other ancillary equipment are often necessary as a regulatory requirement for pressure vessels and are usually planned activities during a plant shutdown and turnaround (Yassir 2006).   Internal vessel inspection is essential to determine possible weakening of the vessel and determine conditions that would develop into leaks. Depending on the corrosivity of the chemicals and the risk of containment release, the frequency of inspection could range from semiannual to every ten years.   To conduct these internal safety inspections, the contents of the vessel need to be purged and any residues should be removed completely (Sanders 1999).   For solvents used in gas treating, the purged solution may not be completely reusable due to various reasons. Consequently this will result in formation of large volumes of highly concentrated

waste solutions which may pose an environmental hazard if not disposed or treated appropriately.

2.2. Industrial Wastewater Treatment

Industrial wastewaters may contain a variety of pollutants depending on the nature of the industry and the specific source of the wastewater. In general terms, industrial wastewaters may be contaminated with suspended solids, organic or inorganic compounds and heavy metals. Technologies to treat industrial wastewater can often be classified according to the mechanistic principle of the treatment process, which is related to the type of contaminant being primarily targeted for treatment. In this regard, industrial wastewater treatment processes are often classified as:

1. Physical treatment

2. Chemical treatment

3. Biological treatment

2.2.1. Physical treatment methods

Physical methods involve processes that remove dissolved and undissolved substances without altering the chemical structure. Physical treatment methods can be further divided into the following general classifications (Woodard 2001):

1. Separation using a physical barrier

2. Granular media filtration

3. Sedimentation

4. Flotation

5. Adsorption

14

6. Ion exchange

2.2.1.1.   Separation using a physical barrier

In these processes, the target pollutants are separated based on the size of the substance as compared to the size of the passageway in the physical barrier. Examples include sieves, bar screens and racks for removal of large particles, sand filtration for removal of finer particles as small as a few microns, and the various types of membrane filters, including semi-permeable reverse osmosis membranes are capable of separating ionic and nonionic compounds. Another type of treatment utilizing physical barriers is the electrodialysis process which utilizes electrical attraction and movement of ions through a solution towards an electrode of opposite charge, combined with selective transport of ionic species through membranes (Woodard 2001).

2.2.1.2.   Granular media filtration

In filtration using granular media, the mechanisms of removal includes one or more of the following: physical entrapment, adsorption, gravity settling, impaction, straining, interception, and flocculation. Granular media filtration involves two distinct operating stages, the filtering phase and the cleaning phase. These phases can be operated either continuously or semi-continuously. Examples of granular media filtration include deep bed filters, pressure or vacuum filters and sand filters (Woodard 2001).

2.2.1.3.   Sedimentation

In sedimentation, particulate matter is separated from the wastewater using the influence of gravity. Clarifiers, settling tanks and lamellar settlers are examples of sedimentation, where quiescent conditions are produced to ensure effective settling of suspended solids. In sedimentation, particles settle according to 3 modes, i.e. discrete

settling, flocculent settling and zone settling. Centrifugation works based on rotation and production of centrifugal forces to enhance the sedimentation and particle separation process (Woodard 2001).

2.2.1.4. *Flotation*

Flotation also utilizes gravity forces to achieve particle removal. In dissolved air flotation (DAF), supersaturated dissolved air is precipitated as tiny bubbles which attach themselves to suspended particles, creating buoyant agglomerates which rise to the surface. At the surface, mechanical skimmers remove the solids which are suspended in a froth. Chemical coagulation is often used to enhance the process.

2.2.1.5. *Adsorption*

Adsorption is the process where a substance is accumulated on the surface of another substance. In water and wastewater treatment, the most common adsorbent is activated carbon. Other adsorbents include synthetic resins, activated alumina, silica gel, fly ash, shredded tires, molecular sieves, and sphagnum peat (Woodard 2001). An important criteria for an effective adsorbent is a high surface-to-volume ratio.

2.2.1.6. *Ion exchange*

Ion exchange process involves the interchange of ions dissolved in the solution with ions associated with functional groups on the surface of the ion exchange media. The process is dependent on the valency and concentration of both the ions in the bulk solution and the ions on the ion exchange media. With proper configuration of ion exchange resin beds and using mixed bed resins, high-purity water can be achieved.

2.2.2. Chemical treatment methods

In chemical treatment methods, the pollutant substance is chemically altered to assist in its removal from the wastewater stream. Examples of chemical methods include chemical precipitation, coagulation and chemical oxidation processes.

2.2.2.1. Chemical precipitation

In industrial wastewaters, the removal of metals is often achieved using either alkaline precipitation, precipitation of the metal as its sulfide, precipitation as its phosphate, precipitation as its carbonate, or co-precipitation with another metal hydroxide, sulfide, phosphate, or carbonate. These processes rely on chemical reactions to form insoluble metal salts which precipitate out of solution. The optimum condition for chemical precipitation is highly dependent on the species of metal to be removed, because theoretical solubilities of different metal compounds vary significantly especially with respect to pH (Woodard 2001).

2.2.2.2. Reduction of surface charge for coagulation

Some particulates, e.g. oil droplets, in the wastewater may exist as stable suspensions, or colloids. A coagulant is a substance that can affect the surface charges of the colloids to destabilize the suspension and cause the dispersed colloids to agglomerate to enhance its separation. The stability of the dispersion is largely a result of the strength of the surface charge of the colloidal particle, which is measured as its zeta potential. The selection of best coagulant or coagulant aid and optimum conditions for charge neutralization is best performed using lab-scale studies (Woodard 2001).

2.2.2.3. Oxidation

Many objectionable substances can be rendered non-objectionable by chemical oxidation. Chemical oxidation involves the use of strongly oxidizing agents which will undergo a redox reaction with the target substance, e.g. include chlorination of

hydrogen sulfide and oxidation of soluble ferrous to insoluble ferric compound using aeration or oxygenation (Woodard 2001). Chemical oxidation may also involve production of free radicals, which are highly reactive radicals that can oxidize organic compounds at a much higher rate. Chemical oxidation processes that involve the generation of free radical (commonly hydroxyl) reactions are commonly referred to as advanced oxidation process (AOP) involving the use of UV, ozone, hydrogen peroxide and other substances.

2.2.3. Biological treatment methods

Biological treatment methods involve the use of living microorganisms to impart a chemical and physical change in the pollutant substance in the effort to remove it from the wastewater stream. This is often achieved in the microorganisms by way of enzyme-catalyzed chemical reactions. In biological treatment, soluble pollutants are chemically transformed into carbon dioxide and nitrogen gas, or into new microbial biomass particulates, which could then be safely separated from the water by physical methods such as sedimentation. In addition to chemical transformation, insoluble organic matter is also entrapped with the microorganisms, resulting in a relatively clean effluent. A portion of the separated insoluble materials may also be returned back to the upstream biological treatment process while the remaining materials are often transferred to a downstream process train for further treatment.

Biological treatment systems can be classified according to three main approaches: (1) the biochemical transformation, (2) the biochemical environment and (3) the bioreactor configuration (Leslie Grady Jr, Daigger and Lim 1999).

2.2.3.1. *Biochemical transformation*

In this approach, biological treatment can be divided based on the nature of the main pollutant transformation that is taking place. There are 3 classifications:

1. Removal of soluble organic matter

2. Stabilization of insoluble organic matter

3. Conversion of soluble organic matter

2.2.3.2. Biochemical environment

The environment in which the microorganism grows is an important factor in biological treatment. Essentially, this relates to whether the environment contains dissolved oxygen in sufficient quantity, i.e. aerobic conditions. Biological treatment can be either aerobic or anaerobic. The aerobic biodegradation process can be represented by Eq. (2-1).

$$C_xH_y + O_2 + (microorganisms/nutrients) \rightarrow H_2O + CO_2 + biomass \qquad (2-1)$$
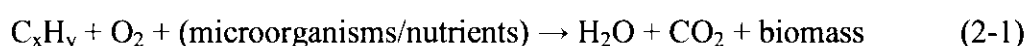
In aerobic biodegradation, pollutants are broken down into CO_2, water, nitrates, sulfates, and biomass (microorganisms). In the conventional aerobic system, the substrate is used as a source of carbon and energy and in the overall redox reaction, is referred to as the electron donor. Under aerobic conditions, the terminal electron acceptor that is preferentially used by the microorganism as they transform the pollutant compounds is oxygen. In aerobic processes, the growth of microorganisms is most efficient and high biomass yield is attained (Doble and Kumar 2005).

In anaerobic degradation, complex organics are first broken down into a mixture of volatile fatty acids (VFAs), such as acetic, propionic, and butyric acid by a consortium of hydrolytic and acidogenic bacteria. Acetogenic (acetogens) and methanogenic (methanogens) bacteria then convert the VFAs to CO_2 and methane, respectively(Doble and Kumar 2005). Anaerobic biodegradation process can be represented by Eq. (2-2).

$$C_xH_y + (microorganisms/nutrients) \rightarrow CO_2 + CH_4 + biomass \qquad (2-2)$$
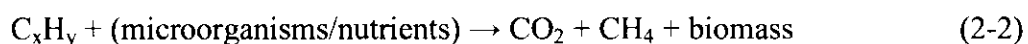
In anaerobic processes, the terminal electron acceptor may be other compounds such as sulfate, carbon dioxide or organic compounds and in anoxic

conditions, compounds such as nitrate/nitrite serve as the main electron acceptor. Under both these conditions, growth rate is less than that which occurs in aerobic conditions. Nonetheless, anaerobic degradation has several advantages over aerobic degradation such as the production of biogas which has calorific value, lesser sludge production, lesser CO_2 generation, and lesser nutrient requirements (Doble and Kumar 2005).

2.2.3.3. *Bioreactor configuration*

There are two major types of bioreactor configuration which encompasses virtually all bioreactors. They are suspended growth and attached growth bioreactors. In suspended growth reactors, the microorganisms are suspended in the liquid medium and conversely, in attached growth reactors, the microorganisms are attached to a solid support.

The most common suspended growth reactor is the activated sludge process, which was developed in 1913 by Clark and Gage at the Lawrence Experiment Station in Massachusetts in the United States and in 1914 by Ardern and Lockett at the Manchester Sewage Works in England (Metcalf & Eddy Inc. 2003). In the activated sludge process, the microbial suspension, called the mixed-liquor suspended solids (MLSS) or mixed-liquor volatile suspended solids (MLVSS) degrades the organics in an aeration tank, in which mechanical mixing and aeration is provided. The mixed liquor is then settled and thickened in a clarifier and part of the settled biomass (the activated sludge) is recycled back into the aeration tank since it still contains active microorganisms. Suspended growth reactors can also be operated anaerobically such as in anaerobic digesters.

In attached growth or fixed film bioreactors, the organic contaminants are removed from the wastewater when it flows past the microbial biofilm attached to a packing material. Many types of packing material are available such as rock, gravel, sand and plastics. The most common type of attached growth reactor is the trickling filter. In attached growth processes, excess biomass sloughs off periodically and has to be separated to ensure the effluent quality (Metcalf & Eddy Inc. 2003).

20

2.2.3.4. Biomass growth and substrate utilization kinetics

The exponential growth of bacteria in the presence of a limiting amount of substrate, and the dependence of the growth rate on the concentration of the limiting substrate, is a basic concept in microbial kinetics (Leslie Grady Jr, Daigger and Lim 1999). Mathematically, the biomass growth rate and substrate utilisation rate are often related to the biomass concentration by the specific growth rate, μ and the specific substrate utilisation rate, k, as indicated in Eq. (2-3) and (2-4), where X, S, μ and k represent the biomass concentration (MLSS, mg/l), substrate concentration (COD, mg/l), specific growth rate (h^{-1}) and specific substrate utilisation rate (h^{-1}) respectively. .

$$\frac{dX}{dt} = \mu X$$

(2-3)

$$\frac{dS}{dt} = kX$$

(2-4)

The dependence of the specific rates, especially μ on the substrate concentration is often described using the well-known equation proposed by Monod as shown in Eq. (2-5), where μ_{max} is the maximum specific growth rate (h^{-1}) and K_S is the half saturation coefficient (mg/l COD). The specific substrate utilization rate, k, can also be described similarly as shown in Eq. (2-6) with the coefficient k_{max} as the maximum substrate utilisation rate (h^{-1}). Graphically, the relationship between μ and S is represented by the curve in Figure 2-2, where μ_{max} is the asymptote of the curve and K_S is the substrate concentration corresponding to one-half of the maximum specific growth rate.

$$\mu = \mu_{max} \frac{S}{K_S + S}$$

(2-5)

$$k = k_{max} \frac{S}{K_S + S}$$

(2-6)

21
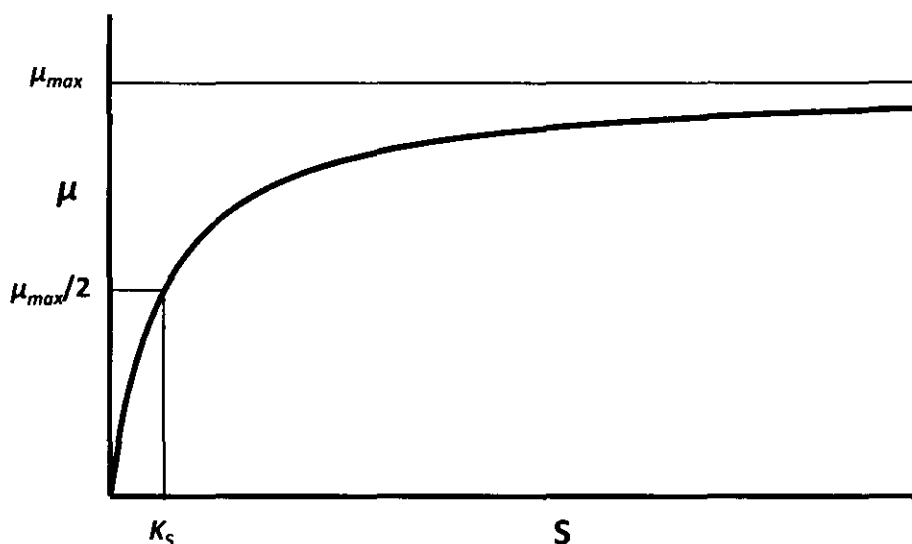
Figure 2-2: Graphical representation of the Monod expression

The Monod expression was first developed to describe pure cultures growing on single substrates. However, in a typical biological treatment system, the substrate is usually a mixture of different organic compounds (although usually treated mathematically as a single aggregate parameter such as COD or BOD) and the biomass invariably consists of a very diverse microbial community. Nonetheless, it has been shown that the Monod equation can be a reasonable model to describe the growth conditions in a wastewater treatment reactor with the provision that the kinetic constants are understood as average values related to the predominant species in the growth conditions being studied (Orhon and Artan 1994).

2.3. Advanced Oxidation Process (AOP)

AOP is a subset of chemical treatment methods in wastewater treatment process. Unlike conventional chemical oxidation methods, which utilize direct reaction between the substrate and a chemical oxidant, AOP can be defined as those processes that aim to achieve water purification by generation of highly reactive ·OH radicals at near ambient temperatures (Glaze, Kang and Chapin 1987). The presence of the unpaired electron in the ·OH radical, make the species a strong electrophile. Therefore, the ·OH radical reacts rapidly with almost all electron-rich organic compounds according to second-order kinetics since the reaction is dependent on both

the target compound concentration and the ·OH radical concentration. Once generated, the radical reactions propagate according to the following reaction mechanisms (Asano, et al. 2007):

Radical addition: When ·OH radical is added to unsaturated organic compounds, an organic radical is generated which could react further to form stable products.

$$R + \cdot OH \rightarrow ROH \qquad (2\text{-}7)$$

Hydrogen abstraction: In this process, a hydrogen atom is removed from the organic compound resulting in the formation of a radical organic compound.

$$R + \cdot OH \rightarrow R\cdot + H_2O \qquad (2\text{-}8)$$

Electron transfer: The transfer of electrons can result in the formation of higher valence ions.

$$R^n + \cdot OH \rightarrow R^{n\text{-}1} + OH^- \qquad (2\text{-}9)$$

Radical combination: Two radicals can combine to form a stable product.

$$\cdot OH + \cdot OH \rightarrow H_2O_2 \qquad (2\text{-}10)$$

There are many ways to generate the ·OH radical, i.e. there are many types of AOPs available. Koprivanac and Kusic (2007) classified AOP's according to the following categories.

1. Chemical and catalytic: These include processes involving the application of ozone, hydrogen peroxide, or homogenous catalyst such as iron or copper. These elements can be used in various combinations to produce hydroxyl radical, for e.g. combination of ferrous catalyst in presence of hydrogen peroxide or Fenton's oxidation and combination of ozone and hydrogen peroxide.

2. Photochemical and photocatalytic: These processes involve application of UV or solar irradiation in combination with oxidants such as ozone and/or hydrogen peroxide or photocatalytic material such as TiO_2 and ZnO.

3. Mechanical and electrical processes: Purely mechanical or electrical energy could be used to generate hydroxyl radicals such as using high-frequency ultrasound to induce cavitation or generation of non-thermal plasma using corona discharge.

Several of these methods have been developed in full-scale for commercial systems, while others are still largely confined to laboratory-scale experimentation. Due to the immense body of literature on each method, only the following shall be reviewed:

1. UV-based processes

2. Ozone-based processes

3. Fenton's oxidation

4. Electrochemical AOPs

2.3.1. UV-based processes

2.3.1.1. UV spectrum

Ultraviolet (UV) light refers to electromagnetic radiation having a wavelength between 100 – 400 nm. The UV region lies between the X-ray region (< 100 nm) and the visible region (400 nm to 700 nm). The UV spectrum is further subdivided into 4 segments; vacuum UV, or V-UV (100 – 200 nm), short-wave UV, or UV-C (200 – 280 nm), middle-wave UV, or UV-B (280 – 315 nm) and long-wave UV, or UV-A (315 – 400 nm) as shown in Figure 2-3.
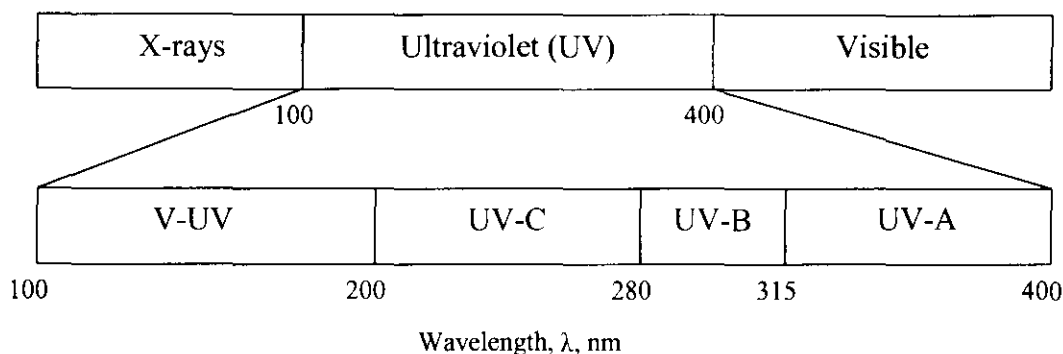
Figure 2-3: The ultraviolet spectrum.

V-UV is absorbed by almost all substances including water, carbon dioxide and oxygen and spectroscopic measurements in this region have to be conducted under vacuum conditions. UV-C radiation is absorbed by many cellular constituents of organisms including DNA, leading to cell mutation and death. This is the basis for UV disinfection, hence this region is also known as the "germicidal region" (Crittenden, Trussell, et al. 2005). All the UV radiation that reaches the surface of the Earth from the sun is in the UV-B and UV-A range; the UV-C and V-UV radiation are efficiently absorbed by the atmosphere (Oppenländer 2003).

2.3.1.2.   Types of UV lamps

In addition to sunlight, UV radiation can be generated by means of UV lamps. Two kinds of lamps are most commonly used in both research and industry, namely the low-pressure (LP) mercury arc lamp and the medium-pressure (MP) mercury arc lamp, both working on the principle of mercury vapor ionization by electrons followed by return to lower energy state.   LP Hg lamps generate almost monochromatic UV radiation and generate a narrow-band emission peak in the UV-C region at λ = 253.7 nm.   The emission spectrum for MP lamps is polychromatic, ranging across the UV-C, UV-B, UV-A, visible and IR regions (Oppenländer 2003).

LP Hg lamps are relatively efficient at converting electrical energy to radiant energy, with electrical efficiency up to 60%, compared to MP Hg lamps (30-40%). However, conventional LP lamps can only be operated at limited electrical input power, typically < 300 W. In comparison, MP lamps can be operated at much higher electrical input power up to 30 kW (Oppenländer 2003). However, the surface temperature of the lamp sleeve in MP lamps can be as high as 900 $^{\circ}$C (Heraeus Noblelight GmbH n.d.), which necessitates the use of open quartz enclosure of the lamp and efficient cooling system in design of reactors. Also, in-situ cleaning mechanisms are necessary to deal with fouling of dissolved solids which precipitate on the quartz sleeve (Lin, Johnston and Blatchley III 1999). High-intensity, low-pressure Hg lamps, known as amalgam lamps, are also available that can produce 10 times the UV power density of conventional, low-intensity LP Hg lamps (Heraeus Noblelight GmbH n.d.).

A relatively new type of UV lamp is the excimer lamp, which does not contain mercury, and is able to produce almost monochromatic emission at either V-UV or UV region depending on the excimer gas or gas mixture applied (Oppenländer 2003). Commercial excimer lamps are available that can be operated with electrical power up to 30 kW (Heraeus Noblelight GmbH n.d.).

2.3.1.3.   Direct UV photolysis

UV-based degradation of pollutants can occur either by direct photolysis, or by generation of oxidizing radicals. In direct photolysis, the target substance absorbs the UV energy and undergoes a chemical change. For this to occur, the absorbance spectrum of the target compound must not only overlap the emission spectrum of the UV source, but the compound must also undergo a chemical change due to the molecular excitation by the UV energy (Linden 2007).

26

2.3.1.4.   UV/H₂O₂

In UV/H$_2$O$_2$ systems, the absorption of UV radiation by H$_2$O$_2$ leads to the formation of ·OH radicals via homolytic cleavage according to Eq. (2-11) with quantum yield of 0.5 (Andreozzi, Caprio and Insola, et al. 1999).

$$H_2O_2 + h\nu \rightarrow 2 \cdot OH \tag{2-11}$$

However, the molar absorption coefficient of H$_2$O$_2$ is low ($\varepsilon_{254\ nm}$ = 18.6 L mol^{-1} cm^{-1}) and as a result, only a small percentage of the incident UV is used for the reaction. In fact, the absorption coefficient of H$_2$O$_2$ is about 200 times less than the coefficient for O$_3$ (Andreozzi, Caprio and Insola, et al. 1999).

Some chemical species in the water matrix may act as inhibitors to the effectiveness of UV/ H$_2$O$_2$ system, either by ·OH radical scavenging or the "inner filter" effect, by absorbing UV radiation in competition to H$_2$O$_2$. Carbonates and bicarbonates are effective ·OH radical scavengers according to Eq. (2-12) and (2-13) with carbonate having a higher reaction rate constant compared to bicarbonate (Oppenländer 2003). In UV/H$_2$O$_2$ degradation of humic acid, Wang et al. (2000) reported that the presence of carbonate and bicarbonate species inhibited the degradation by 70%. Humic acids themselves are often present in some surface waters as natural organic matter (NOM) and are also effective radical scavengers (Wang, Hsieh and Hong 2000). H$_2$O$_2$ itself can act as radical scavenger, according to Eq. (2-14) and at high concentrations can reduce the rate of the desired reaction.

$$HCO_3^- + \ ^{\bullet}OH \rightarrow CO_3^{-\bullet} + H_2O \tag{2-12}$$

$$CO_3^{2-} + \ ^{\bullet}OH \rightarrow CO_3^{-\bullet} + OH^- \tag{2-13}$$

$$^{\bullet}OH + H_2O_2 \rightarrow HOO^{\bullet} + H_2O \tag{2-14}$$

Other organic compounds that are strongly UV-absorbing, including intermediate oxidation products, would compete with H$_2$O$_2$ photolysis, resulting in the "inner filter" effect. At wavelength of 200 nm, nitrate has a very high molar absorption coefficient ($\varepsilon_{200\ nm} \approx$ 10,000 L mol^{-1} cm^{-1}) compared to H$_2$O$_2$ and is an

effective "inner filter", but the molar absorption of nitrate decreases dramatically at 254 nm (Oppenländer 2003). The nitrate content in water can greatly increase the background water absorption and reduce the efficiency of •OH radical formation (Rosenfeldt, et al. 2006). In addition, nitrate photolysis leads to formation of nitrite which is a hydroxyl radical scavenger. A strong nitrite radical scavenger effect was reported for the degradation of diethyl phthalate by UV/ H_2O_2 (Park, et al. 2007).

The UV/ H_2O_2 process is pH dependent. At high pH, H_2O_2 deprotonates to form the hydroperoxide ion HO_2^- in acid-base equilibrium according to Eq. (2-15). The HO_2^- ion has a significantly higher absorption coefficient ($\varepsilon_{254\ nm}$ = 240 L mol^{-1} cm^{-1}) compared to H_2O_2 and is photolysed more effectively into •OH radicals according to Eq. (2-16) (Andreozzi, Caprio and Insola, et al. 1999).

$$H_2O_2 \leftrightarrow HO_2^- + H^+ \tag{2-15}$$

$$HO_2^- + h\nu \rightarrow •OH + O•^- \tag{2-16}$$

However, at neutral to high pH, H_2O_2 itself decomposes according to Eq. (2-17) (Shemer and Linden 2006). In addition, at higher pH, the higher concentration of carbonate ions increases the radical scavenging effect. Thus, there usually exists an optimum pH for the UV/ H_2O_2 process, which would be dependent on the amount of scavenger and oxidant used in the system.

Table 2-2 shows some pH optima values for pollutant degradation using UV/H_2O_2 process.

$$H_2O_2 \rightarrow \frac{1}{2} O_2 + H_2O \tag{2-17}$$

Temperature effects on organic degradation under UV/H_2O_2 process have not received much attention in the scientific literature. Generally, experiments are conducted without temperature control or at ambient temperature. However, for halogenated aliphatics, the rate of degradation has been found to increase with temperature (Sundstrom, et al. 1986).

Table 2-2: Optimum pH values for UV/H$_2$O$_2$ degradation of selected pollutants

Substrate	pH range investigated	Optimum pH	Reference
MTBE	7 and 9	7 (pH-controlled)	(Sutherland, Adams and Kekobad 2004)
Treated wool scouring effluent	3 - 11	No difference across range	(Poole 2004)
Tetrahydrofuran	4 - 11	11 but marginal after pH 7	(Chidambara Raj and Quen 2005)
Azo dye Reactive Red 45	3 - 11	6 (initial pH)	(Peternel, Koprivanac and Kusic 2006)
Phenol	3 - 11	8 (initial pH) based on TOC	(Kusic, Koprivanac and Bozic 2006)
Pulp mill effluent	3 - 11	11 (initial pH) but marginal	(Catalkaya and Kargi 2007)
Polycyclic aromatic hydrocarbons	4 - 10	7 (buffered)	(Shemer and Linden 2006)

2.3.2. Ozone-based processes

Ozone (O$_3$) is an unstable allotrope of oxygen with three oxygen atoms and is a highly oxidizing molecule. It can be used to degrade contaminants in water either by direct oxidation or by generation of secondary oxidizing radicals such as the •OH radical.

2.3.2.1. Generation of ozone

Ozone can be produced by electrical discharge, electrolysis, UV irradiation (λ < 185 nm), ionizing radiation such as x-rays and γ-rays and thermal ionization. Of these methods, only electrical discharge and electrolysis are practical in bench-scale and full-scale applications (Gottschalk, Libra and Saupe 2000).

Electrical discharge ozone generators produce ozone by applying high power alternating current to ionize molecular oxygen. The ionized oxygen atom and unionized molecular oxygen then recombine to form ozone. A large amount of heat is produced and a cooling system is necessary to maintain temperatures below 50°C; the critical value for rapid ozone decay. The feed gas can be either air or pure oxygen.

Although ambient air is cheap and ubiquitous, it requires compression, cooling, filtering and drying and produces lower ozone concentrations compared to pure oxygen feed (Gottschalk, Libra and Saupe 2000).

Electrolytic ozone generators produce dissolved ozone from electrolysis of water. The advantage of this process is that since dissolved ozone is produced, no gas to liquid phase mass transfer is necessary. However, the specific energy consumption is 15 to 20 times the value for electrical discharge generation. In addition, highly purified water is required to prevent damage to the electrodes, limiting the applications to areas where ultrapure water is already being produced or can be produced economically (Gottschalk, Libra and Saupe 2000).

2.3.2.2.   *Low-pH and high-pH ozonation*

Although O_3 is a strong oxidant, its reaction with organic compounds is selective and depends much on the type of functional groups present. In particular, direct ozonation is known to react efficiently with compounds containing amino groups (unprotonated), double bonds, sulfidic groups or activated aromatic compounds. The reactivities of ozone to protonated amines, carboxylic acids, aldehydes and saturated organics in general are negligible (von Gunten 2003). Complete mineralization of organics is usually not possible with direct ozonation reactions, due to the formation of intermediate products with lower O_3 reactivity (Beltran, Garcia-Araya and Alvarez 2001).

Direct O_3 reactions with organics are exclusive only at low pH. At higher pH, hydroxide ions, OH^- catalyze the decay of O_3 leading to the formation of •OH radicals. Therefore, high-pH ozonation can be properly classified as an AOP. The decay of ozone at high pH is described according to the following reaction sequence (Andreozzi, 1999).

$$HO^- + O_3 \rightarrow O_2 + HO_2^- \tag{2-18}$$

$$HO_2^- + O_3 \rightarrow HO_2\bullet + O_3\bullet^- \tag{2-19}$$

$$HO_2\bullet \leftrightarrow H^+ + O_2\bullet^- \qquad\qquad (2\text{-}20)$$

$$O_2\bullet^- + O_3 \rightarrow O_2 + O_3\bullet^- \qquad\qquad (2\text{-}21)$$

$$O_3\bullet^- + H^+ \rightarrow HO_3\bullet \qquad\qquad (2\text{-}22)$$

$$HO_3\bullet \rightarrow HO\bullet + O_2 \qquad\qquad (2\text{-}23)$$

$$HO\bullet + O_3 \rightarrow HO_2\bullet + O_2 \qquad\qquad (2\text{-}24)$$
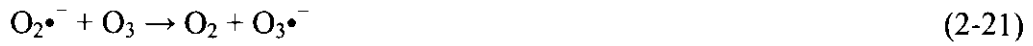
Some examples of substrates that have been successfully treated by high-pH ozonation include phenol (Esplugas, et al. 2002) (Kusic, Koprivanac and Bozic 2006), pulp mill effluent (Bijan and Mohseni 2005), penicillin formulation effluent (Cokgor, et al. 2004) and landfill leachate (Kurniawan, Lo and Chan 2006), although there are various pH optima for different substrates and experimental conditions (e.g. synthetic or natural, buffered or unbuffered wastewater) since at higher pH, the radical reactions tend to be inhibited by higher levels of radical scavengers, especially carbonate ions. However, if the components in the wastewater are already highly reactive to O_3, increasing the pH may not give any apparent benefit as shown by Beltran (1997) for distillery wastewater treatment.

2.3.2.3. O_3/H_2O_2 process

If H_2O_2 is added, the HO_2^- anion, which is an initiator of O_3 degradation to $\bullet$OH radical as shown in Eq. (2-19), can also be generated by acid-base dissociation of H_2O_2 according to Eq. (2-15), enhancing O_3 decomposition and $\bullet$OH radical formation, even at neutral pH. This is the basis of the O_3/H_2O_2 advanced oxidation process. The reaction of O_3 with H_2O_2 itself is negligible (Gottschalk, Libra and Saupe 2000).

Increasing the pH will lead to higher radical formation due to increased H_2O_2 dissociation, but at higher pH, scavenging effect of the carbonate anion increases. The optimum pH of the O_3/H_2O_2 process varies with the substance to be treated as shown in Table 2-3.

Table 2-3: Optimum pH values for O₃/H₂O₂ process to degrade selected pollutants

Substrate	pH range investigated	Optimum pH	Reference
1,4-dioxane	5 - 11	9 (initial pH) constant with further increase	(Suh and Mohseni 2004)
MTBE	7 and 9	7 (pH controlled)	(Sutherland, Adams and Kekobad 2004)
Phenol	3-12	11 (initial pH)	(Kusic, Koprivanac and Bozic 2006)
Phenol	5.7 - 9.4	6.8 (buffered)	(Esplugas, et al. 2002)
Pulp mill effluent	3-11	11 (initial pH)	(Catalkaya and Kargi 2007)

Also, since H_2O_2 itself is a radical scavenger, many investigators reported the existence of H_2O_2 optima beyond which the reaction is inhibited (Suh & Mohseni, 2004, Kusic et al.,2006, Tizaoui et al., 2007 & Kurniawan et al., 2006).

2.3.2.4. O₃/UV process

O_3 is photolyzed by UV irradiation to produce H_2O_2 and O_2 with a relatively strong molar extinction coefficient of 3,300 L mol^{-1} cm^{-1} at 254 nm (Gottschalk, Libra and Saupe 2000).

In O_3/UV process, up to 3 initiation steps are possible to produce •OH radicals, which include the reaction of O_3 with hydroxide ion as per Eq. (2-18), reaction of O_3 with hydroperoxide ion as per Eq. (2-19) and photolysis of H_2O_2 as per Eq. (2-11). In addition, direct reaction of ozone with organics may also occur (Beltran, Encinar and Gonzalez 1997). The process can be further enhanced by supplemental addition of H_2O_2, although the initiation reactions involved remain the same. The O_3/UV process is also less dependent on pH for efficient radical oxidation because of the various radical initiation routes. For example, Wenzel et al. (1999) investigated the degradation of leachate using a thin-film reactor and was forced to conduct the experiments at low pH to prevent foaming. However, the O_3/UV process, not solely dependent on the H_2O_2 dissociation to HO_2^- for radical initiation, which is negligible at low pH, proved to be more efficient at TOC removal compared to

UV/H_2O_2. Similar results were obtained by Andreozzi et al. (2000) in treating mineral-oil contaminated wastewater at pH of 5.

2.3.3. Fenton's oxidation

Conventional or classical Fenton's oxidation is characterized by ·OH formation by the well-known Fenton's reaction in which ferrous ions, Fe^{2+} catalytically hydrolyses H_2O_2 according to Eq. (2-25). The mixture of ferrous ion and hydrogen peroxide is called Fenton's reagent and is well known as a powerful oxidant for degradation of organic compounds (Crittenden, Trussell, et al. 2005).

$$Fe^{2+} + H_2O_2 + H^+ \rightarrow Fe^{3+} + H_2O + \cdot OH \quad (2-25)$$

Because the Fe^{3+} (in the form of the dominant Fe^{3+}-hydroxo complex) which is formed in the reaction above can be regenerated back to Fe^{2+} (according to Eq. (2-26) to (2-28)), Fenton's oxidation can be considered as an iron-catalyzed reaction. Nonetheless, the rate of the ferric reduction reactions are relatively slow compared to the oxidation of ferrous ions from Eq. (2-25) which leads to the accumulation of ferric ions which readily precipitate at acidic conditions (pH 3 – 7) and lead to generation of ferric hydroxide sludge (Ikehata and Gamal El-Din 2006).

$$Fe^{3+} + H_2O_2 \rightarrow Fe^{2+} + HO_2 \cdot + H^+ \quad (2-26)$$

$$Fe^{3+} + HO_2 \cdot \rightarrow Fe^{2+} + O_2 + H^+ \quad (2-27)$$

$$Fe^{3+} + R \cdot \rightarrow Fe^{2+} + R^+ \quad (2-28)$$

The reaction outlined in Eq. (2-25) is rate limiting and also the chain initiation step of the Fenton reaction. A proton is required to initiate the reaction; hence Fenton's oxidation is generally conducted under acidic conditions. Studies by Oliveros, et al. (1997), Farrokhi, et al. (2003) and Tekin, et al. (2006) have indicated that pH of about 3 is usually suitable for Fenton's oxidation. At even lower pH (< 2), the reaction rate is decreased due to the formation of complex iron species and formation of the oxonium ion $[H_3O_2]^+$, which reduces the degradation efficiency. On

the other hand, at higher pH (> 4), the rate of generation of hydroxyl radical becomes slower due to the formation of ferric-hydroxo complexes, causing a decrease in the free iron species in solution, which inhibits the regeneration of Fe^{2+} (Tekin, et al. 2006).

Fenton's oxidation is especially advantageous in cases where the wastewater contains high concentration of organics since the reaction rate is very high compared to other AOPs (Martinez, et al. 2003). However, the dependence of the reaction on the solution pH, the consumption of ferrous ions and also generation of sludge at the end of the reaction are disadvantages for classical Fenton's oxidation processes.

2.3.3.1.   *Photo-Fenton process*

Researchers have found that applying UV/VIS radiation to the Fenton's reagent results in the photoreduction of the ferric ions or ferric complexes, thus increasing the rate of Fe^{2+} regeneration and preventing its depletion. The dominant Fe^{3+}-hydroxo complex absorbs UV/VIS radiation in the wavelength range below 400 nm, but with a relatively low quantum yield of 0.14. However, the quantum yield of the photoproduction of Fe^{2+} can be significantly increased by the addition of oxalate ions which produces ferrioxalate ions, which is highly photosensitive with a quantum yield of 0.86 at approximately 500 nm and even greater at lower wavelengths (Oppenländer 2003). The ferrioxalate-based photo-Fenton process also has a wider available pH range although depending on the concentration of H_2O_2 added to the system, there is either a positive or negative dependence of the ·OH radical production on the solution pH (Jeong and Yoon 2005).

2.3.4. Electrochemical Advanced Oxidation

Electrochemical advanced oxidation (EAOP) is a subset of the general term electrooxidation, in which oxidation of substances (e.g. organic pollutants) is achieved via electrochemical processes which may or may not involve hydroxyl radicals. Although electrooxidation has been studied since the 19th century, EAOPs

34

have only been extensively investigated since early 1990s (Chen 2004). Similar to other electrochemical processes, EAOP systems comprise of electronic conductors i.e. electrodes (anode and cathode) placed in an ionic conductor i.e. electrolyte and an external voltage is applied to induce chemical reactions in the electrolyte and at the electrolyte-electrode interface.

Electrooxidation (including EAOP) can be broadly classified into indirect or direct oxidation (Grimm, Bessarabov and Sanderson 1998). Indirect electrooxidation processes achieve pollutant destruction via electrochemical generation of intermediates; i.e. substances that either promote oxidation or act as oxidizing agents themselves. Examples of indirect electrooxidation include: anodic generation of chlorine or hypochlorite, cathodic generation of hydrogen peroxide from oxygen, electro-fenton (EF) process (electrically-assisted Fenton's oxidation) and mediated electrooxidation (generation of high valence state metal ions) (Chen 2004). Most of the techniques involved in indirect electrooxidation processes do not generate hydroxyl radicals and are therefore not defined as AOP. Among the various indirect oxidation processes, only the EF process shall be reviewed here.

Direct electrooxidation, also commonly known as direct anodic oxidation, is a process where the pollutant is directly oxidized at the anode surface (Chen 2004). Direct anodic oxidation does not suffer from some of the limitations that are pertinent to indirect oxidation processes, such as generation of secondary pollutants (e.g. chlorinated organics, heavy metals), supplementary feeding of oxygen and limited efficiency window (highly acidic, high chloride).

2.3.4.1.   Electrofenton (indirect electrooxidation)

In electrofenton (EF) process, electrical current is used to assist Fenton's oxidation. Depending on the objective of the supplying the electrical current, EF processes can be divided into several groups as follows:

1. Electro-regeneration of Fe^{2+}

2. Electro-generation of H_2O_2

3. Electro-generation of Fe^{2+} via sacrificial anode

4. Simultaneous electro-generation of H_2O_2 and Fe^{2+}

In conventional Fenton's oxidation, it is necessary to supply a large amount of Fe^{2+} (usually in the form of hydrated ferrous sulfate solution) to ensure adequate production of hydroxyl radicals for efficient contaminant degradation. This would also lead to the production of large amounts of ferric hydroxide sludge during the subsequent neutralization stage, which would require additional separation (Zhang, Zhang and Zhou 2006).

To reduce the amount of ferric sludge, Fe^{2+} can be regenerated electrochemically at the cathode according to Eq. (2-29), while H_2O_2 can be externally supplied to complete the Fenton's reagent system. The process is commonly known as EF-FeRe (i.e. ElectroFenton - Ferric Reduction).

$$Fe^{3+} + e^- \rightarrow Fe^{2+} \qquad (2\text{-}29)$$

Electrical current can also be used to generate H_2O_2 electrochemically by reducing dissolved molecular oxygen (obtained by bubbling air or oxygen) at the cathode according to Eq. (2-30). Fe^{2+} is usually externally supplied under acidic conditions, but Fe^{2+} will also be regenerated at the cathode simultaneously. The process is commonly termed as EF-H_2O_2-FeRe. EF-H_2O_2-FeRe systems are essentially similar to EF-FeRe systems with exception of introduction of oxygen or air at the cathode.

$$O_2 + 2H^+ + 2e^- \rightarrow H_2O_2 \qquad (2\text{-}30)$$

A sacrificial iron anode can also be used to generate Fe^{2+} according to Eq. (2-31). H_2O_2 is externally supplied to complete the Fenton's reagent system. This process is commonly known as EF-FeOx (Electro Fenton – Fe Oxidation). EF-FeOx set-ups are relatively simple, requiring only cast iron electrodes in undivided electrolytic cells.

$$Fe \rightarrow Fe^{2+} + 2e^- \qquad (2\text{-}31)$$

Another variation is the EF-H_2O_2-FeOx process, where electro-generation of H_2O_2 is coupled with electro-generation of Fe^{2+} from a sacrificial anode. There are limited number of studies that utilize this process. However, using a simple undivided electrolytic cell with hollow cylindrical iron anode and graphite cathode, Moreno et al. has demonstrated the feasibility of using this method to treat municipal wastewater for reclamation (Moreno 2004).

In addition to the electrofenton processes mentioned above, many researchers have also studied the effect of combining photochemical processes with electrofenton to enhance degradation of pollutants. Typically, photo-electrofenton (photo-EF) combines UV irradiation with electrogeneration of H_2O_2. The mechanism governing photo-EF reactions is the same as in photofenton in that ferric ions (in the form of the dominant Fe^{3+}-hydroxo complex) can be photoreduced by UV radiation at wavelengths below 400 nm according to Eq. (2-32), thus enhancing the regeneration of ferrous ions. Hence, the process is able to increase production of hydroxyl radicals.

$$Fe(OH)^{2+} + hv \rightarrow Fe^{2+} + \cdot OH \tag{2-32}$$

Ferric complexes with organic byproducts such as oxalic and oxamic acids also undergoes photodecomposition with UV irradiation, preventing accumulation of these stable complexes and further enhancing the treatment efficiency (Boye, Brillas and Dieng 2003).

2.3.4.2. *Anodic electrooxidation*

Direct anodic oxidation involves the oxidation of compounds on the surface of the anode itself. The anode is normally a base metal coated with a metallic oxide and the oxidation of water on the active sites available on the anode surface produces adsorbed hydroxyl radicals according to Eq. (2-33) (Brillas, Calpe and Casado 2000). A competing reaction is electrolysis of water at the anode leading to oxygen evolution, so anodes with high overpotentials for O_2 evolution are required.

37

$$H_2O \rightarrow OH\cdot_{ads} + H^+ + e^- \qquad\qquad (2\text{-}33)$$

Typically, anodes such as Pt, PbO_2, doped SnO_2 and IrO_2 are used. However, since the reaction occurs on the anode surface, the low concentration of adsorbed hydroxyl ions that can be achieved with these anode materials limit the efficiency of this method especially for complete mineralization of pollutants (Brillas, Calpe and Casado 2000).

Recently, boron-doped diamond (BDD) thin film anodes, which have much higher oxygen overvoltages compared to conventional anode materials, have shown to be more effective. The presence of inorganic salts such as chlorides significantly increases the mineralization efficiency by producing secondary oxidizing agents such as hypochlorites (Canizares, et al. 2006). BDD anodes also have a greater ability compared to conventional anodes to degrade the stable Fe^{3+}-oxalate complex generated as a by-product of aromatic degradation, which is particularly difficult to degrade in Fenton's (and EF) oxidation (Sires, et al. 2007). Another advantage of BDD over conventional anodes is the exceptional stability and resistance to deterioration (Wright, et al. 2003).

2.4. Taguchi Method of Statistical Design of Experiments

In design of experiments (DOE), statistical methods are used to systematically plan a set of experiments to determine cause-and-effect relationship. The purpose of DOE is to enable the collection of the maximum amount of information from a set of experiments using the minimum amount of time and resources. In the traditional (or classical) approach in empirical research, investigation into each factor is conducted by varying the factor while keeping all other factors constant. There are a number of disadvantages to this approach. Firstly, the total number of trials or experiments to completely test all the factor-level combinations is very large as the number of factors and levels increase. For example, to completely test five factors, each varied at four levels, will require a total of $4^5 = 1024$ experiments. In practice, the number of experiments is much reduced by neglecting all the interaction experiments. However, this approach will likely lead to overestimation of the effect of the referential trial. In

addition, to obtain the experimental error, trials have to be repeated without yielding any additional information other than the experimental error. Using DOE, these deficiencies can be eliminated by using statistical methods to achieve more precise and complete information using much fewer experimental trials and repetition (Lazic 2004).

DOE was first introduced by Sir R. A. Fisher in England in the 1920s in the Rothamsted Agricultural Field Research Station, where he developed a statistical method to determine the effect of various fertilizers on different plots of land. Using the method, he could differentiate between the effect of fertilizer and the effect of other factors to the final condition of the crop. Since then DOE has been widely accepted and applied in many fields especially in the manufacturing industries in the last two decades (Antony 2003).

Originally, Sir Fisher studied the effects of multiple factors simultaneously using full factorial analysis. Although a vast improvement over the classical approach to empirical research, full factorial analysis takes into account all of the possible combinations of factors and leads to very large number of experiments. Fractional factorial was later developed by Frank Yates and Oscar Kempthorne to find a smaller set of factorial experiments. However, in the 1940s, Dr Genechi Taguchi of Japan developed the Taguchi approach to DOE by proposing a special set of orthogonal arrays that standardized fractional factorial designs. Some of the advantages of the Taguchi approach include the reduction of rework costs, scrap work and manufacturing costs; as a result, the Taguchi approach is now used extensively in industry and scientific research (Roy 2001).

CHAPTER 3

EXPERIMENTAL

3.1. Materials

3.1.1. Chemical reagents

The chemicals used in the present experiments are listed in Table 3-1.

Table 3-1: List of chemicals used

Chemical	Supplier	MW (g/mol)	T_m (°C)	T_b (°C)	ρ (g·cm^{-3})
Monoethanolamine, MEA (99.8%)	Merck	61.08	10	170	1.02
Hydrogen peroxide solution, H_2O_2 (30% w/v)	R&M Chemicals	34	-25	108	1.11
Potassium permanganate, $KMnO_4$	Merck	158.03	240	N/A	2.7
Sulfuric acid, H_2SO_4 (98%)	Systerm	98.08	-15	330	1.84
Sodium hydroxide solution, NaOH (1 M)	R&M Chemicals	40	~0	~100	1.02-1.05
Potassium dihydrogen phosphate (KH_2PO_4)	HmbG Chemicals	136.09	253	400	2.34

40

3.1.2. Biomass inoculums

The biomass inoculum was obtained from the recycled activated sludge (RAS) line from an activated sludge sewage treatment plant in Universiti Teknologi PETRONAS (Malaysia) using a sludge trapper. The sludge was then brought to the lab and aerated for 1 day and the mixed liquor suspended solids (MLSS) of the sludge was determined. Then, the sludge was added to the bioreactors in addition to the mineral medium and substrate solution to achieve initial biomass concentration of approximately 100 mg/L MLSS in the bioreactor.

3.1.3. Mineral medium

To ensure biomass growth, a mineral medium was prepared according to specifications in the Zahn-Wellens/EMPA Test in the US Environmental Protection Agency (EPA) method OPPTS 835.3200 (US EPA 1998). The mineral medium was prepared in four separate stocks, i.e. stock A, stock B, stock C and stock D.

Stock A was prepared by dissolving the components listed below in 1 liter aqueous solution. The pH of the solution was adjusted to 7.4.

1. KH_2PO_4 (8.5 g)

2. K_2HPO_4 (21.75 g)

3. Na_2HPO_4, $2H_2O$ (33.4 g)

4. NH_4Cl (0.5 g)

The composition of stock B, C and D are as follows:

B: 1 liter contains 36.4 g $CaCl_2$, $2H_2O$

C: 1 liter contains 22.5 g $MgSO_4$, $7H_2O$

D: 1 liter contains 0.15 g $FeCl_3$ anhydrous

A fresh mineral medium was prepared by mixing of 10 ml stock A and 1 ml each stock B, C and D per liter solution and was prepared fresh before each biological oxidation experiment.

3.2. Photoreactor

Two sizes of photoreactors were used in the experiments as shown in Figure 3-1. The first reactor is a cylindrical, jacketed glass photoreactor, with a working volume of 1.1 L that can be fitted with up to 3 low-pressure, mercury vapor UV lamps with input power rating of 4 W each. The lamps are placed in 1-inch diameter closed-end quartz tubes. The second reactor is a smaller cylindrical, jacketed glass photoreactor, with a working volume of 390 mL and fitted with a low-pressure, mercury vapor UV lamp with nominal power rating of 8 W placed inside a quartz tube. The incident photon flux of the system was varied between 0.67, 1.52, 2.44 and 4.13 W, as measured by hydrogen peroxide actinometry (outlined in Section 3.5), depending on the reactor size and number and type of lamps used. The outside of the reactor was covered with reflective aluminium foil to minimize UV exposure to researchers during the experiments. A mercury thermometer was inserted in the reactor to monitor solution temperature. The temperature was controlled by a recirculating water bath.

In the experiment, approximately 800 mg/L solution of MEA was poured into the reactor. For some of the experiments, potassium dihydrogen phosphate was added to the reactor at low concentration of 8 mM or high concentration of 240 mM. The initial solution pH was adjusted accordingly by adding sulfuric acid or sodium hydroxide. H_2O_2 at 30 % w/v was then added to achieve the required concentration based on the stoichiometric amount for complete mineralization of MEA. The UV lamp was then switched on and the reaction was allowed to proceed for 60 mins. Depending on the run, sample aliquots were taken periodically to determine the COD, H_2O_2, MEA and other chemical species at various times during the course of the reaction. In several of the experimental runs, sample aliquots were also taken temporarily for pH measurement but these samples were then immediately returned into the reactor after measurement.

42
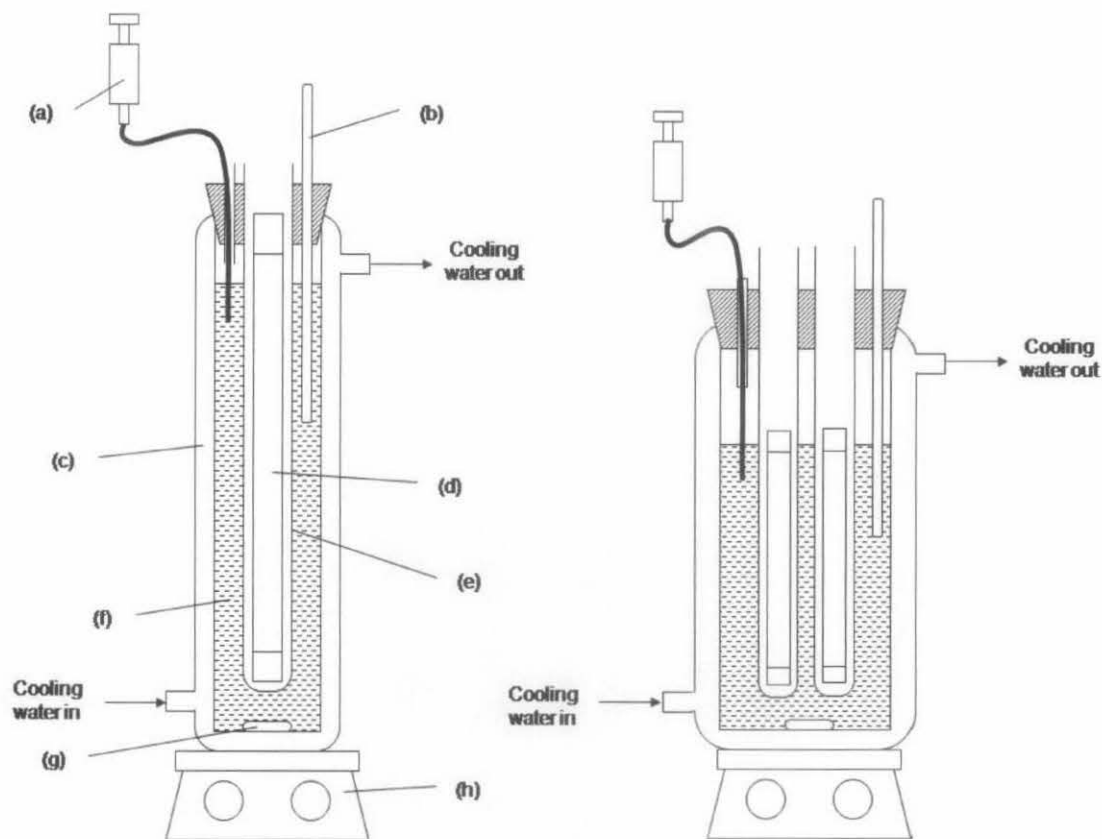
Figure 3-1: Photoreactors used in the study showing (a) sampling syringe, (b) mercury thermometer, (c) glass cooling jacket, (d) UV lamp, (e) closed ended quartz tube, (f) irradiated solution, (g) stir bar and (h) magnetic hotplate stirrer

3.3. Aerobic bioreactor

Biological oxidation experiments were conducted using a programmable bioreactor, model Biosys 7L X 6 Plus, from Biosys (Figure 3-2), which can accommodate a maximum of 6 reactors operating simultaneously. In the experiments, the pH and temperature were kept constant by the equipment using programmable logic control (PLC). The pH was adjusted by automatic dosing of sulfuric acid (1M) or sodium hydroxide (1M). Temperature was automatically controlled by heating jackets and cooling coils. Perforated coils provide aeration from compressed air supply to all the reactors at constant, but manually adjustable flowrate. To provide the required trace mineral nutrients, mineral medium solution was added (as described in Section 3.1.3) in each reactor. The bacterial sludge seed was obtained from the waste activated

sludge (WAS) from the UTP sewage plant. The experimental conditions for all the reactors were as follows:

1. Reactor volume: 2 L

2. Temperature: 30 deg. C

3. pH: 7.5

4. Air flowrate: 6 l/min
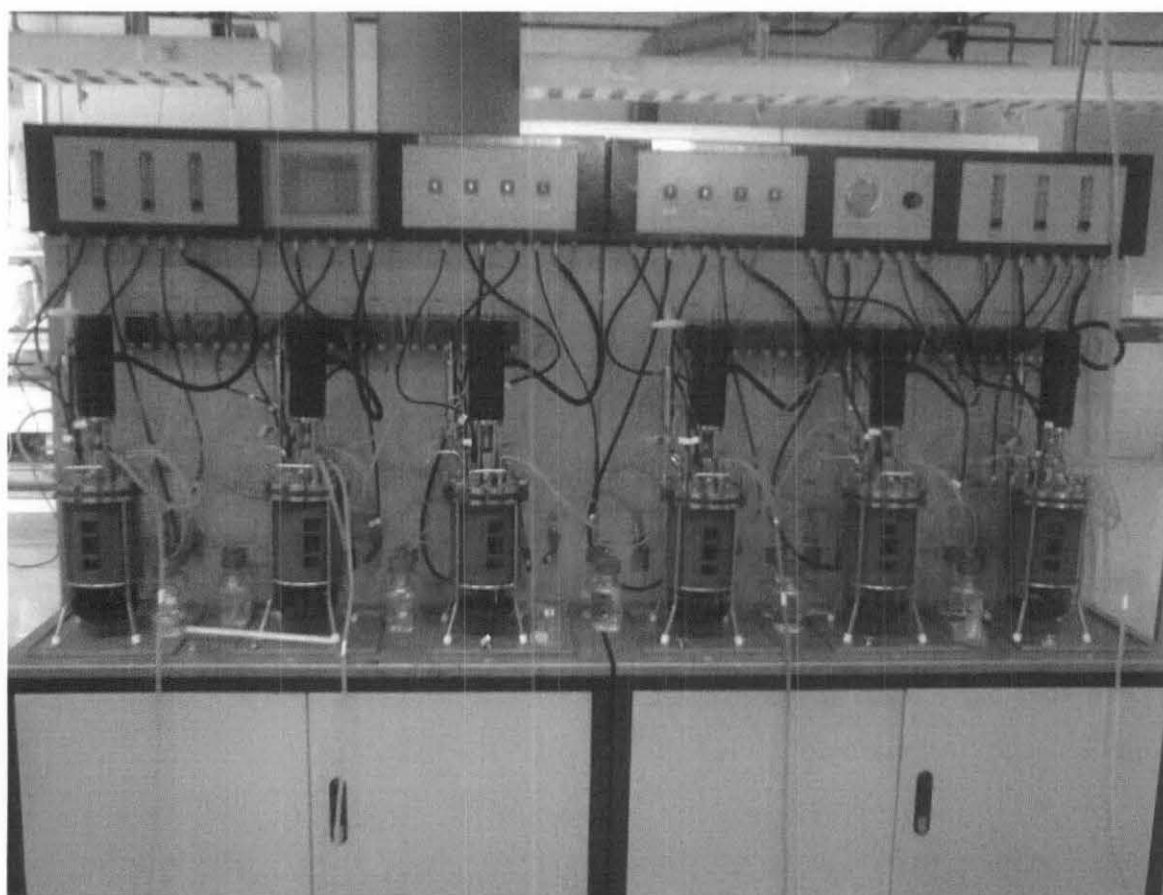
Figure 3-2: Programmable bioreactor used for biodegradation experiments

Table 3-2 shows the volumes of each component added in the aerobic bioreactor for the biodegradability experiments.

Table 3-2: Volumes of component mixtures (mL)

	MEA*	Pretreated MEA**	Blank
Substrate	220	330	-
Mineral medium	1450	1450	1450
Bacterial seed	80	80	80
Distilled H$_2$O makeup	250	140	470

Note:

* MEA concentration = 6750 mg/l, COD = 9000 mg/l

** Pretreated MEA COD = 6080 mg/l. Residual H$_2$O$_2$ was removed from the pretreated MEA by raising the pH and mild heating for 5 hours. The residual H$_2$O$_2$ was confirmed to be completely removed by analysis using HACH H$_2$O$_2$ test kit.

3.4. Analytical methods

3.4.1. Chemical Oxygen Demand

Chemical oxygen demand (COD) is a measure of the total oxidizable organic content in the water sample and is defined as mg of O$_2$ consumed per liter of sample under the conditions of the analytical test method. In this work, COD was determined using the dichromate reactor digestion method (Hach Company Method 8000) using high-range COD reagent vials (for 20 – 1500 mg/L COD), a block heating reactor and a spectrophotometer. The method is approved by USEPA for NPDES compliance monitoring (Hach Company 1999) and is similar in principle to the APHA 5220 A Standard Methods (Clescerl, Greenberg and Eaton 1999).

Since residual H$_2$O$_2$ interferes with COD analysis, the residual H$_2$O$_2$ was removed by raising the pH of the sample with sodium hydroxide and heating the sample in a boiling water bath for 20 minutes.

45

3.4.2. pH

The solution pH was measured using Hach SensION1 portable pH meter. Calibration of the pH meter was conducted weekly or before starting experiments after an extended idle period.

3.4.3. NH_3

Dissolved ammonia (NH_3) was measured using Hach ammonia ion-selective electrode (ISE) connected to Hach SensION 4 Benchtop pH/ISE meter. Calibration of the meter was conducted weekly.

3.4.4. Residual H_2O_2

Determination of the residual H_2O_2 in the solution was performed by titration of the sample with $KMnO_4$ solution (0.05 M). The sample is initially acidified by adding some H_2SO_4 solution (1 M) and then titrated until the end point which is indicated by the appearance of the first persistent light pink colour. To standardize the stock $KMnO_4$ solution used to prepare the titrant, sodium thiosulphate (NaS_2O_3) iodometry was conducted using 1% starch solution as an indicator (Mendham, et al. 2000).

For determination of low-level residual H_2O_2, a test kit for H_2O_2 analysis (Hach model HYP-1) was used. In test method, the sample is acidified and the reaction is catalyzed by the addition of the ammonium molybdate solution. Iodide and starch are then added (Sulfite 1 reagent). Iodide reduces the hydrogen peroxide resulting in the formation of water and free iodine. Titration of iodine to a colorless end point using sodium thiosulfate is then conducted. The added starch enhances the determination of the end point by producing a color change from dark blue to colorless. The amount of hydrogen peroxide in the sample is then calculated from the quantity of the sodium thiosulfate titrant used.

3.4.5. Monoethanolamine using high performance liquid chromatography (HPLC)

MEA was analysed using high-performance liquid chromatograph (Agilent) equipped with YMC-Pack PolymerC18 column using 100 mM Na_2HPO_4/100 mM NaOH (60/40, pH 12) as eluent and UV-Vis detector (215 nm and 253nm) at flow rate of 1 ml/minute. Quantitative analysis of MEA was based on calibration curve obtained using prepared standard solutions of MEA of various known concentrations.

3.4.6. Organic and inorganic anions using ion chromatography (IC)

Organic and inorganic acids were measured using Metrohm 761 Compact IC ion chromatograph using suppressed anion method and MetroSep A Supp 5 – 150 anion column. The eluent used composed of 3.2 mM Na_2CO_3/ 1.0 mM $NaHCO_3$ at a flowrate of 0.70 mL/min at 20 °C and 6.8 MPa. Quantitation of the anions was based on calibration curves obtained using standard solutions of the anions at various known concentrations.

3.4.7. Mixed liquor suspended solids (MLSS)

MLSS was measured using a Hach turbidimeter based on this calibration curve prepared using the seed sludge: [MLSS] = 1.0001·Turbidity (NTU), with coefficient of correlation R^2 = 0.995. To prepare the calibration curve, the total suspended solids content of the seed sludge was measured by filtration through standard 0.45 μm glass-fibre membrane and drying the residue to constant weight at 103-105 °C in accordance with APHA 2540 D in the Standard Methods (Clescerl, Greenberg and Eaton 1999).

3.4.8. Turbidity

Turbidity was measured using the Model 2100P Hach Portable Turbidimeter. The instrument measures light scattered at 90° from incident source and displays the results in Nephelometric Turbidity Units (NTU).

3.5. UV fluence using hydrogen peroxide actinometry

Calculation of the UV fluence, or photonic flux of the lamp and reactor system was conducted in accordance with Nicole et al. (1990). For monochromatic radiation source and no wall reflection, the rate of photolysis of H_2O_2 is given by the general kinetic equation (3-1).

$$-\frac{d[H_2O_2]}{dt} = \Phi_{H_2O_2} I_0 (1 - e^{-2.3D}) \qquad (3\text{-}1)$$

where $\Phi_{H_2O_2}$ is the primary quantum yield of hydrogen peroxide photolysis, I_0 is the volumetric UV photonic flux and D is the optical density of the solution. At high total absorbance, equation (1) reduces to equation (3-2), in which the consumption of photolyte is zero-order.

$$-\frac{d[H_2O_2]}{dt} = \Phi_{H_2O_2} I_0 \qquad (3\text{-}2)$$

Since $\Phi_{H_2O_2}$ is well-known to be unity, the rate of H_2O_2 photolysis can be further simplified to equation (3-3). Therefore, I_0 can be determined by the slope of H_2O_2 photolysis in the reactor-lamp system.

$$-\frac{d[H_2O_2]}{dt} = I_0 \qquad (3\text{-}3)$$

In the actinometry measurements, 4 mL of stock H_2O_2 solution (approximately 30% w/v) was added to the photoreactor and diluted with 386 mL of distilled water. Approximately 8 mM of potassium dihydrogen phosphate was added as a pH buffer. The UV source was activated and the concentration profile of H_2O_2 with time was determined. It was found that the H_2O_2 decay was zero-order and therefore I_0 can be

determined from the slope of the H_2O_2 decay. The results of the actinometry measurements for the different photoreactor sizes and number of UV lamps are provided in Appendix A.

3.6. Statistical design of experiment

The L-16 (4^5) modified orthogonal array was used which can accommodate a maximum of five factors at four levels with a total of 16 experimental runs. For this study, only four factors with four levels were selected as shown in Table 3-3. One column of the orthogonal array was left unused to enable enough degrees of freedom for quantitative determination of the error term in analysis of variance (ANOVA) calculations. Since chemical oxygen demand (COD) gives a practical estimate of the presence of organics in wastewater, we used this parameter as a measure of the degree of degradation of the substrate (MEA). The response of the experiments was given by the fractional COD reduction calculated from the COD after 60 minutes of reaction compared to the initial COD. The quality characteristic for the response is determined to be *bigger-the-better*.

Table 3-3: Factors and levels used in the experiment

Factors		Levels 1	2	3	4
A	UV dose (W/L)	3.6	7.3	12.0	26.7
B	Temperature (°C)	20	25	30	35
C	H_2O_2 dose (x stoichiometric)	0.50	0.75	1.00	1.25
D	pH	2	3	4	5

CHAPTER 4

RESULTS AND DISCUSSION

4.1. Overall Effects of Various Parameters on Gross Organic Destruction Using Taguchi Method of Experimental Design

4.1.1. Main effects

The design orthogonal array used in this study and the experimental results are presented in Table 4-1. Figure 4-1 shows the main effects plots for the results obtained in the study. The main effects plot provides a quick graphical representation of the average effect of each factor to the response. From the main effects plots, it is clear that the UV dose has the highest effect on the COD reduction compared to other factors studied, as indicated by the large slope of the plot for UV dose. As expected, the COD reduction increased significantly as the UV dose is increased. Surprisingly, temperature and H_2O_2 dose do not seem to have any appreciable effect on the COD reduction as would have been expected. The main effects plots also indicate that on average, reducing the pH from 5 to 2 increases the COD reduction to a small extent.

Table 4-1: Experimental design array (based on modified L-16 array) with results of the study.

Run	A	B	C	D	Column unused	Fractional COD removal
1	1	1	1	1	-	0.168
2	1	2	2	2	-	0.124
3	1	3	3	3	-	0.164
4	1	4	4	4	-	0.150
5	2	1	2	3	-	0.304
6	2	2	1	4	-	0.292
7	2	3	4	1	-	0.290
8	2	4	3	2	-	0.294
9	3	1	3	4	-	0.300
10	3	2	4	3	-	0.366
11	3	3	1	2	-	0.420
12	3	4	2	1	-	0.428
13	4	1	4	2	-	0.693
14	4	2	3	1	-	0.738
15	4	3	2	4	-	0.618
16	4	4	1	3	-	0.558
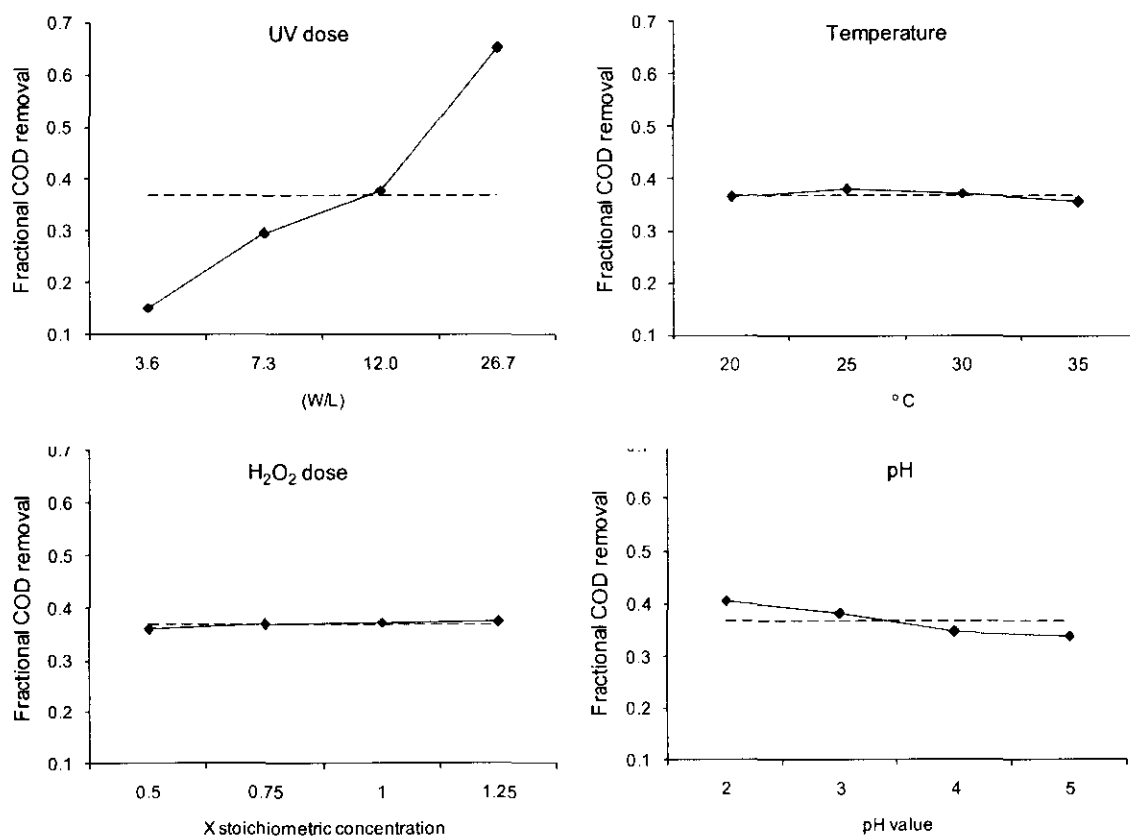
Figure 4-1: Main effects plot for the factors involved in the study

The average effects of factors, the ranking of the factors based on the factor contribution to the response and the optimum conditions for each factor is shown in Table 4-2. At the optimum conditions, the mean optimum response can be determined by adding the contribution (to the response) of each factor at its optimum condition to the grand average of the response. Based on this, the predicted COD reduction at the optimum condition is 0.705. The confidence interval for the predicted response can be calculated upon conducting the analysis of variance.

Table 4-2: Average response table showing optimum levels, factor contributions and rank.

Level	UV dose	Temperature	H_2O_2 dose	pH
1	0.152	0.366	0.360	0.406
2	0.295	0.380	0.369	0.383
3	0.379	0.373	0.374	0.348
4	0.652	0.358	0.375	0.340
Average	0.369	0.369	0.369	0.369
Optimum	4	2	4	1
Contribution	0.282	0.011	0.006	0.037
Rank	1	3	4	2

4.1.2. Analysis of variance (ANOVA)

Analysis of variance (ANOVA) results are shown in Table 4-3. The last column of the ANOVA table shows the relative percentage influence of each factor. The results clearly indicate that, at more than 91% relative percentage influence the UV dose has by far the greatest effect on the response compared to any other factors. The results also show that the effect of experimental errors, factors not included and uncontrollable factors, which comprise the error term, occupy the rest of the effect to the response at almost 9%. The relative influence of other factors including pH is negligible compared to UV dose and the error term.

The confidence interval (C.I.) at the optimum conditions can be calculated based on the required confidence level, the variance of the error term and the degree of freedom values (Roy 2001). At 90% confidence level, the C.I. is computed to be ± 0.13. This means that the optimum response of fractional COD reduction is given by 0.705 ± 0.13 with 90% confidence level.

52

Table 4-3: Analysis of variance results for the study.

Factor	DOF (f)	Sum of Sqrs (S)	Variance (V)	F Ratio (F)	Pure Sum (S')	Percent P (%)
UV dose	3	0.5309	0.1770	29.886	0.513	91.36
Temperature	3	0.0011	0.0004	0.062	0.000	0.00
H_2O_2 dose	3	0.0006	0.0002	0.033	0.000	0.00
pH	3	0.0113	0.0038	0.637	0.000	0.00
Other/Error	3	0.0178	0.0059			8.64
Total	15	0.5617				100.00

4.1.3. Confirmation results

A confirmation experiment was then conducted at the optimum conditions. At 60 minutes, the fractional COD reduction for the confirmation experiment is equal to 0.636, which is within the range of the predicted optimum response of 0.705 ± 0.13. This result confirms that the Taguchi analysis conducted in this study was sound and can provide a reasonably accurate prediction of the optimum response as well as a good measurement of the effects of the factors studied.

4.1.4. Conclusions

The effect of each factor and optimum conditions for degradation of MEA in UV/ H_2O_2 system has been determined. The response at optimum conditions has been verified by a confirmation experiment. It has been shown that the main and controlling factor at the experimental conditions is the UV dose. The results do not indicate that optimum UV dose has been reached and increasing the UV dose should increase the COD reduction further. This can be achieved using different reactor geometry, the use of high output amalgam lamps, or medium pressure UV lamps. Degradation of higher concentrations of MEA would necessitate higher output lamps to be able to achieve appreciable COD reduction in short residence times.

Because other factors such as H_2O_2 dose, pH and temperature seem to have very minimal impact, those factors could be set at a more cost-effective level and still achieve appreciable COD reduction, especially if the process is scaled-up. For

example, a scaled-up process could be run at lower H_2O_2 dosing, minimal pH adjustment and minimal cooling to minimize the chemical and energy cost but still achieve good COD reduction.

4.2. Detailed effects of various parameters on substrate kinetics, gross organic degradation, oxidant decay and breakdown product identification

4.2.1. Effect of initial pH

Experiments were conducted at various initial pH values and the pH change was monitored as the reaction proceeds. As it was found that the pH of the sample dropped considerably without addition of pH buffer, a small amount of buffer (8 mM of KH_2PO_4) was used initially. The temperature of the solution was maintained at approximately $28^{o}C$ using a recirculating water bath. At these conditions, the reduction in COD over time at various pH are shown in Figure 4-2 (a). Replicate experiments showed less than 3% average standard deviations, therefore error bars were not included in this and subsequent figures as they would not be visible due to overlap of the data markers. The results show that COD degradation after 60 minutes varied between 70 % to more than 90 % of initial COD. It is also clear that as the initial pH increases, the final COD degradation also increases significantly, with the highest COD removal at pH 8 (the highest pH studied for this condition). It can be seen from the COD decay that the COD removal rate is almost the same for all the initial pH values used between 0 – 15 minutes, after which the curves start to deviate from one another. Figure 4-2 (b) shows the same plots for the condition of high buffer concentration (240 mM of KH_2PO_4). It can be seen that the addition of higher buffer amounts did not significantly affect the COD reduction, as the trend of higher COD removal at higher initial pH remains, with the highest COD reduction achieved at initial pH of 9.

Figure 4-2: Effect of (a) initial pH at low buffer concentration, (b) initial pH at high buffer concentration, (c) temperature, (d) UV dose and (e) initial H_2O_2 concentration on COD degradation of MEA

The improvement of contaminant degradation at high pH in UV/H_2O_2 was also noted in the degradation of other substances such as pulp mill effluent (Catalkaya and Kargi 2007) and also for the colour removal of reactive dyes (Riga, et al. 2007). On the other hand, other studies have found that a low solution pH was more conducive to substrate degradation (Catalkaya and Sengul 2006, Sutherland, Adams and Kekobad 2004). The effect of bicarbonate/carbonate radical scavenging at high pH may be the main influence to the reduced degradation at high pH seen in those studies where a low pH optimum was obtained (Andreozzi, Caprio and Insola, et al. 1999). Since the solution used in this study does not contain bicarbonate or carbonate ions (no chemicals were introduced containing the species, except for dissolution of carbon dioxide from the atmosphere as carbonic acid, which can be considered to be negligible), this well-known effect was not observed in this study.

The kinetic data for the degradation of MEA at different pH under low buffer condition is shown in Figure 4-3 (a) in terms of the negative of the natural logarithm of the relative concentrations versus time. MEA measurements were not taken for high buffer conditions. The resulting plots show linear trends and this indicates that MEA oxidation via UV/H_2O_2 process obeys pseudo-first-order kinetics. All other runs exhibit similar results. The pseudo first-order rate constant, k_0, and 95 % confidence interval, or $CI_{95\%}$, values for the experimental runs were estimated accordingly and listed in Table 4-4. In contrast to the COD results, the results of pH variation indicate that the rate constant for degradation of MEA is not significantly affected by pH since the range of the rate constants based on $CI_{95\%}$ overlap each other. It is noted that for degradation of synthetic substrates, other researchers have found the same independence of pH on kinetics. For example, Thiruvenkatachari et. al (2007) found that between pH 6 and 8, there is no effect of pH on kinetics of terephthalic acid degradation using UV/H_2O_2. The same was found for clofibric acid degradation between pH 4 to 7 (Andreozzi, Caprio and Marotta, et al. 2003). It is presumable that without the alkalinity scavenging effect in synthetic samples, the kinetics of the main substrate degradation is largely unaffected. The highest pseudo first-order rate constant for MEA degradation achieved in this study is $k_{pH2} = 0.0922 \pm 0.0138 \ min^{-1}$.
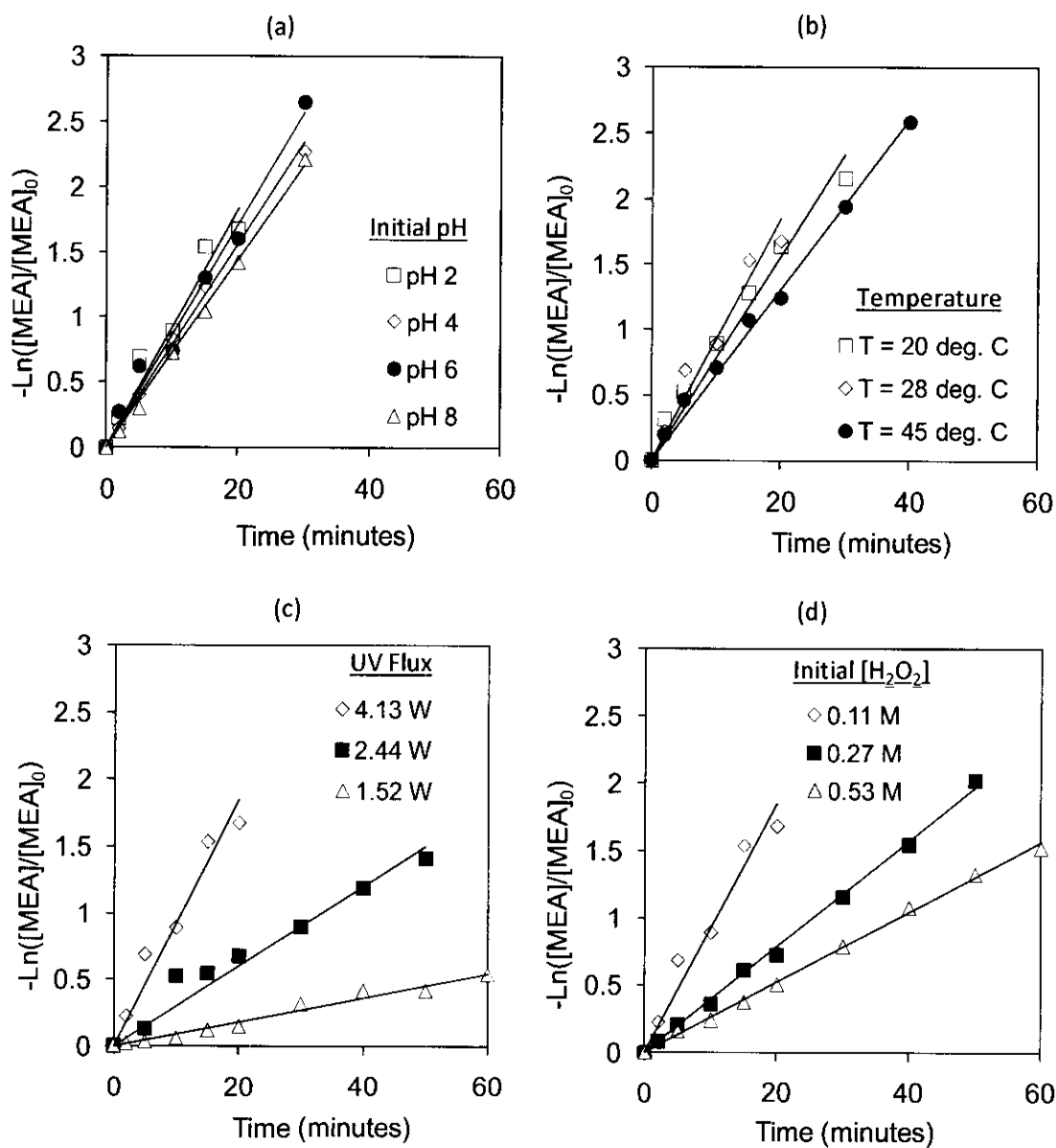
Figure 4-3: Effect of (a) initial pH, (b) temperature, (c) UV flux and (d) initial H_2O_2 concentration (on MEA degradation first-order kinetics.

Table 4-4: Observed pseudo-first order rate constant for MEA oxidation via UV/H_2O_2 process

Init. pH	temperature (deg C)	Init. $[H_2O_2]$ (M)[1]	UV flux (W)[2]	k_0 (min^{-1})	$CI_{95\%}$
2	28	0.11	4.13	0.092209	0.013812
4	28	0.11	4.13	0.078329	0.002905
6	28	0.11	4.13	0.085936	0.006907
8	28	0.11	4.13	0.072335	0.002215
2	20	0.11	4.13	0.077843	0.007973
2	45	0.11	4.13	0.065299	0.003096
2	28	0.53	4.13	0.025961	0.000633
2	28	0.27	4.13	0.039256	0.001052
2	28	0.11	1.52	0.009045	0.000723
2	28	0.11	2.44	0.029993	0.0032

At high pH, the equilibrium shift to the deprotonated form of hydrogen peroxide into the hydroperoxide (HO_2^-) ion occurs. Since this ion has a higher absorption coefficient (240 L mol^{-1} cm^{-1}) compared to the protonated form (19 L mol^{-1} cm^{-1}), H_2O_2 decay is accelerated, leading to increased production of •OH radicals (Andreozzi, Caprio and Insola, et al. 1999). This would presumably increase the overall degradation of organic compounds and accelerate COD removal. However, the results obtained from the MEA degradation seem to suggest that the effect of increased UV absorption of the hydroperoxide ion at high pH in this case may not be significant to the increased COD removal since a corresponding increase of MEA degradation kinetics would be expected if it were so. Instead, the increased COD removal at higher pH may be due to the formation of pH dependent breakdown products that have increased reactivities at higher pH.

---

[1] 0.11 M = 1× stoichiometric, 0.27 = 2.5× stoichiometric, 0.53 = 5× stoichiometric based on complete MEA mineralization.

[2] 4.13 W = One 8 W lamp placed in 390 ml reactor. 2.44 W, 1.52 W and 0.67 W correspond to three, two and one 4W lamp(s) placed in 1.1L reactor respectively. Measured using hydrogen peroxide actinometry.
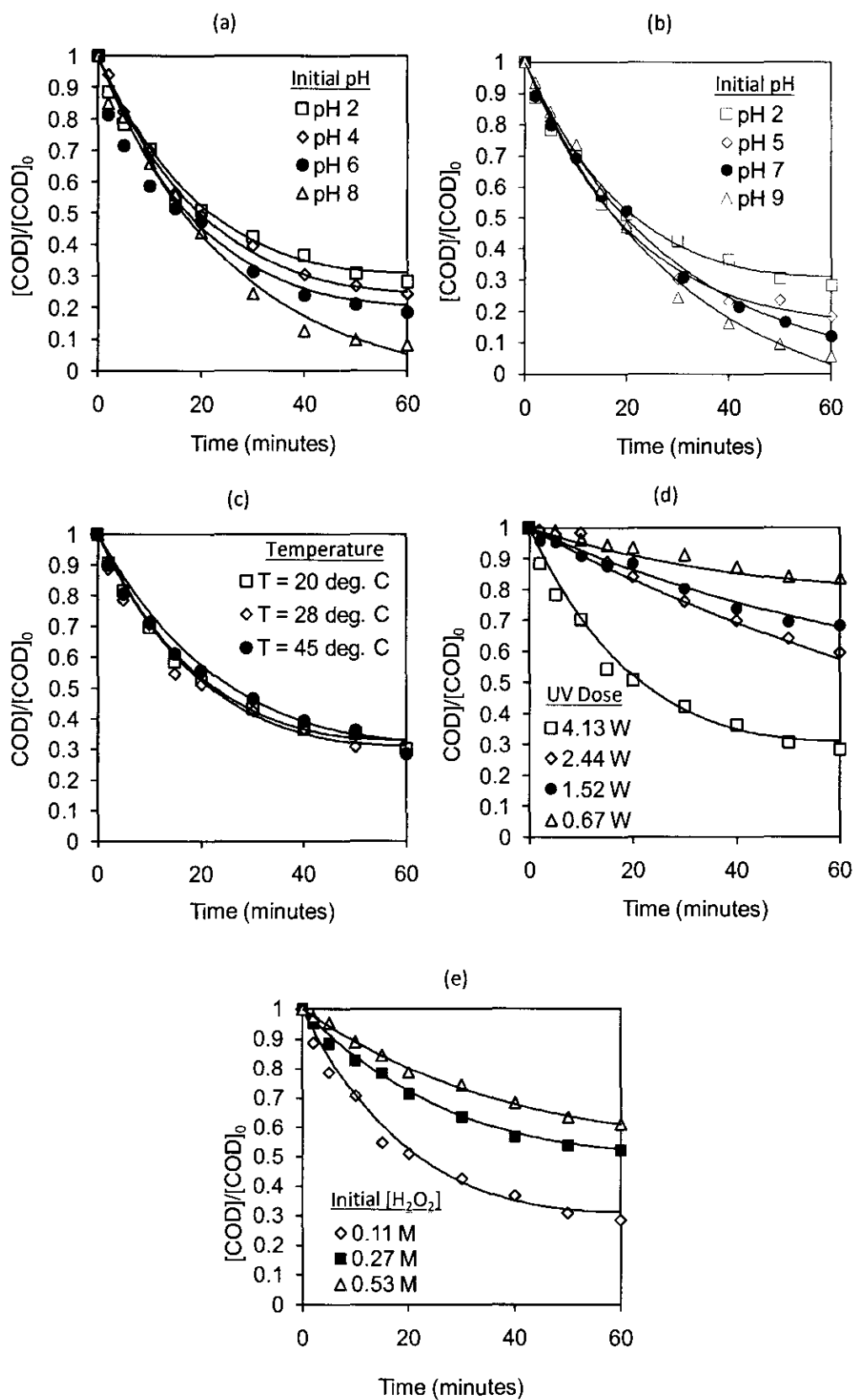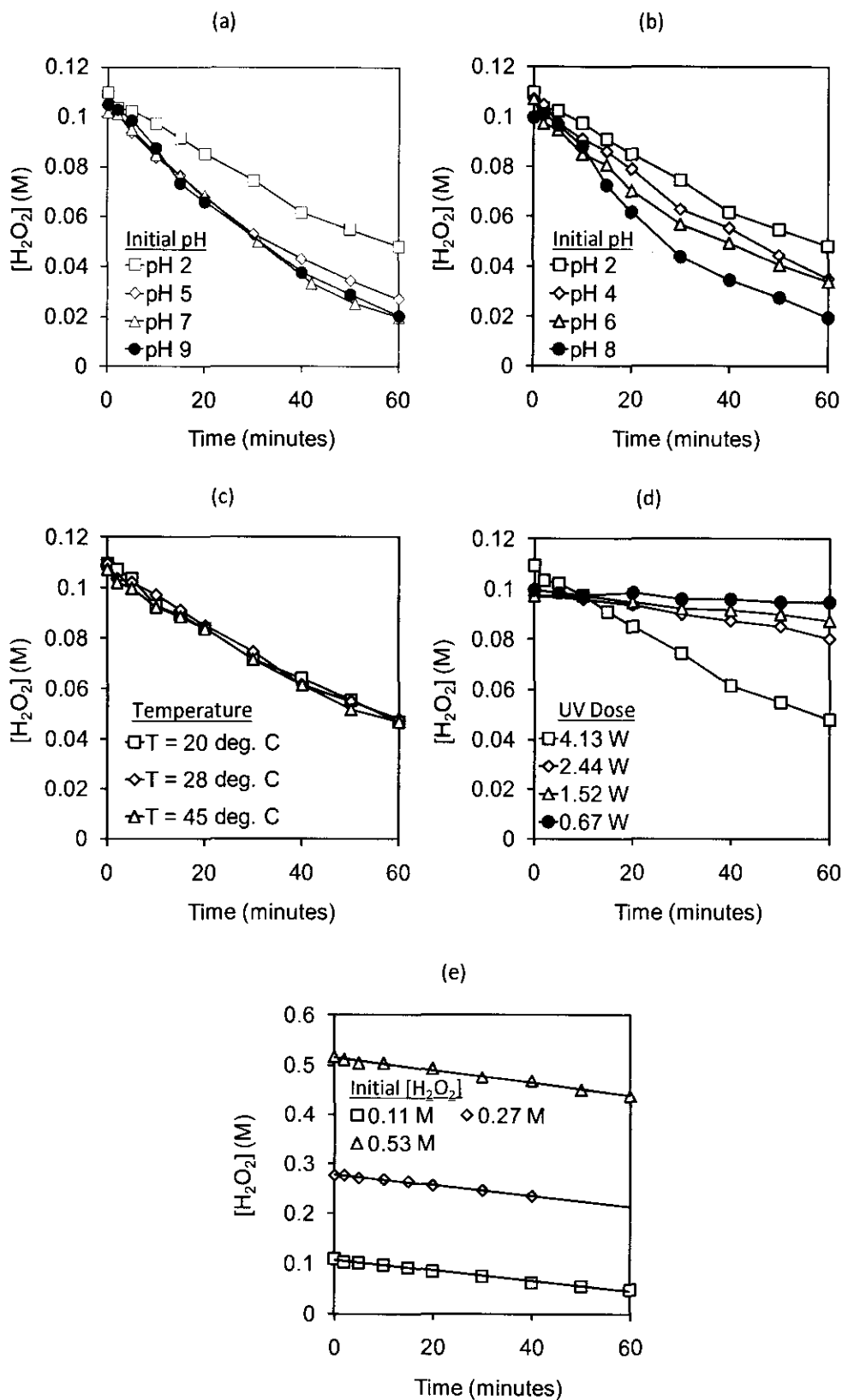
Figure 4-4: Effect of (a) initial pH at high buffer concentration, (b) initial pH at low buffer concentration, (c) temperature, (d) UV flux and (d) initial H₂O₂ concentration on H₂O₂ decay.

Figure 4-4 (a) and (b) shows the change in H_2O_2 concentration with time at different initial pH values. It can be seen clearly that higher pH results in higher H_2O_2 consumption for both high and low buffer conditions. The increased H_2O_2 decay may have been caused by the increased rate of spontaneous decomposition to oxygen and water at high pH (Shemer and Linden 2007). Figure 4-5 shows the pH change in the solution at different pH values and buffer additions. It can be observed that without any buffer addition, the uncorrected pH drops significantly from approximately 10 to 6. Starting at pH 9, addition of a small amount of buffer reduces the pH change by one pH point compared to unbuffered condition. Addition of higher buffer concentration significantly reduced but did not totally eliminate the pH dip that was observed with lower buffer concentrations. This large pH depression effect strongly suggests the presence of some highly acidic byproducts that are formed during the course of the reaction.
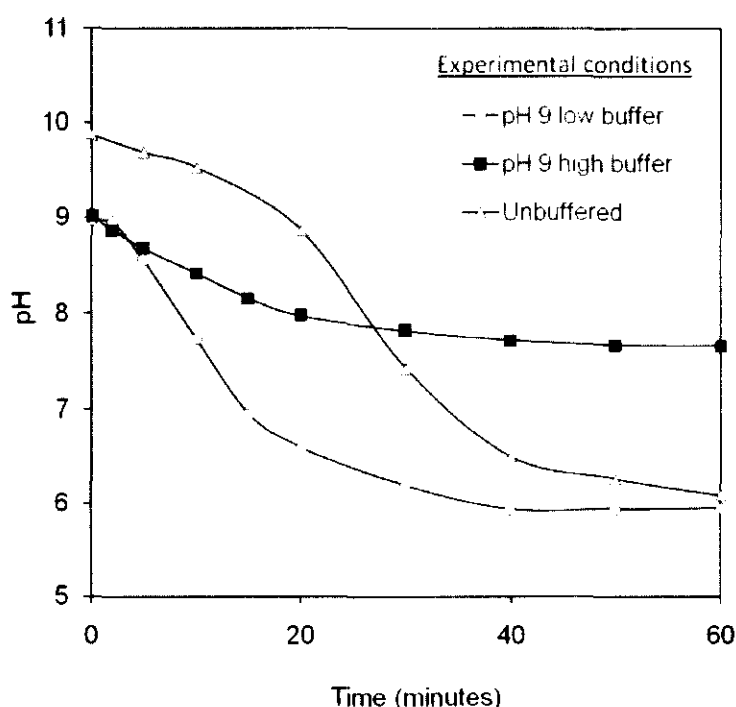
Figure 4-5: Trends of solution pH during experiment at different buffer concentrations.

4.2.2. Effect of temperature

The effect of temperature on the rate of COD removal was studied at 3 temperature levels i.e. 20, 28 and 45 °C. The results of the experiments are shown in Figure 4-2 (c). In contrast to the strong dependence on pH, it appears that temperature does not seem to have any appreciable or noticeable effect on COD degradation for the range of temperature used in this work. The H_2O_2 consumption during the course of the reaction was also unchanged, as shown by the virtually overlapping and identical plots for H_2O_2 decay at different temperatures in Figure 4-4 (c). Pseudo-first order kinetics plot in Figure 4-3 (b) also indicate the kinetics of MEA degradation is not significantly affected by temperature. These results suggest that the overall mechanism and rate of H_2O_2 photolysis, •OH radical generation and organic degradation are unaffected by temperature changes within the parameters of this study.

4.2.3. Effect of UV flux

The UV flux (as measured by the total incident photon flow, Φ) was varied between 0.67, 1.52, 2.44 and 4.13 W to investigate the effect of UV flux on the organic degradation rate. The COD change with time at different UV fluxes is shown in Figure 4-2 (d). As expected, the COD degradation rate increases with increase in UV dose with the highest COD removal at 71% after 60 minutes reaction for incident photon flux of 4.13 W. The lowest COD removal was found for the lowest UV flux of 0.67 W, which only resulted in a COD removal of 16% after 60 minutes of reaction. The rate of H_2O_2 decay at various UV dosages and the slope of the H_2O_2 decay show that H_2O_2 decay is directly affected by the total UV dose applied as indicated in Figure 4-4 (d). The decay in H_2O_2 concentration is caused by the cleavage of the H_2O_2 molecule by the UV photon energy as described by equation (4-3) (Table 4-5), producing the hydroxyl radicals. A higher UV flux therefore directly influences the rate of generation of hydroxyl radicals and therefore the rate of organic destruction.

The UV flux also exerted a highly significant impact on MEA degradation kinetics as shown in Figure 4-3 (c). Empirically, the k_0 value is found to obey a power law with respect to UV flux in the form $k_0 = 0.0035 \cdot \Phi^{2.3194}$ as shown in Figure 4-6. This highlights the importance of UV flux and that the kinetics of MEA degradation can be increased by many-fold with a relatively modest change in UV intensity.

$$y = 0.003x^{2.319}$$
$$R^2 = 0.997$$
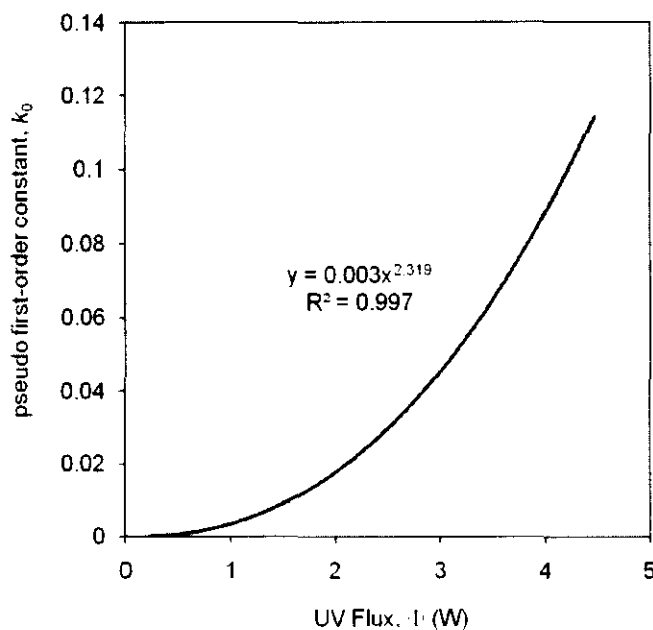
Figure 4-6: Measured k_0 value as a function of UV flux.

4.2.4. Effect of initial H_2O_2 dose

The COD reduction at different initial H_2O_2 dosages was also investigated. The initial H_2O_2 concentration was varied between 0.11, 0.27 and 0.53 M as measured using permanganate titration. These concentrations correspond to 1, 2.5 and 5 times the stoichiometric requirement of H_2O_2 for complete mineralization of MEA as indicated in equation (4-1).

$$2C_2H_7NO + 13H_2O_2 \rightarrow 4CO_2 + N_2 + 20H_2O \qquad (4-1)$$
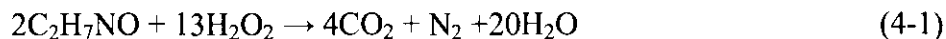
Other experimental conditions were kept constant with UV flux at 4.13 W, pH at 2 and temperature at $28^\circ C$. The results for COD reduction at different initial H_2O_2

concentration and the resultant H_2O_2 concentration profile are shown in Figure 4-2 (e) and Figure 4-4 (e). A significant reduction of the COD removal was observed as the initial H_2O_2 dose was increased. Similarly, kinetics data also showed a significant reduction of MEA degradation with an increase in initial H_2O_2 dose as shown in Figure 4-3 (d). These results indicate that the effect of radical scavenging by H_2O_2 is already significant at the concentrations used in the experimental study. In Section 4.1, it was shown that between $0.5 - 1.25$ times the stoichiometric H_2O_2 concentration (corresponding to $0.05 - 0.16$ M), the effect of initial H_2O_2 concentration on COD degradation of MEA using UV/H_2O_2 process was not statistically significant. Therefore, the optimum initial concentration of H_2O_2 is either 0.05 M (50 mM) or less and any increase above 0.16 M will result in a decrease in the efficiency of COD removal rate. This is in accordance with the optimum initial concentration obtained by other researchers using UV/H_2O_2 for pulp mill effluent (50 mM) (Catalkaya and Kargi 2007), tannery wastewater (approx. 14 mM) (Sauer, et al. 2006), terephthalic acid (3 mM) (Thiruvenkatachari, et al. 2007), azo dye (50 mM) (Peternel, Koprivanac and Kusic 2006) and humic acid (approx. 3 mM) (Wang, Hsieh and Hong 2000). However, in this study, it was not possible to conduct tests at such low initial H_2O_2 concentrations because there is possibility that the H_2O_2 will be completely photolysed before 60 minutes reaction time. It is also evident that the H_2O_2 degradation rate is largely unaffected by the initial H_2O_2 dose as indicated by the slope, which is unchanged. Since the H_2O_2 decay is caused by molecular cleavage into ·OH radicals, the rate of formation of these radicals does not seem to be much affected by the initial H_2O_2 concentration. Rather, the reduced rate of COD and MEA degradation is caused by the increased rate of the radical termination reaction between H_2O_2 and the ·OH radical.

4.2.5. Identification of organic and inorganic anions

Analysis of the breakdown products have been conducted using ion chromatography. This method was selected to identify the presence of organic acids and inorganic acids in the solution after the reaction. The presence of organic and inorganic acids was suspected due to the large drop in pH observed during the reaction.

A sample of the solution after 60 minutes of reaction was analysed using anion suppression technique. To prevent column overloading by sulfate and phosphate species, the sample was taken from an experimental run without pH correction or addition of phosphate buffer. The resultant chromatogram is shown in Figure 4-7 (a). Comparison of resultant chromatogram with standard peaks confirm the presence of the anions formate (t_R = 4.5 minutes) and nitrate (t_R = 10.5 minutes). At a retention time of about 4.1 minutes, a peak which is suspected to be acetate was also observed, however this cannot be confirmed due to interference from H_2O_2 at that location. A clearly separated peak at t_R = 8.1 minutes is observed but this peak was not able to be identified. Although no literature was found specifically on MEA degradation, for many organic compounds such as acetone, 1,4-dioxane and MTBE, the production of by-products such as acetate, formate, oxalate and glycolate were observed during UV/H_2O_2 process (Oppenländer 2003). In this study, the formation of these organic and inorganic acids, especially nitric acid, seems adequate to explain the large pH reduction that is observed in the solution during UV/H_2O_2 treatment. Figure 4-7 (b) shows the evolution of both formate and nitrate during the course of the experimental run, together with the MEA decay on a separate axis, which shows that formate is formed as an intermediate byproduct and has a peak concentration of approximately 200 mg/l after 20 minutes of reaction. Nitrate is probably formed as a terminal byproduct as it continues to increase in concentration throughout the reaction duration. The presence of nitrate is of significance due to its potential to compete with H_2O_2 to absorb UV radiation (Oppenländer 2003).
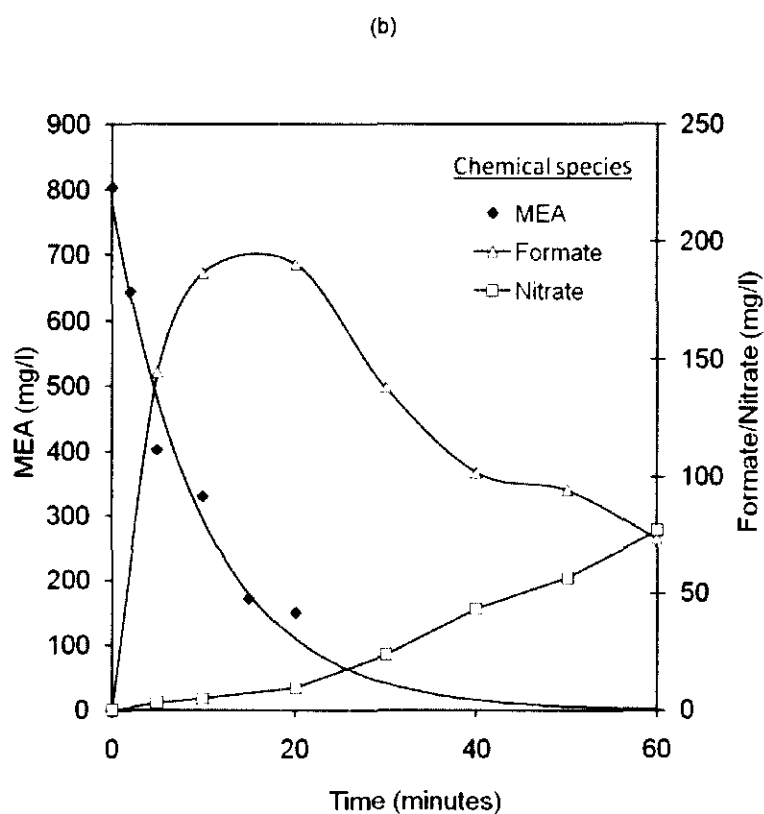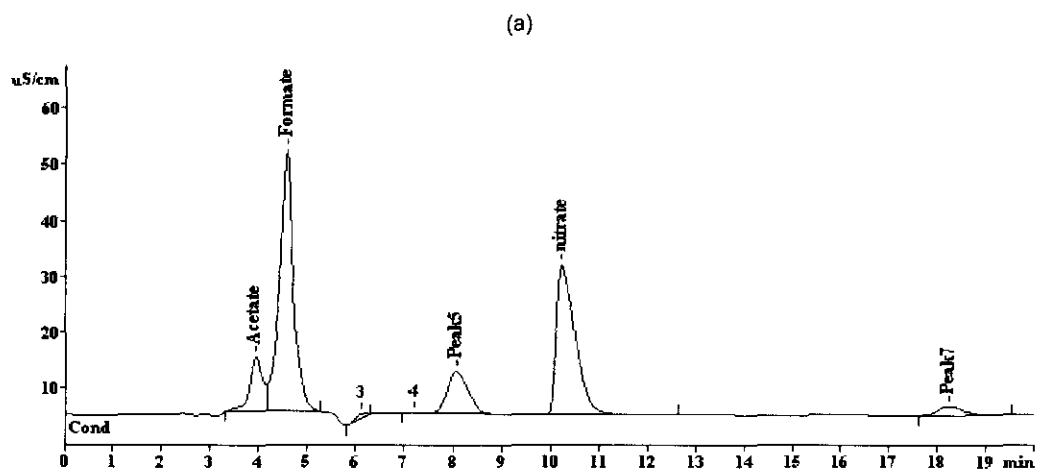
Figure 4-7: Ion chromatograph showing presence of acetate, formate and nitrate and (b) concentration profile of MEA, formate and nitrate with time.

4.2.6. Conclusions

In this work, a study into the effects of initial solution pH, temperature, initial H_2O_2 dose and UV dose on the reduction of COD in MEA solution using the UV/H_2O_2 method was conducted using a batch photoreactor. It was found that degradation of MEA via the UV/H_2O_2 process is very much possible, and the MEA decay was found to obey pseudo first-order kinetics with the maximum rate constant of $k_0 = 0.0922 \pm 0.0138$ min^{-1}. It was found that the initial solution pH was a crucial factor in influencing the rate of COD degradation, whereby increasing the pH from $2 - 9$ resulted in significant increase of COD reduction rate, but had a minimal impact on MEA degradation kinetics, indicating that the pH is affecting the reaction rate of intermediate by-products formed during the reaction. The temperature of the solution did not seem to exhibit any impact on either COD or MEA degradation. The initial H_2O_2 dose was found to significantly affect both COD and MEA degradation rate, owing to the effect of hydroxyl radical scavenging by high H_2O_2 concentration. Increasing the UV dose also resulted in significant increase in the degradation rate as expected.

Ion chromatography analysis confirmed the presence of formate and nitrate as reaction by-products. The formation of nitrate is of particular importance due to its effect as a UV absorber and radical scavenger, potentially reducing the effectiveness of UV-based AOP on the degradation of MEA or other alkanolamines.

4.3. Development of quasi-mechanistic kinetic rate model for COD degradation and H_2O_2 decay

4.3.1. Photolysis model of hydrogen peroxide

It is generally accepted that the initiation reaction in the UV/H_2O_2 process is the photolysis of hydrogen peroxide producing two ·OH radicals. For this reaction, the rate of photolysis of hydrogen peroxide can be represented by equation (4-2):

$$-\left[\frac{d[H_2O_2]}{dt}\right]_{phot} = \Phi_{H_2O_2} I_0 f_{H_2O_2}(1-e^{-A})$$

(4-2)

where $\Phi_{H_2O_2}$ is the primary quantum yield of hydrogen peroxide photolysis, I_0 is the monochromatic UV intensity, A is the absorbance of the solution and $f_{H_2O_2}$ is the fraction of UV irradiation absorbed by hydrogen peroxide.

The value of $\Phi_{H_2O_2}$ is widely accepted to be unity (Glaze, Lay and Kang 1995). The value of I_0 for this work was obtained by hydrogen peroxide actinometry at high total absorbance in accordance with the method outlined by Nicole et al. (1990) and will depend on the characteristics of the lamp and reactor system. The assumption of high total absorbance for the actinometry measurements was justified based on the zero-order decay of hydrogen peroxide that was observed in the actinometry runs.

For the value of $f_{H_2O_2}$, an experimental run was conducted where MEA solution was irradiated with UV light without presence of hydrogen peroxide. It was found that no COD degradation was observed after 60 minutes of irradiation time; indicating that rate of MEA photolysis is negligible, therefore $f_{H_2O_2}$ is assumed to be unity.

The solution absorbance, A, is given by $= 2.303b(\varepsilon_{H_2O_2}[H_2O_2] + \varepsilon_{HO_2^-}[HO_2^-])$, where b is the effective irradiation path length and ε is the molar extinction coefficient for each respective species. The path length was measured as 1.4 cm for the small annular reactor used in this study. For the larger reactor with multiple lamps, the path

length was assumed to be the same, since it was found that the model results were not affected by increasing the path length.

Depending on the pH, the acid-base deprotonation of hydrogen peroxide to the hydroperoxide ions will affect the solution absorbance due to the difference in molar extinction coefficient of the deprotonated species. For this study, the value of ε for hydrogen peroxide and the hydroperoxide ion is assumed to be 19 and 228 M^{-1} cm^{-1} respectively (Crittenden, Hu, et al. 1999).

4.3.2. Reaction scheme

The overall reaction scheme used in the kinetic model is shown in Table 4-5. This reaction scheme is based on the principal reactions for the radical initiation, propagation and termination and substrate decomposition, also known as the *Haber-Weiss* mechanism, as outlined by Glaze et al. (1992). This scheme has subsequently been used successfully by a number of other researchers to model the degradation of various compounds such as phenol (Huang and Shu 1995), 2,4-dichlorophenoxyacetic acid (Alfano, Brandi and Cassano 2001) and dimethyl phthalate (Xu, et al. 2008) using UV/H_2O_2 process. However, in this work, the radical propagation reaction between hydrogen peroxide and the $HO_2\cdot$ radical was not considered in the kinetic model because of its low reaction rate constant (3 M^{-1} s^{-1}) as compared with other principal reactions (which have kinetic constants which are many orders of magnitude higher) in the scheme. Also, to obtain a better fit to the observed values, the rate of substrate decomposition is modeled in this work as an n^{-th} order reaction with the $\cdot OH$ radical with respect to the COD concentration. The kinetic constant values for the reactions in the scheme are obtained largely based on work by Crittenden, Hu, et al. (1999). Since the effect of carbonate and bicarbonate radical scavenging was not studied, the reactions that involve those species were not considered in the model. The effect of nitrogen was also not considered in the mechanism. In applying the kinetic model to the degradation of MEA using UV/H_2O_2 process, the following assumptions were made: (1) acid-base dissociation of hydrogen peroxide is presumed to be instantaneous and (2) pH of solution remains constant (i.e. same as initial pH).

Table 4-5: Reactions in the proposed mechanism of MEA degradation by UV/H₂O₂.

Reaction step	Reaction no.	Rate/equilibrium expression
Radical initiation		
$H_2O_2/HO_2^- + h\upsilon \rightarrow 2\cdot OH$	(4-3)	$-\left[\dfrac{d[H_2O_2]}{dt}\right]_{phot} = \Phi_{H_2O_2} I_0 f_{H_2O_2} (1 - e^{-A})$
Radical propagation		
$H_2O_2 + \cdot OH \rightarrow H_2O + HO_2\cdot$	(4-4)	$k_4 = 2.7 \times 10^7 \ M^{-1} \ s^{-1}$
Radical termination		
$\cdot OH + \cdot OH \rightarrow H_2O_2$	(4-5)	$k_5 = 5.5 \times 10^9 \ M^{-1} \ s^{-1}$
$\cdot OH + HO_2\cdot \rightarrow H_2O + O_2$	(4-6)	$k_6 = 6.6 \times 10^9 \ M^{-1} \ s^{-1}$
$HO_2\cdot + HO_2\cdot \rightarrow H_2O_2 + O_2$	(4-7)	$k_7 = 8.3 \times 10^5 \ M^{-1} \ s^{-1}$
Substrate decomposition		
$S + \cdot OH \rightarrow$ Oxidation products	(4-8)	$k_8 = ?$
Acid/base equilibrium		
$H_2O_2 \leftrightarrow H^+ + HO_2^-$	(4-9)	$pK_a = 11.6$

4.3.3. Kinetic model derivation

From the reactions listed in Table 4-5, a kinetic model was derived for the UV/H₂O₂ process that predicts the concentrations of COD and hydrogen peroxide as a function of time. The derivation of the kinetic model here is similar to the approach used by Glaze et al. (1995) in the kinetic modeling of the decomposition of 1,2-dibromo-3-chloropropane using UV/H₂O₂, in which a numerical or computational method was used. In this model derivation, a steady-state concentration is assumed for both HO· and HO₂· radicals, as represented by equations (4-10) and (4-11) below, based on the reactions listed in Table 4-5. These equations can then be rearranged and expressed in the time-discrete form as indicated in equations (4-12) and (4-13) below:

$$\frac{d[HO\cdot]}{dt} = 2r_{OH} - k_4[H_2O_2][HO\cdot] - k_8[S]^n[HO\cdot] - k_5[HO\cdot]^2 - k_6[HO\cdot][HO_2\cdot] = 0 \quad (4\text{-}10)$$

$$\frac{d[HO_2\cdot]}{dt} = k_4[H_2O_2][HO\cdot] - k_6[HO\cdot][HO_2\cdot] - k_7[HO_2\cdot]^2 = 0 \quad (4\text{-}11)$$

$$[HO\cdot]_{i+1} = \frac{2r_{OH}}{k_4[H_2O_2]_i + k_8[S]_i^n + k_5[HO\cdot]_i + k_6[HO_2\cdot]_i} \qquad (4\text{-}12)$$

$$[HO_2\cdot]_{i+1}^2 = \frac{k_4[H_2O_2]_i[HO\cdot]_i - k_6[HO\cdot]_i[HO_2\cdot]_i}{k_7} \qquad (4\text{-}13)$$

where i is the time index from 0 to 3600 s. The rate of OH radical generation, r_{OH} will depend on the extent of deprotonation of H_2O_2, calculated from the difference between pH and pK_a. The rate of substrate ([COD]) degradation is considered to be n^- th order with respect to the COD and hydroxyl radical concentration and represented by equation (4-14) below. The substrate concentration can thus be expressed in the same fashion as the radical species by equation (4-15). Similarly, the rate of H_2O_2 decay and its time-discrete concentration can be adequately represented by equation (4-16) and (4-17).

$$\frac{d[S]}{dt} = -k_8[S]^n[HO\cdot] \qquad (4\text{-}14)$$

$$[S]_{i+1} = [S]_i - k_8[S]_i^n[HO\cdot]_i \qquad (4\text{-}15)$$

$$\frac{d[H_2O_2]}{dt} = k_5[HO\cdot]^2 + k_7[HO_2\cdot]^2 - r_{OH} - k_4[H_2O_2][HO\cdot] \qquad (4\text{-}16)$$

$$[H_2O_2]_{i+1} = [H_2O_2]_i + k_5[HO\cdot]_i^2 + k_7[HO_2\cdot]_i^2 - r_{OH} - k_4[H_2O_2]_i[HO\cdot]_i \qquad (4\text{-}17)$$

To calculate the concentrations of the various species using the model, initial concentrations ($t = 0$) of COD, H_2O_2 and pH were assumed based on the observed data in the experimental run to be modeled. Values of the reaction order, n and the kinetic constant, k_8 for the substrate decomposition reaction are not known in literature and must be chosen arbitrarily at the initial step. The concentrations of radicals were assumed to be zero at initial conditions. Using equations (4-12), (4-13), (4-16) and (4-17), the concentrations of HO· and HO$_2$· radicals, COD and H_2O_2 were determined at each $t=i+1$s by calculation based on values at $t=i$. This calculation is

71

repeated for every second from $t = 1s$ to $t = 3600s$ (i.e. 60 minutes of reaction) using Microsoft ® Office Excel spreadsheet to obtain the concentration profile of the species. Then, the rate constant, k_8 was obtained using Solver tool in Excel by minimising the residual sum-of-squares between the actual and predicted concentration of COD. Trial-and-error method was used to refine the fit by choosing the best values of n and Solver-optimized k_8.

4.3.4. Model generalization and validation

Optimized fitting of both the kinetic constant, k_8 and the reaction order, n was conducted as described above, for the experimental runs. The results are shown in Table 4-6, which also indicates the experimental conditions for each of the runs. It can be observed that, at low initial solution pH ~ 2, the COD decomposition can be modeled as a 3rd order reaction with kinetic constant values ranging from 4.7×10^{10} to 1.5×10^{11} M^{-3} s^{-1}. As the initial pH of the solution is increased, the reaction order of the overall organic content as measured by the COD, n is found to decrease. This is illustrated more clearly in Figure 4-8 (a) and (b), which shows the effect of initial solution pH on the apparent reaction order, for both low and high phosphate buffer conditions, and the direct relationship between the reaction order and the kinetic constant.

72

Table 4-6: Calculated reaction rate constant and reaction order results for COD degradation using UV/H₂O₂ showing both individual fitting and generalized model results.

Run	pH	Temp (°C)	[H₂O₂]	UV flux (W/l)	Individual fitting results		Generalised model results		
					n	k_8	n	k_8	R^2
1	2	28	0.11	10.58974	3	6.16E+10	3	7.41E+10	0.9801
2	4	28	0.11	10.58974	3	7.14E+10	2.63	1.98E+10	0.9934
3	6	28	0.11	10.58974	3	1.17E+11	2.2	4.28E+09	0.947
4	8	28	0.11	10.58974	2	2.70E+09	1.77	9.25E+08	0.9857
5	9	28	0.11	10.58974	1.2	1.04E+08	1.55	4.24E+08	0.9911
6	2	20	0.11	10.58974	3	5.68E+10	3	7.41E+10	0.9733
8	2	45	0.11	10.58974	3	4.68E+10	3	7.14E+10	0.9363
9	7	28	0.11	10.58974	2	2.02E+09	2	2.10E+09	0.9938
10	9	28	0.11	10.58974	1.5	3.51E+08	1.55	4.24E+08	0.9932
11	5	28	0.11	10.58974	2.5	1.40E+10	2.4	9.08E+09	0.9919
14	2	28	0.53	10.58974	3	6.28E+10	3	6.28E+10	0.9722
15	2	28	0.27	10.58974	3	6.15E+10	3	7.41E+10	0.9611
16	2	28	0.11	0.609091	3	1.53E+11	3	7.41E+10	0.8511
17	2	28	0.11	1.381818	3	1.39E+11	3	7.41E+10	0.9551
18	2	28	0.11	2.218182	3	1.10E+11	3	7.41E+10	0.9701
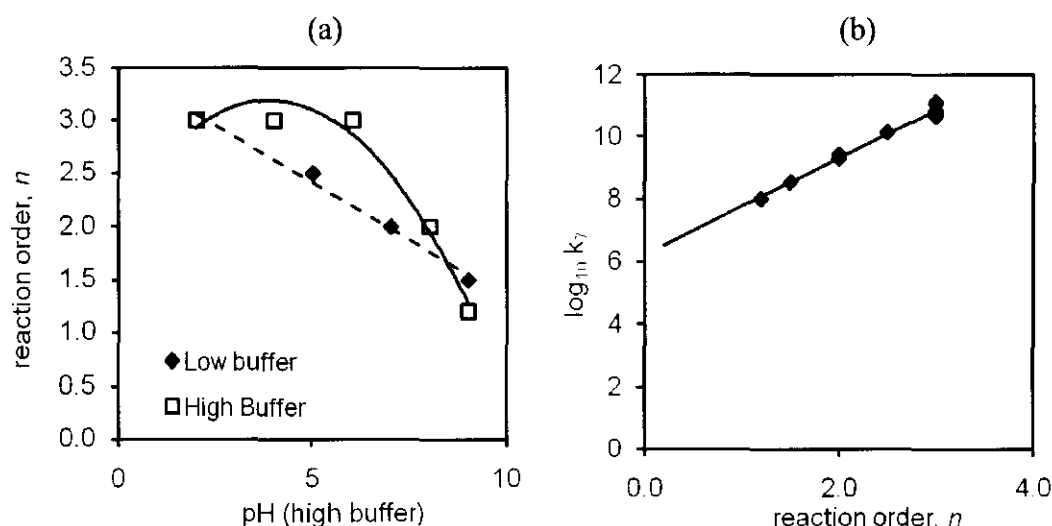
Figure 4-8: (a) Dependence of reaction order, n on pH and (b) linear relationship between kinetic constant k_8 and reaction order, n

Based on the model prediction, the dependence of the substrate decomposition rate on the pH is not primarily a consequence of the higher molar absorption coefficient of the hydroperoxide ion, which tend to form at high pH. As shown in Figure 4-9 (a), by maintaining the value of n and k_8 to be constant (i.e., by using the 3rd order fit only), the model predicts that the fractional COD removal at the end of the reaction duration is not affected at all for pH values lower than approximately 11. Only beyond the pH of 11, does the fractional COD removal predicted by the 3rd -

73

order model show an increasing trend. In contrast, the observed COD fractional removal rate shows a gradual increasing trend as the pH is raised from 2 – 9. The reason is that in the reaction scheme, the main effect of pH is to determine the equilibrium concentrations of H_2O_2 and the hydroperoxide ion, which have differing UV absorption values. However, the pK_a of that deprotonation reaction is 11.6, therefore the concentration of the hydroperoxide ion, which has the higher molar absorption coefficient of 228 M^{-1} cm^{-1}, is quite negligible at low pH until the pH is close to 11.6. Therefore, some other mechanism is responsible for the increased COD decomposition of the MEA solution at high pH and change in reaction order and kinetic constant in the observed data, but unfortunately it is beyond the scope of this study. However, it is reasonable to expect that this mechanism is caused by the formation of unidentified reaction byproducts that have pH-dependent reaction rates with the ·OH radical, since the kinetic constants for MEA itself was shown earlier to have no correlation with the initial solution pH.

Fitting of each experimental run separately will result in very good correlations with the observed data; however, a more generalized model is desirable, in which reasonably accurate kinetic data can be derived with minimal numerical fitting and optimization, using initial reaction conditions. To achieve this, based on the correlation in Figure 4-8 (b), it is proposed that the dependence of the reaction order to the initial solution pH can be described (using the low buffer results as a simple model) by equation (4-18) below:

$$n = 3.486 - 0.215\text{pH} \tag{4-18}$$

and the kinetic constant for COD reduction of MEA can be described as a function of the reaction order as shown in equation (4-19):

$$\log_{10} k_8 = 1.548n + 6.226 \tag{4-19}$$

74
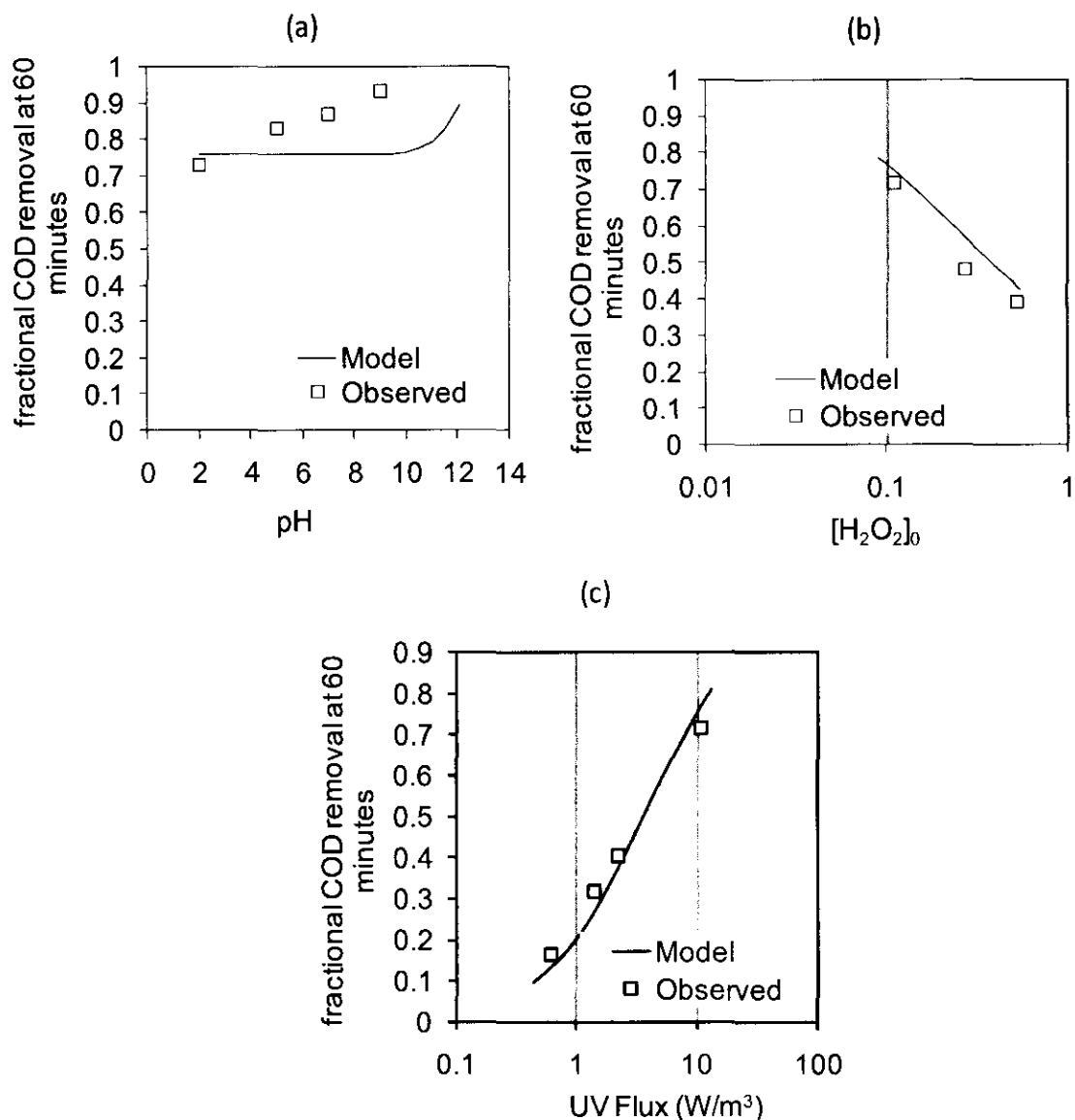
Figure 4-9: Comparison of fractional COD removal after 60 minutes of reaction between observed (measured) data and the results predicted by model (generalised based on equation (4-18) and (4-19)). The comparison is made by varying (a) pH ($n = 3$, $k_8 = 7.41 \times 1010$ M^{-3} s^{-1}, initial [H_2O_2] = 0.107 M, initial [COD] = 0.036 M, UV flux = 10.53 W/m^3), (b) initial H_2O_2 concentration ($n = 3$, $k_8 = 7.41 \times 10^{10}$ M^{-3} s^{-1}, pH = 2, initial [COD] = 0.036 M, UV flux = 10.53 W/m^3) and (c) UV flux ($n = 3$, $k_8 = 7.41 \times 10^{10}$ M^{-3} s^{-1}, pH = 2, initial [H_2O_2] = 0.1 M, initial [COD] = 0.036 M,).

For example, using equation (4-18) and (4-19), at initial solution pH = 2, the reaction order, n and kinetic constant, k_8 can be calculated to be 3rd order and 7.41×10^{10} M^{-3} s^{-1} respectively. Using this approach, the correlation of the kinetic model with observed data were recalculated for all the experimental runs and shown in Table 4-6 under "Generalised model results" column. The results indicate that the correlation between the model prediction and observed data for the selected runs were found to be good, with the R-squared value ranging between 0.851 and 0.993. The

model was then used to predict the fractional COD removal at 60 minutes of reaction as a function of UV dose, and initial H_2O_2 concentration as shown in Figure 4-9 (b) and (c). The model was found to be reasonably accurate in predicting the reaction rate and fractional COD removal as a function of UV dose and H_2O_2 concentration with R-squared value of 0.960 and 0.804 respectively.

Figure 4-10 shows some examples of experimental data compared to the kinetic model, showing a reasonably good prediction of both the COD decay and H_2O_2 decomposition. However, in some of the runs, there appears to be a systematic deviation of the observed values for H_2O_2 compared with the prediction, especially nearing the end of the reaction, where the observed data showed a gradual decrease in decay rate compared to the model prediction. One possible explanation is the influence of nitrate photolysis, which is not considered in the reaction scheme. As indicated earlier, the formation of nitrate was positively identified by ion chromatography, and the nitrate ion, NO_3^-, has been shown to be a potential "inner filter", by absorption of UV in competition to hydrogen peroxide (Mack and Bolton 1999). Although the molar absorption coefficient for NO_3^- photolysis at 254 nm is relatively weak (approximately 4 M^{-1} cm^{-1}) (Oppenländer 2003), the "inner filter" effect of NO_3^- would continue to increase as the NO_3^- continue to be formed from the decomposition of the intermediate nitrogen compounds, as is apparently the case in the present study. The photolysis of NO_3^- leads to a number of intermediate products via a complex reaction sequence, and includes the formation of nitrite, NO_2^- (Sharpless, Page and Linden 2003). Since NO_2^- reacts rapidly with ·OH radicals, and the photolysis of NO_2^- results in formation of NO· radicals which also react rapidly with ·OH radicals, the formation of nitrates ultimately leads to a strong radical scavenging effect as noted by Park et al. (2007). The high reaction rate of NO_2^- with ·OH radicals also explains the absence of the NO_2^- peak in the ion chromatography analysis, since it would be expected that any NO_2^- formed would have been completely reacted. Therefore, in the UV/H_2O_2 treatment of MEA or any other alkanolamines, the formation of nitrates is an important consideration as it can potentially affect the desired COD reduction by being an effective "inner filter" and also by the radical scavenging effect, especially if polychromatic UV sources are used

which have significant emission peaks at the wavelengths where nitrate absorption is much greater.
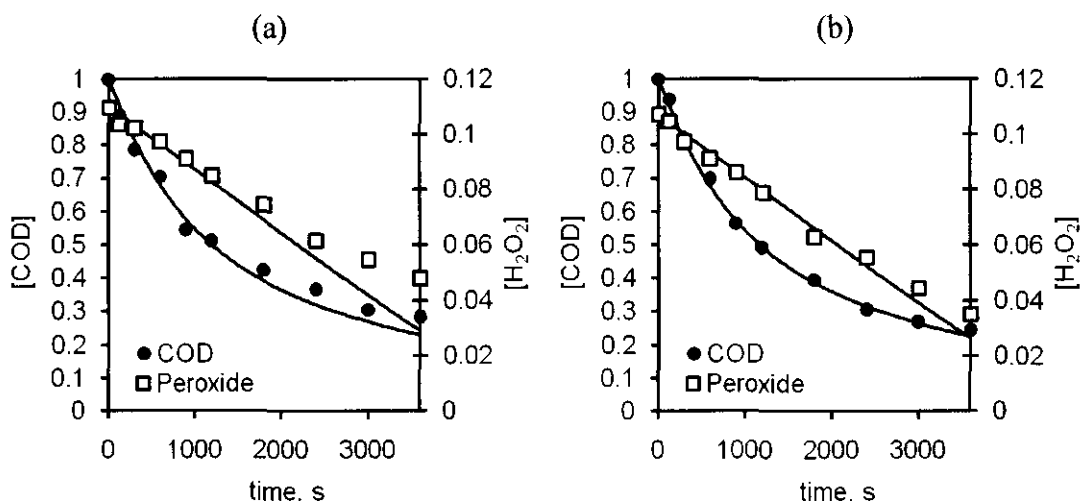
Figure 4-10: Examples of experimental run data plotted against model prediction ([KH$_2$PO$_4$] = 8 mM, [H$_2$O$_2$]$_0$ = 0.11 M, T = 28 deg. C, Φ_{UV} = 4.13 W) for (a) initial pH =2 and (b) initial pH = 4.

4.3.5. Conclusions

A quasi-mechanistic kinetic rate model was described to predict the COD degradation rate and H$_2$O$_2$ concentration in MEA treatment using UV/H$_2$O$_2$ process, based on established literature values for the principal reactions involved, to which is added the n-th order reaction of the substrate (COD) with ·OH radical. The model was optimized using the MEA experimental run data and a generalized form was tested with the experimental data. It was found that the model was in good agreement with the observed data. The model confirms that the pH dependence of the rate of COD degradation is a consequence of the property of unidentified reactive intermediates, and not as a result of effect of the higher UV molar absorption of H$_2$O$_2$ at high pH. Since the approach to the model derivation (using n-th order reaction with the ·OH radical) is relatively simple and the results were shown to be reasonably accurate, the approach could potentially be used in the description and prediction of other pollutants by the UV/H$_2$O$_2$ process, especially in cases where the gross organic content rather than individual compounds is of greater concern. In conclusion, the UV/H$_2$O$_2$ process as a method to decompose MEA and other alkanolamines in

wastewater has a high potential to be an effective solution. However, the effect of nitrate formation, the reaction pathways, the pH dependence of intermediates and other aspects such as effects of inorganic carbon radical scavengers have yet to be studied and further investigation into these areas is recommended.

4.4. Effect of UV/H$_2$O$_2$ Advanced Oxidation Pretreatment on Aerobic Biodegradation

To determine the effect of UV/H$_2$O$_2$ AOP pretreatment to the biodegradability of MEA solution, partially degraded MEA was prepared by UV/H$_2$O$_2$ treatment of MEA in which the COD was reduced from 9000 mg/l to 6080 mg/l. Residual H$_2$O$_2$ was then removed by raising the pH (> 10) and moderate heating for approximately 5 hours. The pretreated MEA was then diluted in the aerobic bioreactor with distilled water, mineral medium and bacterial seed to achieve COD of approximately 900 mg/L as described in Chapter 3.1.3. The same procedure was applied for untreated MEA solution and blank solution.

4.4.1. Kinetic model for substrate degradation and biomass growth

The Monod equation, described in Chapter 2.2.3.4, was used in this work to describe the microbiological growth rate and organic degradation rate. To obtain the kinetic coefficients which describes the Monod equation, biomass (X) and concentration (S) vs. time data were fitted to a sigmoid equation of the form indicated in equation (4-20), which adequately describes the lag, acceleration, exponential, declining and stationary phases of biomass growth. The sigmoid equation is similar to the form used by Cabrero et al. (1998) in their experiment to model activated sludge bacterial growth, but in this present work, the exponential term was used instead of the half-life term. During the observation of the effects of changing the parameter values in equation (4-20), it was found that the coefficients k represent the slope of the sigmoid, a represents the distance from the lag to the stationary phase, b relates to the acclimatization time and c represents the initial biomass concentration or the final substrate concentration as shown in Figure 4-11 and Figure 4-12.
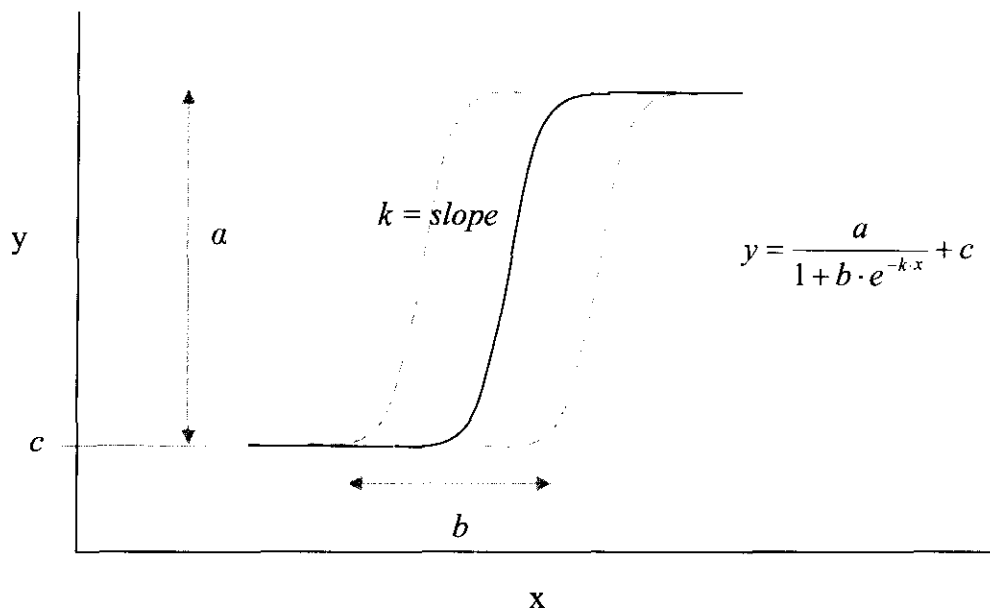
Figure 4-11: Sigmoid curve used for describing biomass growth

$$y = \frac{a}{1 + b \cdot e^{-k \cdot x}} + c$$
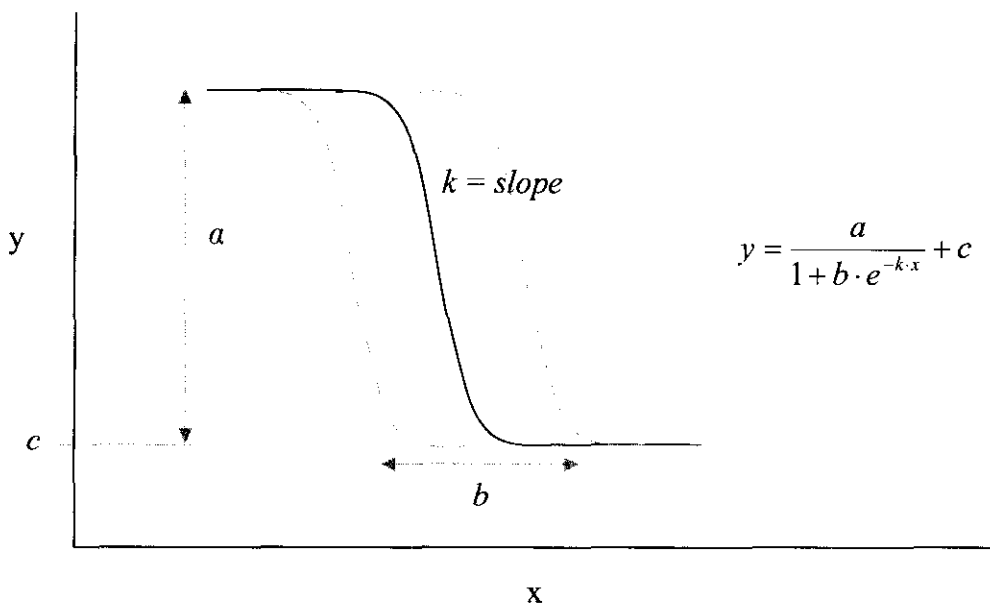
Figure 4-12: Sigmoid curve used for describing substrate utilisation

$$y = \frac{a}{1 + b \cdot e^{-k \cdot x}} + c$$

80

The best fit of the sigmoid equation to the actual measured values was obtained using the Solver tool in Microsoft ® Office Excel 2003 by minimizing the residual sum-of-squares between the actual and predicted values. Trial-and-error method was used to determine the best initial conditions to arrive at a good optimum fit based on visual judgement.

$$y = \frac{a}{b + e^{-kt}} + c \qquad (4\text{-}20)$$

Once the sigmoid equation has been fitted and the sigmoid coefficients obtained, the slope of equation (4-20) can then be calculated by differentiation to obtain equation (4-21) below.

$$\frac{dy}{dt} = \frac{a \cdot b \cdot k \cdot e^{-kt}}{\left(1 + b^{-kt}\right)^2} \qquad (4\text{-}21)$$

The specific growth rate is calculated from equation (2-3) by dividing equation (4-21) with the predicted biomass concentration at each designated time. Taking the inverse of equation (2-5) yields the following equation.

$$\frac{1}{\mu} = \frac{K_S}{\mu_{max}} \cdot \frac{1}{S} + \frac{1}{\mu_{max}} \qquad (4\text{-}22)$$

A plot of $1/\mu$ vs. $1/S$ will yield a straight line with slope K_S/μ_{max} and y-intercept $1/\mu_{max}$. To obtain the values of μ_{max} and K_S, a linear fit is found using principles of linear regression, also using tools available in Microsoft ® Excel. The biomass yield, $Y_{X/S}$ can then be calculated by dividing the total biomass growth by the substrate consumed (i.e. a_X/a_{COD}). The maximum substrate utilisation rate, or k_{max} can be estimated using equation (4-23).

$$k_{max} = \frac{\mu_{max}}{Y_{X/S}} \qquad (4\text{-}23)$$

4.4.2. Results of post AOP biological treatment based on Monod model

Figure 4-13 shows the biomass and substrate profile and fitted sigmoid curve for degradation of both untreated MEA solution and AOP-pretreated MEA solution. It is apparent from visual comparison of the curves that the biomass growth rate and the COD degradation rate are reduced for the pre-treated MEA compared to the untreated MEA. Acclimatization times (i.e. time taken until biomass growth initiates) does not seem to be affected by the AOP pretreatment. It is also apparent that the yield of biomass and the completeness of substrate degradation are also reduced in the pretreated MEA compared to the treated MEA solution. This suggests that the biodegradability of MEA solution is actually detrimentally affected by pretreating the solution using UV/H₂O₂ process.
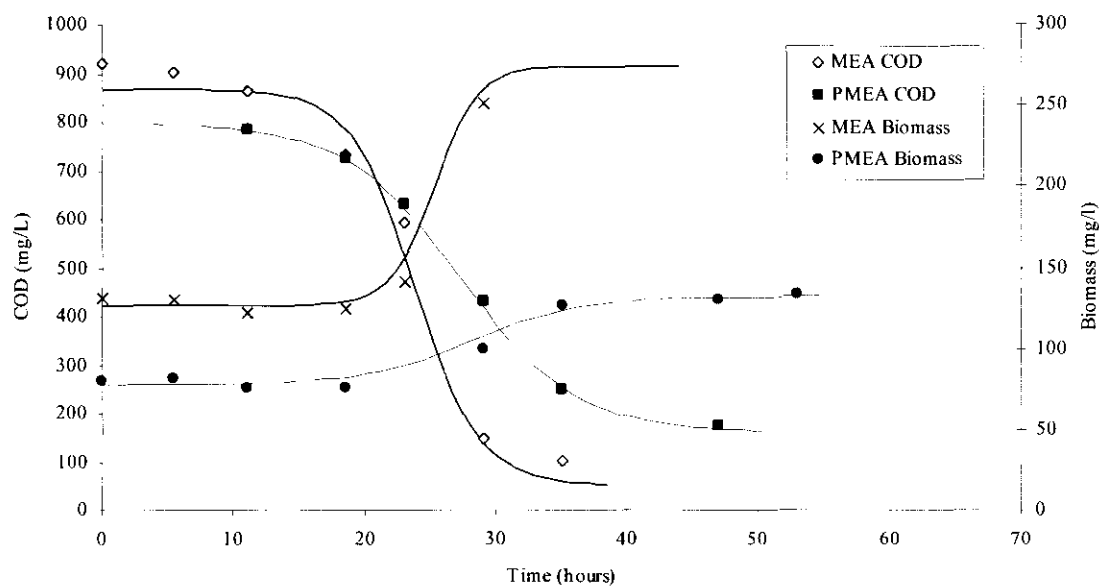
Figure 4-13: Biomass growth and organic removal for AOP-pretreated and untreated MEA solution

82

Table 4-7: Fitted sigmoid coefficients for biomass growth and substrate utilisation (organic degradation) rate

Coefficient.	Biomass growth		Substrate utilisation	
	MEA	Pretreated MEA	MEA	Pretreated MEA
k	0.60	0.25	-0.41	-0.23
a	147.7	54.1	815.1	637.5
b	4.06E+06	1.09E+03	5.67E-05	2.00E-03
c	126.7	78.0	52.0	160.2

Table 4-7 shows the values of the fitted sigmoid coefficients used to plot the biomass and substrate profile in Figure 4-13. Using these coefficients, the linearized Monod's equation could be calculated to determine the Monod coefficients. Table 4-8 shows the calculated data used to plot the linearized Monod equation for MEA and pretreated MEA biodegradation. Since the Monod expression is an approximation of the batch growth process and assumes that the lag, acceleration and declining growth phases do not exist (Striggul, Dette and Melas 2009), the calculations were based on model data during the exponential phase only. It was also found that outside of that region, the plot of $1/\mu$ against $1/S$ ceases to exhibit linear behaviour.

Table 4-8: Calculated data for plotting of the linearized Monod expression to determine the Monod coefficients

t (h)	X (mg/l)	COD (mg/l)	S (mg/l)	dX/dt (mg/l/h)	u (h⁻¹)	-dS/dt (mg/l/h)	k (h⁻¹)	1/S (l/mg)	1/u (h)	1/k (h)
Untreated MEA										
25.0	190.8	372.1	320.1	21.80	0.114	-79.7	0.418	0.00312	8.76	2.39
25.3	199.7	340.8	288.8	22.17	0.111	-76.5	0.383	0.00346	9.00	2.61
25.7	206.3	318.3	266.3	22.04	0.107	-73.5	0.356	0.00376	9.36	2.81
26.0	212.8	296.7	244.7	21.56	0.101	-70.2	0.330	0.00409	9.87	3.03
26.3	221.3	269.6	217.6	20.43	0.092	-65.4	0.296	0.00460	10.83	3.38
26.7	227.2	250.5	198.5	19.28	0.085	-61.6	0.271	0.00504	11.78	3.69
27.0	232.8	232.6	180.6	17.94	0.077	-57.7	0.248	0.00554	12.97	4.04
27.3	239.6	210.6	158.6	15.97	0.067	-52.4	0.219	0.00630	15.00	4.57
27.7	244.2	195.5	143.5	14.44	0.059	-48.5	0.199	0.00697	16.91	5.04
28.0	248.3	181.5	129.5	12.92	0.052	-44.7	0.180	0.00772	19.22	5.56
AOP-pretreated MEA										
30.0	110.9	387.7	227.5	3.20	0.029	-33.3	0.300	0.00440	34.61	3.33
30.4	112.4	371.3	211.1	3.11	0.028	-32.1	0.286	0.00474	36.19	3.50
30.9	113.7	358.7	198.5	3.02	0.027	-31.1	0.274	0.00504	37.68	3.66
31.3	115.1	343.5	183.3	2.89	0.025	-29.7	0.258	0.00546	39.85	3.88
31.8	116.3	331.8	171.6	2.78	0.024	-28.5	0.245	0.00583	41.85	4.08
32.2	117.6	317.9	157.7	2.63	0.022	-27.0	0.230	0.00634	44.73	4.36
32.7	118.7	307.4	147.2	2.51	0.021	-25.8	0.217	0.00679	47.35	4.61
33.1	119.9	294.9	134.7	2.35	0.020	-24.2	0.202	0.00742	51.07	4.96
33.6	120.8	285.5	125.3	2.22	0.018	-22.9	0.190	0.00798	54.43	5.27
34.0	121.6	276.6	116.4	2.09	0.017	-21.6	0.178	0.00859	58.18	5.62

Figure 4-14 shows the linearized Monod plot for the aerobic biodegradation of both MEA and pretreated MEA. Based on the slope and y-intercept of the plot, the Monod kinetic coefficients could be calculated and the values are shown in Table 4-9. The data shows that the maximum specific biomass growth rate and the maximum specific substrate utilization rate are markedly reduced by pre-oxidation of the MEA solution using the UV/H₂O₂ process. The biomass yield was also reduced by half in the pre-treated MEA biodegradation. This confirms the visual indication from the biomass/substrate – time plots which seem to show a general decrease in biodegradability. The reduction in the half-saturation coefficient, K_S for pre-treated MEA may suggest that the biomass affinity for the substrate has increased. However, for practical bioreactors, a low K_S value is generally not preferred since this indicates sensitivity of the growth rate to small changes in the substrate concentration, which would lead to reduced stability of the bioreactor operations (Orhon and Artan 1994).
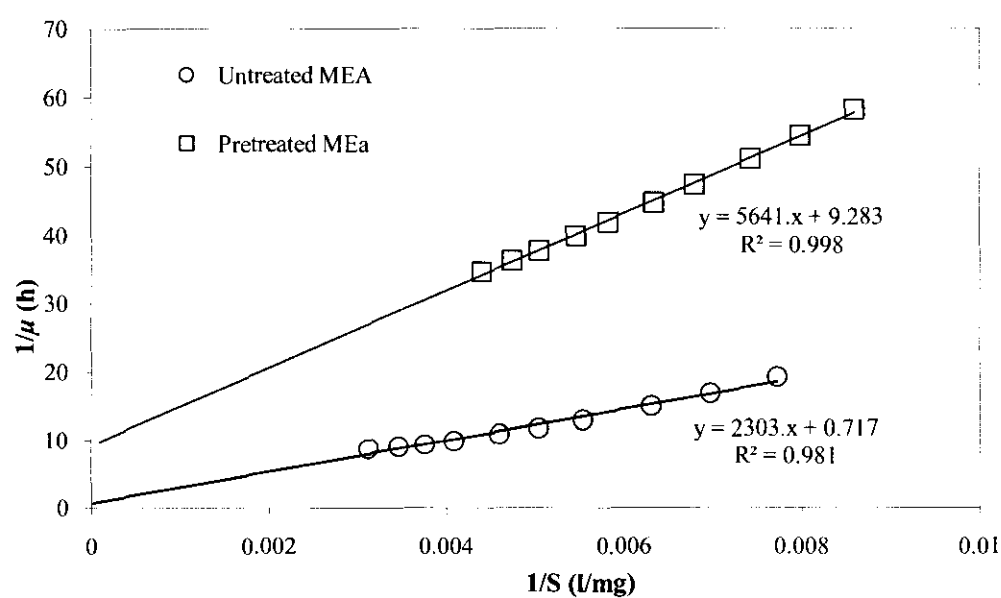
Figure 4-14: Linearized Monod plots for MEA and Pretreated MEA

Table 4-9: Monod coefficients for untreated and AOP-pretreated MEA

	μ_{max} (h⁻¹)	K_s (mg/l)	$Y_{X/S}$	k_{max} (h⁻¹)
MEA	1.39	3210.7	0.181	7.69
Pretreated MEA	0.11	607.7	0.085	1.27

At this point, it is not known what has caused the reduction in biodegradability after AOP treatment as indicated by the Monod coefficients. The most probable cause is the formation of chemical by-product of the radical oxidation such as formaldehyde that is actually toxic to the microbial community in the aerobic bioreactor. AOP involves the action of the highly reactive ·OH radical, which rapidly and non-selectively reacts with organic compounds and typically generates a wide and complex range of degradation products, some of which may be highly inhibitory to microbial growth, while most others may be quite biodegradable. However, since MEA itself is considered to be generally biodegradable, even small amounts of inhibitory compounds can lead to a reduction in the overall biological degradation rate.

4.4.3. Ammonia formation

Measurements of ammonia were also conducted to determine the extent of ammonia formation from the hydrolysis of the nitrogenous compounds. It should be noted that the pre-oxidation of MEA actually resulted in the formation of high concentrations of ammonia, at approximately 935 mg/l. However, prior to aerobic biodegradation, all of the ammonia was removed in the process for the removal of residual H_2O_2, which was found to greatly inhibit the biomass growth in a previous test run. Figure 4-15 shows the ammonia formation at different biodegradation times. Ammonia measurement was not taken for MEA at 47 hours due to reaction completion after approximately 40 hours. It is clear that ammonia is generated in significant amounts both for pretreated and untreated MEA with maximum values approximately 250 mg/L N as ammonia. This value is approximately equal to the theoretical concentration of ammonia that is potentially generated if all of the nitrogen in the MEA compound is converted to ammonia based on 1 mole of MEA producing 1 mole of NH_3 from stoichiometry. Therefore, it appears that the bacteria population used in this experiment is able to completely hydrolyze the organic nitrogen in the MEA solution to ammonia. For pretreated MEA, it is not known the amount of organic nitrogen at the start of the biodegradation, since the proportion of nitrogen has changed from the advanced oxidation process.
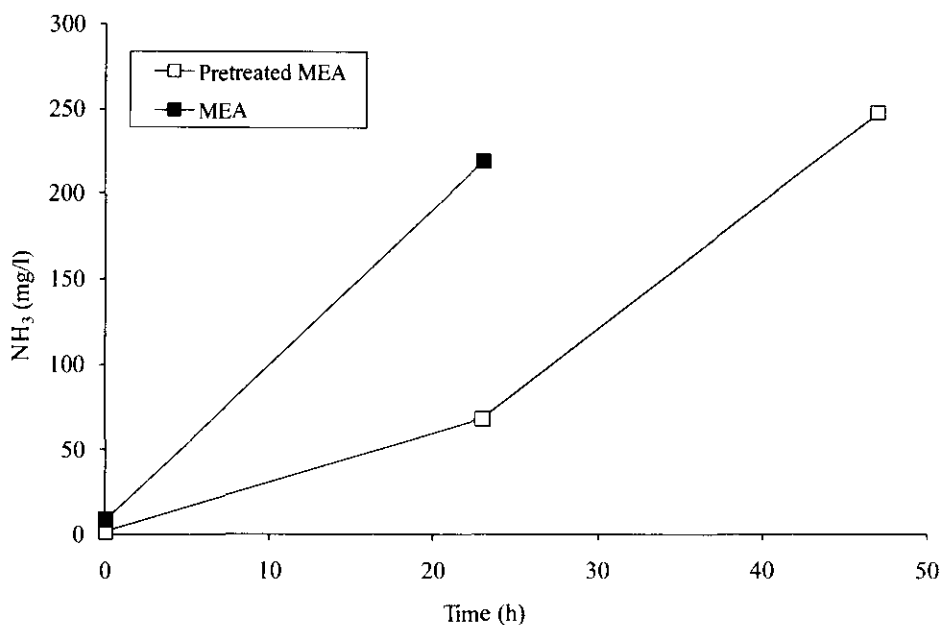
Figure 4-15: Ammonia formation during aerobic biodegradation of MEA and pretreated MEA.

The high concentrations of ammonia that was generated from aerobic biodegradation of MEA and pretreated MEA have a number of practical consequences. Firstly, environmental regulations usually prohibit high concentrations of ammonia to be discharged into waterways, primarily due to the potential of causing excessive algal growth or eutrophication and also due to odor issues. Also, advanced oxidation pretreatment of MEA waste solutions will lead to high levels of ammonia, which would increase the pH of the solution necessitating chemical pH adjustment to ensure the downstream biological treatment system is not adversely affected. To remove the ammonia from the wastewater, specific ammonia removal treatment processes may be necessary either at the discharge of the AOP or at the final discharge. This can be achieved by means of air stripping of the wastewater stream at high pH (>11) or by modifying the biological treatment process to include nitrification and denitrification (by the combination of anoxic and aerobic processes) to completely convert the ammonia to nitrogen gas (Metcalf & Eddy Inc. 2003).

86

4.4.4. Conclusions

The biodegradability of MEA solution that has been partially degraded via UV/H_2O_2 was studied using batch growth reactor operated under aerobic conditions. The kinetic rate constants based on the Monod model, namely the maximum specific biomass growth, maximum specific substrate utilisation, half-saturation coefficient and yield constant, were calculated and formed the basis of comparison. The biomass concentration was determined by measurement of solids concentration, which was correlated to solution turbidity. The total substrate concentration was based on COD. Using the batch data, the kinetic constants were determined by fitting the growth and utilisation data to a sigmoid equation to determine the slope which correspond to the specific rates. The acclimatization times were also studied. The results indicated that, for MEA solution which was partially treated with UV/H_2O_2 at 30% COD degradation, the acclimatization time for aerobic biodegradation was unaffected. However, the estimated Monod kinetic constants showed that the biomass growth rate, substrate utilisation rate and biomass yield was reduced for the partially treated MEA compared to untreated MEA. The half-saturation coefficient was also reduced indicating reduced operational stability for pretreated MEA compared to untreated MEA. This effect may be attributed to the formation of some unidentified inhibitory compound at the level of pretreatment that was applied. Biodegradation of both MEA and partially treated MEA was found to generate high levels of ammonia as by-product.

CHAPTER 5

CONCLUSIONS AND RECOMMENDATIONS

5.1. Conclusions

In the present work, the kinetics and parametric effects in the degradation of MEA using UV/H_2O_2 advanced oxidation process was studied in terms of both substrate and organic removal. Biological treatment of pre-oxidized MEA was also investigated. From these studies, the following conclusions can be drawn:

1. The most significant factor affecting the COD removal in the process is the UV flux. Increasing UV flux will significantly increase the COD removal rate and this can be achieved by use of high output UV lamps such as low-pressure high output lamps or medium-pressure lamps. Increasing UV flux also results in higher MEA degradation rates.

2. The pH of solution is an important factor in the process. In particular, increasing the solution pH from 2 – 9 results in significant increase in COD removal rates, but do not seem to affect the MEA degradation rate. The mechanism for this pH dependence is most likely due to the formation of intermediate by-products which have pH-dependent kinetic removal rates. However, in most wastewaters with natural alkalinity, higher pH will result in the increase in bicarbonate and carbonate ions, which will have a large radical scavenging effect.

3. H_2O_2 concentration also significantly affects the COD removal rate with optimum concentration in the range of 0.05 - 0.16 M. Further increase in H_2O_2

dose results in significant scavenging of the ·OH radical, reducing the overall organic degradation rate.

4. The formation of nitrate and formate was identified as by-products of the UV/H$_2$O$_2$ treatment of MEA. These acidic species explain the large pH depression that was observed during the course of the experimental runs.

5. A quasi-mechanistic model was developed to describe the kinetics of COD degradation and H$_2$O$_2$ decay observed in the experiments. The model utilizes empirical "lumped" n-th order reaction for COD in combination with literature values of rate constants for principal reactions involved in the UV-induced radical reactions. The model was validated using experimental data and was found to be in good agreement. The model also confirms that pH dependence is likely due to the effects of by-products.

6. Pre-oxidation of MEA using UV/H$_2$O$_2$ resulted in a decrease in biodegradability, as indicated by the Monod rate constants in a batch aerobic bioreactor, when compared with untreated controls. It is likely that formation of biologically inhibitory by-products occur during the AOP treatment. Significant concentrations of ammonia was also formed both during UV/H$_2$O$_2$ pretreatment and during biological oxidation with important consequences for process selection.

5.2. Recommendations

The following recommendations are made:

1. Further studies using actual wastewaters containing MEA should be conducted to evaluate the effects of other constituents, particularly known radical scavengers such as inorganic carbon species and humic acids. Additionally, studies into the fate of nitrogen in the course of the breakdown of the amine is important due to its various effects such as role as "inner filter" of UV.

89

2. More insight into the breakdown products should be obtained by means of analytical instrumentation with greater sensitivity and ease of use such as LC-MS to elucidate the reaction mechanism in more detail. Such studies could help to explain the processes involved during oxidation and shed light into the influence of oxidation by-products on pH dependence and other factors.

3. From the results, it is clear that a careful study should be conducted if AOPs are intended to be used for improving biodegradability. It is recommended that any attempt to introduce AOPs as a pre-treatment system for a biological process must be preceded with detailed biokinetics studies at different pretreatment levels to ensure that toxicity effects are well-understood. Factors such as formation of ammonia or nitrates as well as issues such as residual peroxide removal should also be given due consideration.

4. The kinetic model for UV/H_2O_2 developed in the present work has a potential to be generalized for the degradation of other compounds, since it is based on gross organic content. However, the model could be made more complete by incorporating reactions from common radical scavengers.

5.3. Contribution of this thesis

This work is the first published study in the author's knowledge, of the use of UV/H_2O_2 process to treat MEA solution both as a standalone process or as a pretreatment to biological oxidation.

In addition to establishing the feasibility of AOP for MEA degradation, the thesis addresses the effects of various important parameters relevant to the process, such as the pH, temperature, UV flux and H_2O_2 concentration and suggests plausible theoretical considerations to describe those effects. Some insight was also gained into the possible effects of byproducts such as organic acids and ammonia to the effectiveness of the treatment process.

Another significant contribution of the thesis is the development of a relatively simple kinetic model which could be used to predict the behaviour of the treatment process.

In theory, this approach can also be used for modeling of UV/H_2O_2 treatment of other substrates since it is based on gross organic degradation, rather than a particular chemical target compound.

Lastly, this thesis highlights the importance of detailed studies of AOP processes for biological pretreatment, especially with nitrogen-containing compounds such as amines, to ensure that inhibitory byproducts do not interfere with the subsequent biological oxidation process.

REFERENCES

[1] Abdi, M Abedinzadegan. "Improve contaminant control in amine systems." *Hydrocarbon Processing*, no. 80 (10) (2001).

[2] Adams, C D, and J J Kuzhikannil. "Effects of UV/H₂O₂ preoxidation on the aerobic biodegradability of quarternary amine surfactants." *Water Research* 34, no. 2 (2000): 668-672.

[3] Alfano, O M, R J Brandi, and A E Cassano. "Degradation kinetics of 2,4-D in water employing hydrogen peroxide and UV radiation." *Chemical Engineering Journal* 82 (2001): 209-218.

[4] Andreozzi, R, V Caprio, A Insola, and R Marotta. "Advanced oxidation processes (AOP) for water purification and recovery." *Catalysis Today* 53 (1999): 51-59.

[5] Andreozzi, R, V Caprio, A Insola, R Marotta, and R Sanchirico. "Advanced oxidation processes for the treatment of mineral-oil contaminated wastewaters." *Water Research* 34, no. 2 (2000): 620-628.

[6] Andreozzi, R, V Caprio, R Marotta, and A Radovnikovic. "Ozonation and H2O2/UV treatment of clofibric acid in water: a kinetic investigation." *Journal of Hazardous Materials* B103 (2003): 233-246.

[7] Antony, J. *Design of Experiments for Engineers and Scientists* . Oxford: Butterworth-Heinemann, 2003.

[8] Arslan-Alaton, Idil, Emine Ubay Cokgor, and Baris Koban. "Integrated photochemical and biological treatment of a commercial textile surfactant: Process optimization, process kinetics and COD fractionation." *Journal of Hazardous Materials*, no. 146 (2007): 453-458.

[9] Asano, Takashi, Metcalf & Eddy, Harold L Leverenz, Ryujiro Tsuchihashi, and George Tchobanoglous. *Water reuse: issues, technologies and applications.* McGraw Hill Professional, 2007.

[10] Beltran, F J, J F Garcia-Araya, and P M Alvarez. "pH sequential ozonation of domestic and wine distillery wastewaters." *Water Research* 35, no. 4 (2001): 929-936.

[11] Beltran, F J, J M Encinar, and J F Gonzalez. "Industrial wastewater advanced oxidation. Part 2. Ozone combined with hydrogen peroxide or UV radiation." *Water Research* 31, no. 10 (1997): 2415-2428.

[12] Bijan, L, and M Mohseni. "Integrated ozone and biotreatment of pulp mill effluent and changes in biodegradability and molecular weight distribution of organic compounds." *Water Research* 39 (2005): 3763–3772.

[13] Boye, B, E Brillas, and M M Dieng. "Anodic oxidation, electro-Fenton and photoelectro-Fenton treatments of 2,4,5-trichlorophenoxyacetic acid." *Journal of Electroanalytical Chemistry* 557 (2003): 135-146.

[14] Brillas, E, J C Calpe, and J Casado. "Mineralization of 2,4-D by advanced electrochemical oxidation processes." *Water Research* 34 (2000): 2253-2262.

[15] Cabrero, Alberto, Sara Fernandez, Fernando Mirada, and Julian Garcia. "Effects of copper and zinc on the activated sludge bacteria growth kinetics." *Water Research* 32, no. 5 (1998): 1355-1362.

[16] Canizares, P, R Paz, J Lobato, C Saez, and M A Rodrigo. "Electrochemical treatment of the effluent of a fine chemical manufacturing plant." *Journal of Hazardous Materials* B138 (2006): 173-181.

[17] Catalkaya, E C, and F Sengul. "Application of Box–Wilson experimental design method for the photodegradation of bakery's yeast industry with UV/H_2O_2 and UV/H_2O_2/Fe(II) process." *Journal of Hazardous Materials* B128 (2006): 201-207.

[18] Catalkaya, Ebru Cokay, and Fikret Kargi. "Color, TOC and AOX removals from pulp mill effluent by advanced oxidation processes: A comparative study." *Journal of Hazardous Materials* B139 (2007): 244–253.

[19] Chen, G. "Electrochemical technologies in wastewater treatment." *Separation and Purification Technology* 38 (2004): 27.

[20] Chidambara Raj, C B, and Han Li Quen. "Advanced oxidation processes forwastewater treatment: Optimization of UV/H_2O_2 process through a statistical technique." *Chemical Engineering Science* 60 (2005): 5305 – 5311.

[21] Clescerl, L S, A E Greenberg, and A D Eaton, . *Standard Methods for the Examination of Water and Wastewater*. 20th Edition. Baltimore: American Public Health Association, 1999.

[22] Cokgor, E U, I A Alaton, O Karahan, S Dogruel, and D Orhon. "Biological treatability of raw and ozonated penicillin formulation effluent." *Journal of Hazardous Materials* B116 (2004): 159–166.

[23] Crittenden, J C, R R Trussell, D W Hand, K J Howe, and G Tchobanoglous. *Water treatment: principles and design*. 2nd Edition. New Jersey: John Wiley and Sons, 2005.

[24] Crittenden, J C, S Hu, D W Hand, and S A Green. "A kinetic model for H_2O_2/UV process in a completely mixed batch reactor." *Water Research* 33, no. 10 (1999): 2315-2328.

[25] Doble, Mukesh, and Anil Kumar. *Biotreatment of Industrial Effluents*. Oxford: Elsevier Butterworth-Heinemann, 2005.

[26] Esplugas, S, J Gimenez, S Contreras, E Pascual, and M Rodriguez. "Comparison of different advanced oxidation processes for phenol degradation." *Water Research* 36 (2002): 1034–1042.

[27] Farrokhi, M, A R Mesdaghinia, S Naseri, and A R Yazdanbakhsh. "Oxidation of pentachlorophenol by Fenton's reagent." *Iranian Journal of Public Health* 32, no. 1 (2003): 6-10.

[28] Gas Processors Suppliers Association. *Engineering Data Book.* 12th Edition. Vol. II. Tulsa: Gas Processors Suppliers Association, 2004.

[29] Glaze, W H, F Beltran, T Tuhkanen, and J W Kang. "Chemical models of advanced oxidation processes." *Water Poll. Res. J. Canada* 27, no. 1 (1992): 23-42.

[30] Glaze, W H, Y Lay, and J W Kang. "Advanced oxidation processes. A kinetic model for the oxidation of 1,2 dibromo-3-chloropropane in water by the combination of hydrogen peroxide and UV radiation." *Ind. Eng. Chem. Res.* 34 (1995): 2314-2323.

[31] Glaze, William H, Joon-Wun Kang, and Douglas H Chapin. "The chemistry of water treatment processes involving ozone, hydrogen peroxide and ultrraviolet radiation." *Ozone Science & Engineering* 9 (1987): 335-352.

[32] Gottschalk, C, J A Libra, and A Saupe. *Ozonation of Water and Waste Water.* Weinheim: Wiley-VCH, 2000.

[33] Grimm, J, D Bessarabov, and R Sanderson. "Review of Electro-assisted methods for water purification." *Desalination* 115 (1998): 288.

[34] Hach Company. "Hach Methods approved/accepted by the USEPA." *Hach - Downloads - Hach Methods EPA Acceptance Letters.* 1999. http://www.hach.com/fmmimghach?/CODE%3AL7951_7-0610550%7C1 (accessed October 21, 2009).

[35] Heraeus Noblelight GmbH. "Water treatment, Low Pressure, Mercury Lamp, Disinfection Lamp, Germicidal Lamp." *Heraeus Noblelight.* http://www.heraeus-noblelight.com/fileadmin/user_upload/PDF/disinfection/Lampe_eng.pdf (accessed July 17, 2009).

[36] Huang, C R, and H Y Shu. "The reaction kinetics, decomposition pathways and intermediate formations of phenol in ozonation, UV/O$_3$, and UV/H$_2$O$_2$ processes." *Journal of Hazardous Materials* 41 (1995): 47-64.

[37] Ikehata, Keisuke, and Mohamed Gamal El-Din. "Aqueous pesticide degradation by hydrogen peroxide/ultraviolet irradiation and Fenton-type advanced oxidation processes: a review." *Journal of Environmental Engineering Science* 5 (2006): 81–135.

[38] Jeong, Joonseon, and Jeyong Yoon. "pH effect on OH radical production in photo/ferrioxalate system." *Water Research* 39 (2005): 2893–2900.

[39] Kidnay, Arthur J, and William R Parrish. *Fundamentals of Natural Gas Processing.* Boca Raton: CRC Press, 2006.

[40] Kohl, A, and R Nielsen. *Gas Purification.* Houston: Gulf Publishing Company, 1997.

[41] Koprivanac, N, and H Kusic. "AOP as an Effective Tool for Minimization of Hazardous Organic Pollutants in Colored Wastewater; Chemical and Photochemical Processes." In *Hazardous Materials and Wastewater.* New York: Nova Science Publisher, 2007.

[42] Kurniawan, T A, Wai-hung Lo, and G Y S Chan. "Radicals-catalyzed oxidation reactions for degradation of recalcitrant compounds from landfill leachate." *Chemical Engineering Journal* 125 (2006): 35–57.

[43] Kusic, Hrvoje, Natalija Koprivanac, and Ana Loncaric Bozic. "Minimization of organic pollutant content in aqueous solution by means of AOPs: UV- and ozone-based technologies." *Chemical Engineering Journal* 123 (2006): 127–137.

[44] Lazic, Z R. *Design of Experiments in Chemical Engineering: A Practical Guide.* Weinheim: Wiley-VCH, 2004.

96

[45] Leslie Grady Jr, C P, G T Daigger, and H C Lim. *Biological Wastewater Treatment.* 2nd Edition. New York: Marcel Dekker, 1999.

[46] Lin, L S, C T Johnston, and E R Blatchley III. "Inorganic fouling at quartz:water interfaces in ultraviolet photoreactors-I. Chemical characterization." *Water Research* 33, no. 15 (1999): 3321-3329.

[47] Linden, K G. "Fundamentals of UV-based advanced oxidation processes." *Proceedings of the 4th IWA Leading-Edge Conference on Water and Wastewater Technology.* Singapore, 2007.

[48] Mack, J, and J R Bolton. "Photochemistry of nitrite and nitrate in aqueous solution: a review." *Journal of Photochemistry and Photobiology A: Chemistry* 128 (1999): 1-13.

[49] Malaysian Industrial Development Authority (MIDA). *Scheduled Waste Treatment Rates.* 2008. http://www.mida.gov.my/en_v2/index.php?page=scheduled-waste-treatment-rates (accessed July 23, 2009).

[50] Martinez, Nora San Sebastián, Josep Figulz Fernández, Xavier Font Segura, and Antoni Sánchez Ferrer. "Pre-oxidation of an extremely polluted industrial wastewater by the Fenton's Reagent." *Journal of Hazardous Materials* B101 (2003): 315-322.

[51] Mendham, J, R C Denney, J D Barnes, and M J K Thomas. *Vogel's Textbook of Quantitative Chemical Analysis.* 6th Edition. Harlow: Prentice Hall, 2000.

[52] Metcalf & Eddy Inc. *Wastewater Engineering: Treatment and Reuse.* 4th. New York: McGraw-Hill, 2003.

[53] Moreno, A D. "Electro-Fenton as a feasible advanced treatment process to produce reclaimed water." *Water Science & Technology* 50 (2004): 83-90.

[54] Mrklas, O, A Chu, S Lunn, and R L Bentley. "Biodegradation of monoethanolamine, ethylene glycol and triethylene glycol in laboratory bioreactors." *Water, Air and Soil Pollution*, no. 159 (2004): 249-263.

[55] Nicole, I, J De Laat, M Dore, J P Duguet, and C Bonnel. "Use of U.V. radiation in water treatment: Measurement of photonic flux by hydrogen peroxide actinometry." *Water Research* 24, no. 2 (1990): 157-168.

[56] Oliveros, E, O Legrini, M Hohl, T Muller, and A M Braun. "Industrial waste water treatment: large scale development of a light-enhanced Fenton reaction." *Chemical Engineering and Processing* 36 (1997): 397-405.

[57] Oppenländer, T. *Photochemical purification of water and air.* Weinheim: Wiley-VCH, 2003.

[58] Orhon, D, and N Artan. *Modelling of Activated Sludge Systems.* Basel: Technomic, 1994.

[59] Park, J H, et al. "Effects of nitrate on the UV photolysis of H_2O_2 for diethyl phthalate degradation in treated effluents." *International Water Association Leading-Edge Technology Conference.* Singapore, 2007.

[60] Peternel, Igor, Natalija Koprivanac, and Hrvoje Kusic. "UV-based processes for reactive azo dye mineralization." *Water Research* 40 (2006): 525-532.

[61] Poole, A J. "Treatment of biorefractory organic compounds in wool scour effluent by hydroxyl radical oxidation." *Water Research* 38 (2004): 3458–3464.

[62] Riga, A, K Soutsas, K Ntampegliotis, V Karayannis, and G Papapolymerou. "Effect of system parameters and of inorganic salts on the decolorization and degradation of Procion H-exl dyes. Comparison of H_2O_2/UV, Fenton, UV/Fenton, TiO_2/UV and TiO_2/UV/H_2O_2 processes." *Desalination* 211 (2007): 72–86.

[63] Robins, G, A Houston, and J Sevigny. "Freshwater aquatic toxicity of the alkanolamines MEA, DEA, TEA, and DIPA." *Proceedings of the Society of Environmental Toxicology and Chemistry's 23rd Annual Meeting.* 2002.

[64] Rosenfeldt, E J, K G Linden, S Canonica, and U von Gunten. "Comparison of the efficiency of OH radical formation during ozonation and the advanced oxidation processes O_3/H_2O_2 and UV/H_2O_2." *Water Research* 40 (2006): 3695-3704.

[65] Roy, R K. *Design of experiments using the Taguchi approach: 16 steps to product and process improvements.* New York: John Wiley and Sons, 2001.

[66] Sanders, Roy E. *Chemical Process Safety: Learning From Case Histories.* Boston: Butterworth-Heinemann, 1999.

[67] Sarria, Victor, Sandra Parra, Nevenka Adler, Paul Peringer, Norberto Benitez, and Cesar Pulgarin. "Recent developments in the coupling of photoassisted and aerobic biological processes for the treatment of biorecalcitrant compounds." *Catalysis Today*, no. 76 (2002): 301-315.

[68] Sauer, T P, L Casaril, A L B Oberziner, H J Jose, and R F P M Moreira. "Advanced oxidation processes applied to tannery wastewater containing Direct Black 38—Elimination and degradation kinetics." *Journal of Hazardous Materials* B135 (2006): 274–279.

[69] Sharpless, C M, M A Page, and K G Linden. "Impact of hydrogen peroxide on nitrite formation during UV disinfection." *Water Research*, 2003: 4730–4736.

[70] Shemer, H, and K G Linden. "Degradation and by-product formation of diazinon in water during UV and UV/H_2O_2 treatment." *Journal of Hazardous Materials* B136 (2006): 553-559.

[71] Shemer, H, and K G Linden. "Photolysis, oxidation and subsequent toxicity of a mixture of polycyclic aromatic hydrocarbons in natural waters." *Journal of Photochemistry and Photobiology A: Chemistry* 187 (2007): 186-195.

[72] Sires, I, J A Garrido, R M Rodriguez, E Brillas, N Oturan, and M A Oturan. "Catalytic behavior of the Fe^{3+}/Fe^{2+} system in the electro-Fenton degradation of the antimicrobial chlorophene." *Applied Catalysis B*, 2007: 382-294.

[73] Striggul, Nikolay, Holger Dette, and Viatcheslav B Melas. "A practical guide for optimal designs of experiments in the Monod model." *Environmental Modelling & Software* 24, no. 9 (2009): 1019-1026.

[74] Suh, J H, and M Mohseni. "A study on the relationship between biodegradability enhancement and oxidation of 1,4-dioxane using ozone and hydrogen peroxide." *Water Research* 38 (2004): 2596–2604.

[75] Sundstrom, D W, H E Klei, T A Nalette, D J Reidy, and B A Weir. "Destruction of Halogenated Aliphatics by Ultraviolet Catalyzed Oxidation with Hydrogen Peroxide." *Hazardous Waste and Hazardous Materials* 3, no. 1 (1986): 101-110.

[76] Sutherland, J, C Adams, and J Kekobad. "Treatment of MTBE by air stripping, carbon adsorption, and advanced oxidation: technical and economic comparison for five groundwaters." *Water Research* 38 (2004): 193-205.

[77] Tekin, H, et al. "Use of Fenton oxidation to improve the biodegradability of a pharmaceutical wastewater." *Journal of Hazardous Materials* 136, no. 2 (2006): 258-265.

[78] The Dow Chemical Company. *Dow Specialty Amines - Literature.* January 12, 2007. [1] http://www.dow.com/PublishedLiterature/dh_0051/0901b80380051133.pdf?filepath=productsafety/pdfs/noreg/233-00265.pdf&fromPage=GetDoc (accessed July 16, 2009).

[79] Thiruvenkatachari, R, T O Kwon, J C Jun, S Balaji, M Matheswaran, and I S Moon. "Application of several advanced oxidation processes for the destruction of terephthalic acid (TPA)." *Journal of Hazardous Materials* 142 (2007): 308–314.

[80] Tizaoui, C, L Bouselmi, L Mansouri, and A Ghrabi. "Landfill leachate treatment with ozone and ozone/hydrogen peroxide systems." *Journal of Hazardous Materials* 140 (2007): 316–324.

[81] United States Department of Energy. *Malaysia Energy Data, Statistics and Analysis - Oil, Gas, Electricity, Coal.* September 2009. http://www.eia.doe.gov/cabs/Malaysia/NaturalGas.html (accessed August 4, 2010).

[82] US EPA. "Fate, Transport and Transformation Test Guidelines." *Zahn-Wellens/EMPA Test.* no. OPPTS 835.3200. 1998.

[83] von Gunten, Urs. "Ozonation of drinking water: Part I. Oxidation kinetics and product formation." *Water Research* 37 (2003): 1443–1467.

[84] Wang, G S, S T Hsieh, and C S Hong. "Destruction of humic acid in water by UV light-catalyzed oxidation with hydrogen peroxide." *Water Research* 34, no. 15 (2000): 3882-3887.

[85] Wenzel, A, A Gahr, and R Niessner. "TOC-removal and degradation of pollutants in leachate using a thin-film photoreactor." *Water Research* 33, no. 4 (1999): 937-946.

[86] Woodard, Frank. "Methods for Treating Wastewaters From Industry." In *Industrial Waste Treatment Handbook*, by Frank Woodard, 219-396. Boston: Butterworth-Heinemann, 2001.

[87] Wright, N, M Potter, N Bains, and M Goosey. "A new method for destroying organic contaminants and recycling wastewater from printed circuit board manufacturing process effluent streams." *Circuit World* 29, no. 4 (2003): 34-41.

[88] Xu, B, N Gao, H Cheng, S Xia, M Rui, and D Zhou. "Oxidative degradation of dimethyl phthalate (DMP) by UV/H2O2 process." *Journal of Hazardous Materials*, 2008: doi:10.1016/j.jhazmat.2008.05.122.

[89] Yassir, M Ammar. *Personal communication.* Bintulu: Malaysia LNG Sdn. Bhd, June 20, 2006.

[90] Zhang, H, D Zhang, and J Zhou. "Removal of COD from landfill leachate by electro-Fenton method." *Journal of Hazardous Materials* B135 (2006): 106-111.

PUBLICATIONS

1. Mohd Ariff, I F, P N F Megat Khamaruddin, S Harimurti and B K Dutta. "Optimisation of UV/H_2O_2 Treatment of Monoethanolamine Using the Taguchi Method of Experimental Design." *Proceedings of the International Conference on Environmental Research and Technology (ICERT),* Penang (2008).

2. Mohd Ariff, I F and B K Dutta. "Effect of pH and temperature on UV/H_2O_2 advanced oxidation treatment of monoethanolamine." *National Postgraduate Conference (NPC),* Perak (2009).

3. Mohd Ariff, I F. "Effect of UV/H_2O_2 Advanced Oxidation on the Aerobic Biodegradability of Monoethanolamine Solution." *International Water Association Malaysia Young Water Professionals Conference (IWAYWP),* Kuala Lumpur (2010).

Appendix A: Hydrogen peroxide actinometric measurements of photoreactor system
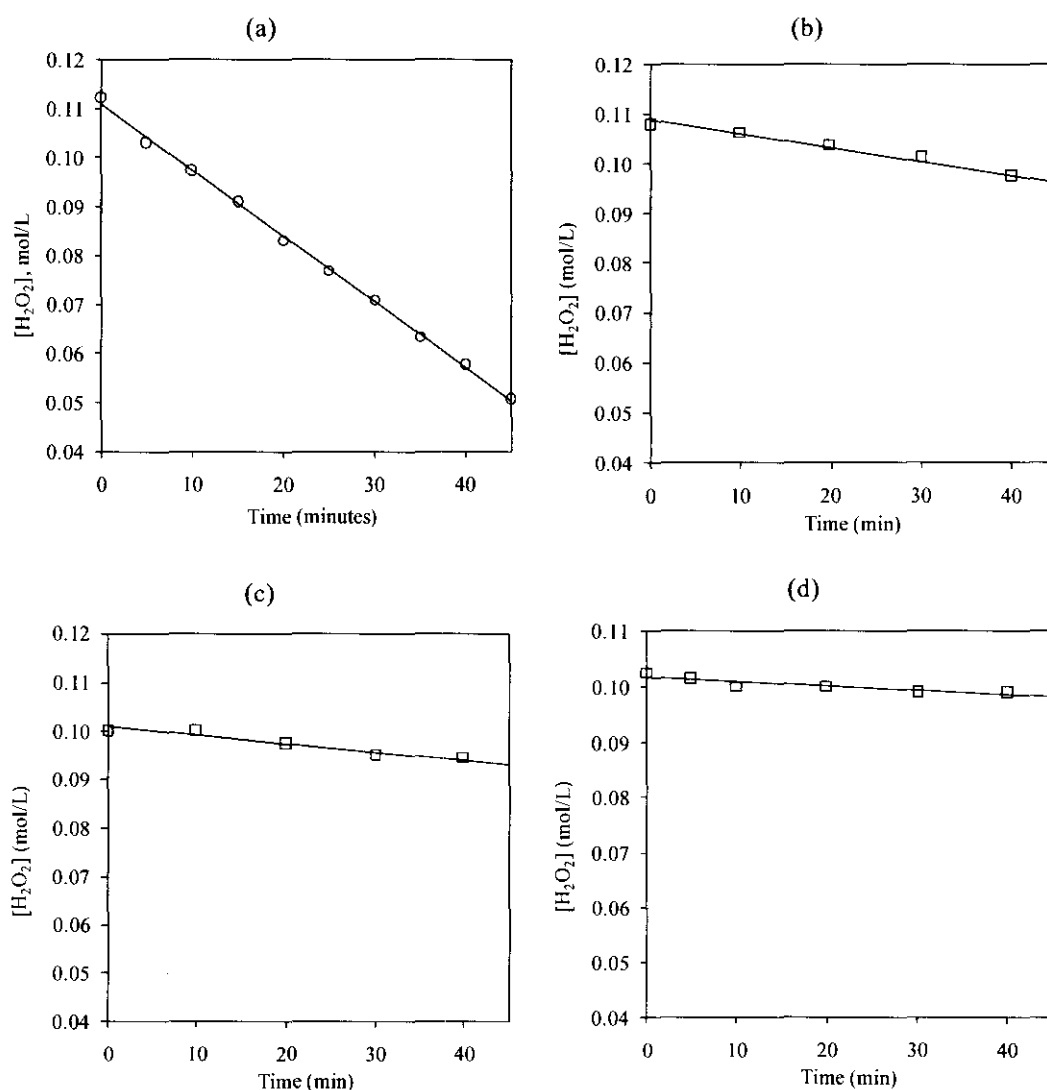
Figure A-5-1: Determination of UV fluence using hydrogen peroxide actinometry using various UV lamp - reactor combinations. (a) One 8 W lamp in 390 mL reactor, (b) One 4 W lamp in 1100 mL reactor, (c)Two 4 W lamp in 1100 mL reactor, (d) Three 4 W lamp in 1100 mL reactor

The calculations for UV fluence, I_0 and radiant power, P_0 for the above cases are given as follows:

(a) I_0 $= - d[H_2O_2]/dt = 0.00134/60 = 2.23 \times 10^{-5}$ Einsteins $\cdot$ L$^{-1} \cdot$ s^{-1}

   P_0 $= 2.23 \times 10^{-5} \times 0.39$ L $/ 8.3593$ Einsteins $\cdot$ W$^{-1} \cdot$ m$^{-1} \cdot$ s$^{-1} / (253.7 \times 10^{-9}$ m)

   $= 4.11$ W

(b) I_0 $= - d[H_2O_2]/dt = 0.00281/60 = 4.68 \times 10^{-6}$ Einsteins $\cdot$ L$^{-1} \cdot$ s^{-1}

   P_0 $= 4.68 \times 10^{-6} \times 1.1$ L $/ 8.3593$ Einsteins $\cdot$ W$^{-1} \cdot$ m$^{-1} \cdot$ s$^{-1} / (253.7 \times 10^{-9}$ m)

   $= 2.43$ W

(c) I_0 $= - d[H_2O_2]/dt = 0.00174/60 = 2.90 \times 10^{-6}$ Einsteins $\cdot$ L$^{-1} \cdot$ s^{-1}

   P_0 $= 2.90 \times 10^{-6} \times 1.1$ L $/ 8.3593$ Einsteins $\cdot$ W$^{-1} \cdot$ m$^{-1} \cdot$ s$^{-1} / (253.7 \times 10^{-9}$ m)

   $= 1.51$ W

(d) I_0 $= - d[H_2O_2]/dt = 0.000774/60 = 1.29 \times 10^{-6}$ Einsteins $\cdot$ L$^{-1} \cdot$ s^{-1}

   P_0 $= 1.29 \times 10^{-6} \times 1.1$ L $/ 8.3593$ Einsteins $\cdot$ W$^{-1} \cdot$ m$^{-1} \cdot$ s$^{-1} / (253.7 \times 10^{-9}$ m)

   $= 0.67$ W

Appendix B: Raw Data for Figures

Figure 4-2. (Page 56) Effect of (a) initial pH at high buffer concentration ($[KH_2PO_4]$ = 240 mM, $[H_2O_2]_0$ = 0.11 M, T = 28 deg. C, Φ_{UV} = 4.13 W), (b) initial pH at low buffer concentration ($[KH_2PO_4]$ = 8 mM, $[H_2O_2]_0$ = 0.11 M, T = 28 deg. C, Φ_{UV} = 4.13 W), (c) temperature ($[H_2O_2]_0$ = 0.11 M, pH_0 = 2, Φ_{UV} = 4.13 W), (d) UV flux ($[H_2O_2]_0$ = 0.11 M, T = 28 deg. C, pH_0 = 2) and (e) initial H_2O_2 concentration (T = 28 deg. C, Φ_{UV} = 4.13 W, pH_0 = 2) on COD degradation of MEA

Figure 4-2 (a)							
pH 2		pH 5		pH 7		pH 9	
Time	Value	Time	Value	Time	Value	Time	Value
0	1	0	1	0	1	0	1
2	0.886513	2		2	0.891339	2	0.93311
5	0.784539	5	0.81	5	0.79685	5	0.841137
10	0.705592	10	0.688333	10	0.692913	10	0.735786
15	0.546053	15	0.586667	15	0.570079	15	0.591973
20	0.509868	20	0.465	20	0.52126	20	0.473244
30	0.424342	30	0.303333	31	0.308661	30	0.245819
40	0.365132	40	0.231667	42	0.215748	40	0.162207
50	0.305921	50	0.235	51	0.165354	50	0.095318
60	0.282895	60	0.183333	60	0.119685	60	0.055184

Figure 4-2 (b)

pH 2		pH 4		pH 6		pH 8	
Time	Value	Time	Value	Time	Value	Time	Value
0	1	0	1	0	1	0	1
2	0.886513	2	0.938776	2	0.814241	2	0.848397
5	0.784539	5	0.822606	5	0.71517	5	0.806122
10	0.705592	10	0.697017	10	0.588235	10	0.66035
15	0.546053	15	0.565149	15	0.51548	15	0.559767
20	0.509868	20	0.491366	20	0.475232	20	0.437318
30	0.424342	30	0.395604	30	0.314241	30	0.24344
40	0.365132	40	0.304553	40	0.239938	40	0.125364
50	0.305921	50	0.268446	50	0.208978	50	0.09621
60	0.282895	60	0.243328	60	0.185759	60	0.081633

Figure 4-2 (c)

T = 28 deg. C		T = 20 deg. C		T = 45 deg. C	
Time	Value	Time	Value	Time	Value
0	1	0	1	0	1
2	0.886513	2	0.907767	2	0.899213
5	0.784539	5	0.815534	5	0.804724
10	0.705592	10	0.695793	10	0.711811
15	0.546053	15	0.584142	15	0.609449
20	0.509868	20	0.527508	20	0.555906
30	0.424342	30	0.432039	30	0.464567
40	0.365132	40	0.364078	40	0.392126
50	0.305921	50	0.351133	50	0.36063
60	0.282895	60	0.300971	60	0.283465

Figure 4-2 (d)							
4.13 W		2.44 W		1.52 W		0.67 W	
Time	Value	Time	Value	Time	Value	Time	Value
0	1	0	1	0	1	0	1
2	0.886513	2	0.994819	2	0.960666	2	1.041739
5	0.784539	5	0.981002	5	0.956127	5	0.991304
10	0.705592	10	0.984456	10	0.912254	10	0.965217
15	0.546053	15	0.891192	15	0.877458	15	0.946087
20	0.509868	20	0.842832	20	0.885023	20	0.935652
30	0.424342	30	0.761658	30	0.803328	30	0.914783
40	0.365132	40	0.699482	40	0.739788	40	0.874783
50	0.305921	50	0.642487	50	0.695915	50	0.841739
60	0.282895	60	0.597582	60	0.683812	60	0.838261

Figure 4-2 (e)					
0.11 M		0.27 M		0.53 M	
Time	Value	Time	Value	Time	Value
0	1	0	1	0	1
2	0.886513	2	0.951786	2	0.973545
5	0.784539	5	0.883929	5	0.952381
10	0.705592	10	0.828571	10	0.888889
15	0.546053	15	0.782143	15	0.843034
20	0.509868	20	0.7125	20	0.784832
30	0.424342	30	0.635714	30	0.744268
40	0.365132	40	0.567857	40	0.68254
50	0.305921	50	0.535714	50	0.633157
60	0.282895	60	0.521429	60	0.608466

Figure 4-3: (Page 59) Effect of (a) initial pH ($[H_2O_2]_0$ = 0.11 M, T = 28 deg. C, Φ_{UV} = 4.13 W), (b) temperature ($[H_2O_2]_0$ = 0.11 M, pH_0 = 2, Φ_{UV} = 4.13 W), (c) UV flux ($[H_2O_2]_0$ = 0.11 M, T = 28 deg. C, pH_0 = 2) and (d) initial H_2O_2 concentration (T = 28 deg. C, Φ_{UV} = 4.13 W, pH_0 = 2) on MEA degradation first-order kinetics.

Figure 4-3 (a)				
Time	pH 2	pH 4	pH 6	pH 8
0	0	0	0	0
2	0.2219005	0.144523	0.269728	0.127833
5	0.6931472	0.408107	0.619816	0.299305
10	0.8905066	0.831591	0.737599	0.728429
15	1.5421048	1.237056	1.302913	1.044124
20	1.678964	1.606803	1.604018	1.427116
30		2.273975	2.649986	2.213354

Figure 4-3 (b)			
Time	T = 20 deg. C	T = 28 deg. C	T = 45 deg. C
0	0	0	0
2	0.311519	0.221901	0.197977
5	0.525928	0.693147	0.460342
10	0.888834	0.890507	0.707817
15	1.278795	1.542105	1.072263
20	1.63547	1.678964	1.2419
30	2.157345		1.943486

Figure 4-3 (c)				Figure 4-3 (d)		
Time	4.13 W	2.44 W	1.52 W	0.11 M	0.27 M	0.53 M
0	0	0	0	0	0	0
2	0.2219005	0.132509	0.021109	0.221901	0.084174	
5	0.6931472	0.528483	0.037238	0.693147	0.207639	0.162367
10	0.8905066	0.540703	0.061931	0.890507	0.363394	0.244692
15	1.5421048	0.671895	0.122035	1.542105	0.613104	0.374928
20	1.678964	0.896207	0.145917	1.678964	0.724896	0.503104
30		1.185841	0.316823		1.154852	0.787941
40		1.412898	0.414646		1.543923	1.075623
50			0.414646		2.018817	1.323696
60			0.536389			1.515773

Figure 4-4. (Page 60) Effect of (a) initial pH at high buffer concentration ($[KH_2PO_4]$ = 240 mM, $[H_2O_2]_0$ = 0.11 M, T = 28 deg. C, Φ_{UV} = 4.13 W), (b) initial pH at low buffer concentration ($[KH_2PO_4]$ = 8 mM, $[H_2O_2]_0$ = 0.11 M, T = 28 deg. C, Φ_{UV} = 4.13 W), (c) temperature ($[H_2O_2]_0$ = 0.11 M, pH_0 = 2, Φ_{UV} = 4.13 W) on H_2O_2 decay, (d) UV flux ($[H_2O_2]_0$ = 0.11 M, T = 28 deg. C, pH_0 = 2) and (d) initial H_2O_2 concentration (T = 28 deg. C, Φ_{UV} = 4.13 W, pH_0 = 2) on H_2O_2 decay.

Figure 4-4 (a)							
pH 2		pH 5		pH 7		pH 9	
Time	Value	Time	Value	Time	Value	Time	Value
0	0.109617	0	0.104074	0	0.101611	0	0.10469
2	0.103459	2	0.100995	2	0.100995	2	0.102843
5	0.102227	5	0.093605	5	0.094837	5	0.098532
10	0.0973	10	0.083752	10	0.084984	10	0.087447
15	0.091142	15	0.076362	15	0.076362	15	0.073283
20	0.084984	20	0.067741	20	0.068357	20	0.065893
30	0.074515	30	0.052961	31	0.049882		
40	0.061583	40	0.043108	42	0.033255	40	0.037565
50	0.054808	50	0.034486	51	0.025249	50	0.028944
60	0.048034	60	0.027096	60	0.019706	60	0.020322

111

Figure 4-4 (b)							
pH 2		pH 4		pH 6		pH 8	
Time	Value	Time	Value	Time	Value	Time	Value
0	0.109617	0	0.107154	0	0.107154	0	0.099764
2	0.103459	2	0.10469	2	0.0973	2	0.100995
5	0.102227	5	0.0973	5	0.094837	5	0.096685
10	0.0973	10	0.091142	10	0.084984	10	0.088063
15	0.091142	15	0.086216	15	0.080673	15	0.072667
20	0.084984	20	0.078826	20	0.070204	20	0.061583
30	0.074515	30	0.062814	30	0.056656	30	0.043724
40	0.061583	40	0.055424	40	0.049266	40	0.034486
50	0.054808	50	0.044339	50	0.040644	50	0.027712
60	0.048034	60	0.035102	60	0.03387	60	0.019706

Figure 4-4 (c)					
T = 28 deg. C		T = 20 deg. C		T = 45 deg. C	
Time	Value	Time	Value	Time	Value
0	0.109617	0	0.109617	0	0.107154
2	0.103459	2	0.107154	2	0.102227
5	0.102227	5	0.103459	5	0.099764
10	0.0973	10	0.09299	10	0.092374
15	0.091142	15	0.089295	15	0.088679
20	0.084984	20	0.083752	20	0.083752
30	0.074515	30	0.071436	30	0.071436
40	0.061583	40	0.064046	40	0.061583
50	0.054808	50	0.055424	50	0.051729
60	0.048034	60	0.046803	60	0.046803

Figure 4-4 (d)							
4.13 W		2.44 W		1.52 W		0.67 W	
Time	Value	Time	Value	Time	Value	Time	Value
0	0.109617	0	0.0973	0	0.0973	0	0.099764
2	0.103459						
5	0.102227					5	0.098532
10	0.0973	10	0.096069	10	0.0973	10	0.0973
15	0.091142						
20	0.084984	20	0.093605	20	0.094837	20	0.098532
30	0.074515	30	0.08991	30	0.092374	30	0.096069
40	0.061583	40	0.087447	40	0.091758	40	0.096069
50	0.054808	50	0.084984	50	0.08991	50	0.094837
60	0.048034	60	0.080057	60	0.087447	60	0.094837

Figure 4-4 (e)					
0.11 M		0.27 M		0.53 M	
Time	Value	Time	Value	Time	Value
0	0.109617	0	0.277121	0	0.517293
2	0.103459	2	0.277121	2	0.511135
5	0.102227	5	0.270963	5	0.504977
10	0.0973	10	0.267884	10	0.504977
15	0.091142	15	0.264805		
20	0.084984	20	0.255567	20	0.49266
30	0.074515	30	0.24633	30	0.474185
40	0.061583	40	0.234014	40	0.468027
50	0.054808			50	0.449552
60	0.048034			60	0.437236

Figure 4-5. (Page 61) Evolution of pH with time at low buffer conditions ($[KH_2PO_4]$ = 8 mM, $[H_2O_2]_0$ = 0.11 M, T = 28 deg. C, Φ_{UV} = 4.13 W), high buffer condition ($[KH_2PO_4]$ = 240 mM, $[H_2O_2]_0$ = 0.11 M, T = 28 deg. C, Φ_{UV} = 4.13 W) and unbuffered solution ($[H_2O_2]_0$ = 0.11 M, T = 28 deg. C, Φ_{UV} = 4.13 W).

Figure 4-5					
pH 9 low buffer		pH 9 high buffer		Unbuffered	
Time	pH	Time	pH	Time	pH
0	8.97	0	9.01	0	9.88
2	8.94	2	8.87	5	9.69
5	8.55	5	8.68	10	9.53
10	7.74	10	8.42		
15	6.95	15	8.16	20	8.87
20	6.6	20	7.98		
30	6.19	30	7.82	30	7.43
40	5.94	40	7.72	40	6.5
50	5.94	50	7.67	50	6.26
60	5.95	60	7.66	60	6.09

Figure 4-6: (Page 62) Measured k_0 value as a function of UV flux.

Figure 4-6	
UV Flux (W)	k_0
1.52	0.009045
2.44	0.029993
4.13	0.092209

114

Figure 4-7 (b) (Page 66) Concentration profile of MEA, formate and nitrate with time.

Figure 4-7 (b)					
Time	MEA		Time	Formate	Nitrate
0	804		0	0	0
2	644		5	144.8293	3.2994
5	402		10	186.9097	4.92645
10	330		20	190.4526	9.49515
15	172		30	138.3505	23.5098
20	150		40	101.768	43.3332
30			50	94.27833	56.57235
40			60	73.63197	76.7025

Figure 4-8 (Page 73) (a) Dependence of reaction order, n on pH and (b) linear relationship between kinetic constant k_8 and reaction order, n.

Figure 4-8 (a)			
Low buffer		High buffer	
pH	n	pH	n
2	3.0	2	3.0
5	2.5	4	3.0
7	2.0	6	3.0
9	1.5	8	2.0
		9	1.2

Figure 4-8 (b)	
n	$\log_{10} k_8$
3.0	10.78
3.0	10.84
3.0	11.06
2.0	9.42
1.2	8.01
3.0	10.75
3.0	10.66
2.0	9.29
1.5	8.54
2.5	10.14
3.0	10.80
3.0	10.79
3.0	11.12

Figure 4-9. (Page 75) Comparison between observed (measured) and predicted fractional COD removal after 60 minutes of reaction as a function of (a) pH ($n = 3$, k_8 = 7.41×10^{10} M^{-3} s^{-1}, initial $[H_2O_2]$ = 0.107 M, initial [COD] = 0.036 M, UV flux = 10.53 W/m^3), (b) initial H_2O_2 concentration ($n = 3$, $k_8 = 7.41 \times 10^{10}$ M^{-3} s^{-1}, pH = 2, initial [COD] = 0.036 M, UV flux = 10.53 W/m^3) and (c) UV flux ($n = 3$, $k_8 = 7.41 \times 10^{10}$ M^{-3} s^{-1}, pH = 2, initial $[H_2O_2]$ = 0.1 M, initial [COD] = 0.036 M,).

Figure 4-9 (a)				Figure 4-9 (b)			
Model		Observed		Model		Observed	
pH_0	$1-[S]/[S]_0$	pH_0	$1-[S]/[S]_0$	$[H_2O_2]_0$	$1-[S]/[S]_0$	$[H_2O_2]_0$	$1-[S]/[S]_0$
2	0.7556	2	0.7286	0.09	0.7834	0.11	0.717105
4	0.7556	5	0.8276	0.095	0.7755	0.27	0.478571
6	0.7556	7	0.8693	0.1	0.7673	0.53	0.391534
8	0.7557	9	0.9319	0.15	0.6894		
9	0.7566			0.2	0.6307		
9.5	0.7585			0.25	0.5853		
10	0.7634			0.3	0.5483		
10.5	0.7733			0.35	0.5170		
11	0.7910			0.4	0.4899		
11.5	0.8259			0.45	0.4660		
12	0.8841			0.5	0.4448		
12.05	0.8914			0.55	0.4258		
				0.6	0.4085		

117

Figure 4-9 (c)			
Model		Observed	
UV flux	$1-[S]/[S]_0$	UV dose (W/m^3)	$1-[S]/[S]_0$
0.43	0.0956	0.609	0.161739
0.64	0.1389	1.382	0.316188
0.86	0.1793	2.218	0.402418
1.29	0.2517	10.590	0.717105
2.14	0.3681		
3	0.4551		
4.29	0.5496		
5.14	0.5967		
6.43	0.6525		
8.57	0.7209		
10.72	0.7711		
12.86	0.8085		

Figure 4-10 (Page 77) Examples of experimental run data plotted against model prediction ([KH_2PO_4] = 8 mM, [H_2O_2]$_0$ = 0.11 M, T = 28 deg. C, Φ_{UV} = 4.13 W) for (a) initial pH =2 (n = 3, k_8 = 7.41×10^{10} M^{-3}s^{-1}) and (b) initial pH = 4 (n = 2.63, k_8 = 1.98×10^{10} M$^{-2.63}$s^{-1}).

	Figure 4-10 (a)*				Figure 4-10 (b)*			
	Experiment		Model		Experiment		Model	
time (s)	[H_2O_2]	[S]/[S]$_0$	[H_2O_2]	[S]/[S]$_0$	[H_2O_2]	[S]/[S]$_0$	[H_2O_2]	[S]/[S]$_0$
0	0.110	1.000	0.109	1.000	0.107	1.000	0.107	1.000
120	0.103	0.887	0.106	0.923	0.105	0.939	0.104	0.925
300	0.102	0.785	0.102	0.821	0.097	0.823	0.100	0.823
600	0.097	0.706	0.095	0.685	0.091	0.697	0.093	0.681
900	0.091	0.546	0.089	0.583	0.086	0.565	0.087	0.572
1200	0.085	0.510	0.082	0.507	0.079	0.491	0.080	0.487
1800	0.075	0.424	0.068	0.401	0.063	0.396	0.066	0.369
2400	0.062	0.365	0.054	0.330	0.055	0.305	0.052	0.292
3000	0.055	0.306	0.041	0.277	0.044	0.268	0.039	0.236
3600	0.048	0.283	0.028	0.237	0.035	0.243	0.027	0.194

*Only model data that correspond to the experimental sampling times are included here.

Figure 4-13 (Page 82) Biomass growth and organic removal for AOP-pretreated and untreated MEA solution

Time	Untreated MEA		Pretreated MEA	
	Biomass (mg/l)	COD (mg/l)	Biomass (mg/l)	COD (mg/l)
0	131.8375	921	80.825	-
5.5	129.85	903	81.4875	-
11	122.5625	864	75.525	786
18.5	124.55	731	75.525	724
23	141.1125	592	-	632
29	251.75	149	99.375	429
35	-	102	126.5375	248
47	-	-	129.85	172
53	-	-	133.1625	-

Run No	Notes	Date	Init. pH	Buffer (mM)	Temperature (deg C)	Volume (mL)	$[H_2O_2]_0$ (M)*	H_2O_2 added (g)	MEA added (g)	UV flux (W)	MEA analysis
1		14-Aug-08	2	8	28	390	0.11	1.41	0.39	4.11	Yes
2		16-Sep-08	4	8	28	390	0.11	1.41	0.39	4.11	Yes
3		19-Sep-08	6	8	28	390	0.11	1.41	0.39	4.11	Yes
4		25-Sep-08	8	8	28	390	0.11	1.41	0.39	4.11	Yes
5		16-Oct-08	9	8	28	390	0.11	1.41	0.39	4.11	No
6		14-Oct-08	2	8	20	390	0.11	1.41	0.39	4.11	Yes
7	Repeat of pH 6	16-Oct-08	6	8	28	390	0.11	1.41	0.39	4.11	No
8		21-Oct-08	2	8	45	390	0.11	1.41	0.39	4.11	Yes
9		12-Nov-08	7	240	28	390	0.11	1.41	0.39	4.11	No
10		17-Nov-08	9	240	28	390	0.11	1.41	0.39	4.11	No
11		19-Nov-08	5	240	28	390	0.11	1.41	0.39	4.11	No
12	Glycine run	24-Nov-08	6	0	28	390	0.11	1.41	n/a	4.11	No
13	Uncorrected pH	26-Nov-08	10	0	28	390	0.11	1.41	0.39	4.11	No
14		5-Jan-09	2	0	28	390	0.53	7.06	0.39	4.11	Yes
15		8-Jan-09	2	0	28	390	0.27	3.53	0.39	4.11	Yes
16		15-Jan-09	2	0	28	1100	0.11	3.98	1.10	0.67	Yes
17		15-Feb-09	2	0	28	1100	0.11	3.98	1.10	1.51	Yes
18		18-Feb-09	2	0	28	1100	0.11	3.98	1.10	2.43	Yes

Table A-2: Raw data for Run 1

Time	[H$_2$O$_2$]	COD (mg/l)	MEA(mg/l)
0	0.110	1216	804
2	0.103	1078	644
5	0.102	954	402
10	0.097	858	330
15	0.091	664	172
20	0.085	620	150
30	0.075	516	-
40	0.062	444	-
50	0.055	372	-
60	0.048	344	-

Table A-3: Raw data for Run 2

Time	[H$_2$O$_2$]	COD (mg/l)	MEA(mg/l)
0	0.107	1274	758
2	0.105	1196	656
5	0.097	1048	504
10	0.091	888	330
15	0.086	720	220
20	0.079	626	152
30	0.063	504	78
40	0.055	388	-
50	0.044	342	-
60	0.035	310	-

Table A-4: Raw data for Run 3

Time	[H$_2$O$_2$]	COD (mg/l)	MEA(mg/l)
0	0.107	1292	736
2	0.097	1052	562
5	0.095	924	396
10	0.085	760	352
15	0.081	666	200
20	0.070	614	148
30	0.057	406	52
40	0.049	310	-
50	0.041	270	-
60	0.034	240	-

Table A-5: Raw data for Run 4

Time	[H$_2$O$_2$]	COD (mg/l)	MEA(mg/l)
0	0.100	1372	750
2	0.101	1164	660
5	0.097	1106	556
10	0.088	906	362
15	0.073	768	264
20	0.062	600	180
30	0.044	334	82
40	0.034	172	-
50	0.028	132	-
60	0.020	112	-

Table A-6: Raw data for Run 5

Time	[H$_2$O$_2$]	COD (mg/l)	MEA(mg/l)	pH
0	0.105	1264	-	8.97
2	0.103	1198	-	8.94
5	0.100	1114	-	8.55
10	0.087	922	-	7.74
15	0.080	780	-	6.95
20	0.068	658	-	6.6
30	0.052	402	-	6.19
40	0.035	182	-	5.94
50	0.027	100	-	5.94
60	0.018	82	-	5.95

Table A-7: Raw data for Run 6

Time	[H$_2$O$_2$]	COD (mg/l)	MEA(mg/l)	pH
0	0.110	1236	934	2
2	0.107	1122	684	-
5	0.103	1008	552	-
10	0.093	860	384	2.11
15	0.089	722	260	-
20	0.084	652	182	2.11
30	0.071	534	108	2.13
40	0.064	450	-	2.13
50	0.055	434	-	2.11
60	0.047	372	-	2.13

Table A-8: Raw data for Run 8

Time	[H$_2$O$_2$]	COD (mg/l)	MEA(mg/l)
0	0.107	1270	824
2	0.102	1142	676
5	0.100	1022	520
10	0.092	904	406
15	0.089	774	282
20	0.084	706	238
30	0.071	590	118
40	0.062	498	62
50	0.052	458	-
60	0.047	360	-

Table A-9: Raw data for Run 9

Time	[H$_2$O$_2$]	COD (mg/l)	MEA(mg/l)	pH
0	0.102	1270	-	7
2	0.101	1132	-	6.98
5	0.095	1012	-	6.97
10	0.085	880	-	6.96
15	0.076	724	-	6.94
20	0.068	662	-	6.92
31	0.050	392	-	6.88
42	0.033	274	-	6.84
51	0.025	210	-	6.85
60	0.020	152	-	6.83

Table A-10: Raw data for Run 10

Time	[H_2O_2]	COD (mg/l)	MEA(mg/l)	pH
0	0.105	1196	-	9.01
2	0.103	1116	-	8.87
5	0.099	1006	-	8.68
10	0.087	880	-	8.42
15	0.073	708	-	8.16
20	0.066	566	-	7.98
30	0.000	294	-	7.82
40	0.038	194	-	7.72
50	0.029	114	-	7.67
60	0.020	66	-	7.66

Table A-11: Raw data for Run 11

Time	[H_2O_2]	COD (mg/l)	MEA(mg/l)	pH
0	0.104	1200	-	5
2	0.101	-	-	
5	0.094	972	-	4.96
10	0.084	826	-	4.86
15	0.076	704	-	4.64
20	0.068	558	-	4.52
30	0.053	364	-	4.33
40	0.043	278	-	4.25
50	0.034	282	-	4.23
60	0.027	220	-	4.3

Table A-12: Raw data for Run 13

Time	[H₂O₂]	COD (mg/l)	MEA(mg/l)	pH
0	-	1254	-	9.88
2	-	-	-	-
5	-	1109	-	9.69
10	-	952	-	9.53
15	-	-	-	-
20	-	762	-	8.87
30	-	573	-	7.43
40	-	459	-	6.5
50	-	341	-	6.26
60	-	279	-	6.09

Table A-12: Raw data for Run 14

Time	[H₂O₂]	COD (mg/l)	MEA(mg/l)
0	0.517	1134	774
2	0.511	1104	658
5	0.505	1080	606
10	0.505	1008	532
15	0.000	956	468
20	0.493	890	352
30	0.474	844	264
40	0.468	774	206
50	0.450	718	170
60	0.437	690	774

Table A-13: Raw data for Run 15

Time	[H$_2$O$_2$]	COD (mg/l)	MEA(mg/l)
0	0.277	1120	768
2	0.277	1066	706
5	0.271	990	624
10	0.268	928	534
15	0.265	876	416
20	0.256	798	372
30	0.246	712	242
40	0.234	636	164
50	-	600	102
60	-	584	-

Table A-14: Raw data for Run 16

Time	[H$_2$O$_2$]	COD (mg/l)	MEA(mg/l)
0	0.100	1150	-
2	-	1198	-
5	0.099	1140	-
10	0.097	1110	-
15	-	1088	-
20	0.099	1076	-
30	0.096	1052	-
40	0.096	1006	-
50	0.095	968	-
60	0.095	964	-

Table A-15: Raw data for Run 17

Time	[H$_2$O$_2$]	COD (mg/l)	MEA(mg/l)
0	0.097	1322	766
2	-	1270	750
5	-	1264	738
10	0.097	1206	720
15	-	1160	678
20	0.095	1170	662
30	0.092	1062	558
40	0.092	978	506
50	0.090	920	506
60	0.087	904	448

Table A-16: Raw data for Run 18

Time	[H$_2$O$_2$]	COD (mg/l)	MEA(mg/l)
0	0.097	1158	838
2	-	1152	-
5	-	1136	734
10	0.096	1140	494
15	-	1032	488
20	0.094	976	428
30	0.090	882	342
40	0.087	810	256
50	0.085	744	204
60	0.080	692	-